ABSTRACT

Late Mississippian (Chesterian) High-Frequency Climate Change
in the Pennington Formation at Pound Gap, KY USA

Julia Amanda Kahmann-Robinson Ph.D.

Mentor: Steven G. Driese, Ph.D.

Climate during the Late Mississippian (Late Chesterian) in the southern Appalachian Basin was characterized by periods of aridity and humidity. The Pennington Formation, exposed at Pound Gap, KY, USA records these changing climatic conditions. The climate signal, however, is partially obscured by longer-term eustatic fluctuations throughout the Late Chesterian. In this clastic-dominated formation, evidence for several orders of cyclicity point to tectonic, glacio-eustatic, and climate controlled-cyclicity. Pennington Formation paleosols provide a record of climate and ecological changes for latest Chesterian time. Forty paleosols were identified, described, and assigned to seven pedotypes ranging from Vertisols to Oxisols. Field and micromorphological evidence suggests a polygenetic character of the Vertisols, resulting from changing soil drainage through time. Using the CIA-K proxy, mean annual precipitation (MAP) estimates range from 519 to 1361 mm/yr. Variations in MAP and quantified soil processes correspond with variation s in soil drainage, resulting from high-frequency paleoclimate change. The temporal distribution of trace elements in paleosols is also related to soil-forming processes and climate. The trace element chemistry (Ti, Ga, Ge, Y, Zr, Nb, Cs, La, Hf,

Ta, W, Ce, Th) of the paleosols is controlled by either organic matter content or lessivage (clay formation and accumulation by feldspar weathering). Climate changes are inferred from the trace element chemistry, which is related to changing MAP and intensity of chemical weathering. This study provides greater resolution of changing climate, controls on sedimentation, and pedogenic processes than what is provided in previous studies of the Late Mississippian. The documented variability in fluvial cyclicity, paleosol types, soil drainage, and trace element chemistry might represent the record of high-frequency climate changes likely associated with expansion and contraction of the paleo-Intertropical Convergence Zone (ITCZ).

Late Mississippian (Chesterian) High-Frequency Climate Change
in the Pennington Formation at Pound Gap, KY, USA

by

Julia Amanda Kahmann-Robinson B.S., M.S.

A Dissertation

Approved by the Department of Geology

_____
Steven G. Driese, Ph.D., Chairperson

Submitted to the Graduate Faculty of
Baylor University in Partial Fulfillment of the
Requirements for the Degree
of
Doctor of Philosophy

Approved by the Dissertation Committee

_____
Steven G. Driese, Ph.D., Chairperson

_____
Stacy C. Atchley, Ph.D.

_____
Stephen I. Dworkin, Ph.D.

_____
Lee C. Nordt, Ph.D., Dean

_____
Joseph D. White, Ph.D.

Accepted by the Graduate School
December 2008

_____
J. Larry Lyon, Ph.D., Dean

Page bearing signatures is kept on file in the Graduate School.

TABLE OF CONTENTS

LIST OF FIGURES

LIST OF TABLES

ACKNOWLEDGMENTS

With great love I would like to thank my husband, Mark Sherman Robinson, for his positive attitude, example, and eternal friendship that helped me see this project to the end. His sacrifice and service to our country in the Iraq War taught me to persevere and work fully-engaged with purpose; a purpose outside of myself. From the beginning, my parents Tony and Karen have been supporters and cheer leaders of my many adventures, ups, downs and turnaround s that brought me to this point in life. The scientist, the teacher, the person that Julia is, was cultivated by my parents. Inspiration to become a scientist came from my high school chemistry teacher Mrs. Cinda Parton, and the drive to become a geologist from Dr. Scott Ritter of Brigham Young University.

The academic success of this dissertation is the result of the mentorship, guidance, and friendship of my advisor Dr. Steven G. Driese. Never were the doors closed, counsel always given, and the opportunity to "become" the scientist always extended. The expertise and guidance of my committee members Drs. Stacy Atchley, Steve Dworkin, and Lee Nordt was amazing and unselfish. Their skill and commitment to university learning is admirable. I would also like to thank Dr. Joseph White for his contributions to my success. Lastly, I am grateful to the journals: Journal of Geology, Chicago Press and Palaeogeography, Palaeoclimatology, Palaeoecology, Elsevier for permission to include Chapter 2 (Kahmann and Driese, 2008) and Chapter 3 (Kahmann et al., 2008) in this dissertation.

To those wanting to extend and enhance the legacy of those gone before. It is humbling to have the opportunity to contribute my part.

"Shall we not go forth in so great a cause?"
-Joseph Smith Jr.

CHAPTER ONE

Introduction

The Late Mississippian marks a transition from icehouse to greenhouse conditions. In addition to this large-scale climatic event, the Late Mississippian in the Appalachian Basin was also characterized by marked high-frequency climate variation characterized by alternating periods of humid and dry conditions (Cecil, 1990). The nature and controls upon these high-frequency climate shifts have not been thoroughly studied because of a perceived lack of available data and application of appropriate paleoclimate proxies. The Pennington Formation at the Pound Gap exposure, KY offers a unique opportunity to study the variability of Late Mississippian (Chesterian) climate. Using tools of pedology, major and trace element chemistry, and sequence stratigraphy, the high-frequency climate variation of the Late Mississippian can be confidently analyzed and interpreted.

The Pennington Fm. records a variety of depositional environments ranging from open marine carbonate ramps to the pedogenic environment. The pedogenic environment and the paleosols developed record Critical Zone processes occurring at the interface between the biosphere, atmosphere, and lithosphere. Consequently, Pennington paleosols are acutely sensitive to paleoenvironmental and paleoclimate change. Utilizing field, micromorphological, and geochemical attributes of over forty Pennington paleosols the following are hypothesized: (1) the Late Mississippian (Chesterian) in the southern Appalachian region was characterized by overall more arid to semi-arid conditions than the earliest Pennsylvanian, (2) that the evidence for overprinting by dry and wet soil

features in the Pennington paleosols indicates effects associated with high-frequency, and seasonal wet/dry conditions, and (3) that seasonal migration of a paleo-Intertropical Convergence Zone (ITCZ), similar to what occurs in tropical regions today, also operated during the latest Mississippian.

Preliminary geochemical analysis of the Pennington Fm. paleosols suggested that another paleoclimate proxy might be available to further enhance paleoclimate interpretation. Plots of certain trace element concentrations (Zr, Nb, Cs, La, Hf, Ta, W, Ce, and Th) versus time were tightly coupled. This coupling was also observed in relation to soil-forming processes, suggesting a potential climate control. Given the low concentrations of trace elements in soils, the temporal and spatial distributions of these elements in soils have been generally overlooked, particularly in relation to soil-forming processes and climate. In order to confidently utilize the trace element soil chemistry as a paleoclimate proxy, both linear and multivariate statistical techniques were employed. It was determined through statistical analysis that trace element chemistry could be a useful tool in paleoclimate interpretation provided that (1) trace element data are statistically analyzed using linear and multivariate methods, (2) data are analyzed temporally (i.e., through time) and not viewed statically, and (3) there is an understanding of the underlying controls on trace element chemistry of soils.

Although paleosol study could confirm climate control upon deposition, other controls needed to be considered to account for cyclicity within other environments of deposition in the Pennington Fm. Using a sequence-stratigraphic approach, other controls such as the waxing and waning of global ice, regional tectonics, and eustasy were evaluated. As a mixed carbonate and siliciclastic system, the above controls are difficult

to differentiate; however, it is proposed that all the above factors contributed to Pennington cyclicity. A three-tiered hierarchy of cyclicity is presented: composite sequence, sequence, and cycle. The highest order within the proposed hierarchy (a cycle) suggests high-frequency climate change. The hierarchy is based strictly upon facie stacking patterns and genetic relationships without rigorous chronostratigraphic controls. In addition to paleosol study, and geochemical proxies, a sequence-stratigraphic study contributed to the overall understanding of Late Mississippian (Chesterian) climate change for the Southern Appalachian Basin region.

CHAPTER TWO

Paleopedology and Geochemistry of Late Mississippian (Chesterian) Pennington Formation Paleosols at Pound Gap, Kentucky, USA: Implications for High-Frequency Climate Variations

Abstract

Climate during the Late Mississippian (late Chesterian) in the southern Appalachian Basin was characterized by alternating periods of aridity and humidity. Pennington Formation paleosols at Pound Gap record climate and ecological changes for latest Chesterian time, ending at the Mississippian-Pennsylvanian systemic boundary. Forty paleosols were identified, described, and assigned to seven pedotypes. Inferred soil orders considered as analogs include Histosols, Entisols, Inceptisols, Alfisols and Oxisols, but are dominated by Vertisols. Classification of an Oxisol was determined by field and geochemical evidence of intense leaching and kaolinite-dominated clay mineralogy. Field and micromorphologicial evidence suggests a polygenetic character of the Vertisols, resulting from changing soil drainage through time. Variations in soil drainage are quantified using proxy estimates of inferred soil processes such as base loss, leaching, lessivage, and oxidation. Using the CIA-K proxy, mean annual precipitation (MAP) estimates range from 519 to 1361 mm/yr. Changes in MAP correspond with variation in inferred soil processes. The flora of this time period, in response to variations in precipitation and soil drainage, also changes through time as evidenced by changes in abundance and depth of root traces. Reconstructed ecosystems range from sparse vegetative cover with shallow, tabular root systems in early Pennington soil development, to dense, deeply penetrating root systems suggestive of arborescent floral

associations at the top of the succession approaching the Mississippian-Pennsylvanian boundary. This study provides greater resolution of changing climate and pedogenic processes than what is provided in previous studies of Late Mississippian climate, and suggests that the documented variability in paleosol types and soil drainage might represent the record of high-frequency climate changes likely associated with expansion and contraction of the paleo-Intertropical Convergence Zone (ITCZ).

Introduction

Late Mississippian climate change in the Appalachian Basin region was interpreted by Cecil (1990) as being relatively dry throughout the Meramecian and into the early Chesterian. By late Chesterian time, however, the paleoclimate became more seasonal, with increased annual rainfall and punctuated periods of humidity and aridity (Cecil, 1990). Various other workers have proposed late Mississippian climate interpretations from continental deposits of alternating periods of aridity and humidity. (Caudill et. al., 1996; Greb and Caudill, 1998; Mora and Driese, 1999; Driese et al., 2000, 2005). Miller and Eriksson (1999) added greater resolution to the Cecil (1990) climate model for the Mississippian by proposing a monsoon-climate forcing of Mississippian sedimentation. This new 'monsoon model', invoking transient wet conditions, was questioned by Beuthin and Bascombe (2002), who suggested that the model should be further investigated.

Paleosols of the Paleozoic and Mesozoic have proven to be a valuable tool in the interpretation of paleoclimate and paleoenvironments utilizing micromorphology (McCarthy et al., 1998; Mora and Driese, 1999; McCarthy, 2002; Driese et al., 2004; Driese and Ober, 2005) and geochemistry (Driese, et al., 2000; Sheldon et al., 2002).

Thin section micromorphology is a valuable technique for the study of paleosols (Retallack and Wright, 1990; Kemp, 1999) where features such as clay coatings, concretions, etc., are useful in paleoenvironmental interpretation (Kemp, 1999) by providing genetic, temporal, and spatial information on soil-forming processes as influenced by the environment of pedogenesis (McCarthy et al., 1998). Bulk geochemical analysis can provide proxies for soil processes (Retallack, 2001) and paleoprecipitation (Sheldon et al., 2002), as well as an understanding of the flux of elements added or removed throughout the soil profile (Chadwick et al., 1990; Driese et al., 2000) using mass-balance. There is evidence that the bulk geochemistry of paleosols remains largely unaltered despite the effects of diagenesis (Driese et al., 2000, 2005; Sheldon et al., 2002; Driese, 2004). In addition to micromorphology and bulk geochemistry we employ clay mineralogy to interpret the magnitude of weathering (Moore and Reynolds, 1997), because weathering intensity can, in turn, be used to interpret paleoclimate.

We therefore hypothesize that: (1) the Late Mississippian (Chesterian) in the southern Appalachian region was characterized by overall more arid to semi-arid conditions than the earliest Pennsylvanian, (2) that the evidence for overprinting by dry and wet soil features in the Pennington paleosols indicates effects associated with high-frequency, and seasonal wet/dry conditions, and (3) that seasonal migration of a paleo-Intertropical Convergence Zone (ITCZ), similar to what occurs in tropical regions today, also operated during the latest Mississippian. In what follows, we utilize field, micromorphological and geochemical study of 40 paleosols spanning latest Chesterian

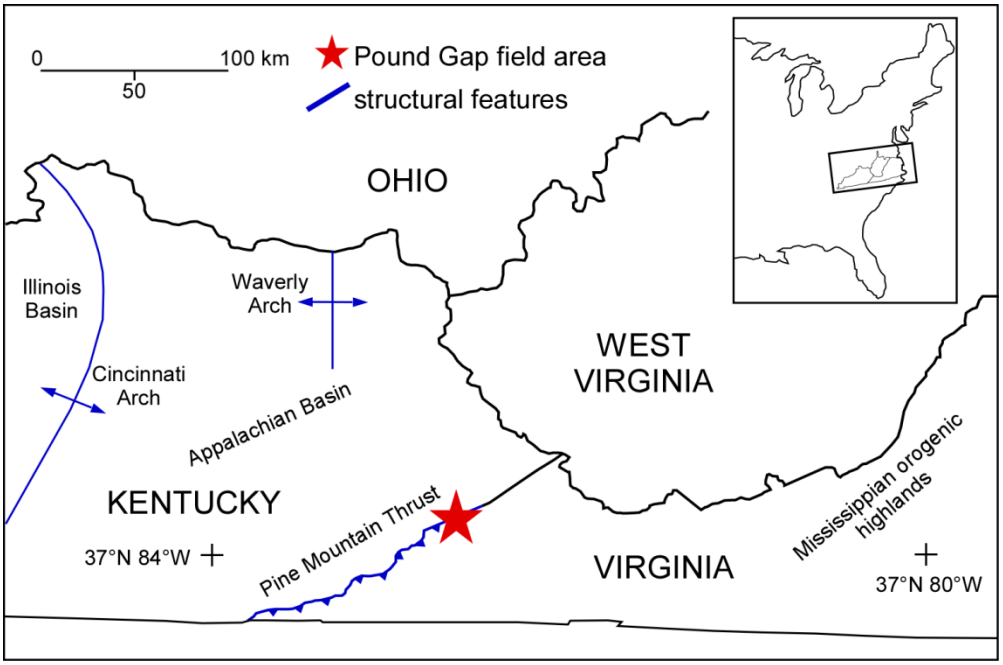

Figure 2.1 Location map for Pound Gap study area in the southeastern USA (adapted from Al-Tawil et al., 2003) showing important late Mississippian paleogeographic features. Star denotes the study are location.

time in an attempt to refine interpretations of Late Mississippian climate change in the southern Appalachian region.

Geologic Setting and Burial History

The study area is located on the Kentucky–Virginia border, along US Highway 58 near the town of Pound, Virginia in southeastern USA (Fig. 2.1). Structural features active during latest Chesterian (Late Mississippian) time influencing the distal foreland (the location of the Pound Gap section) include the Cincinnati Arch to the west, the Waverly Arch to the north-northwest (Woodward, 1961) and the Pine Mountain thrust to the east. The Cincinnati arch was only mildly active until late Chesterian time (Sable and Dever, 1990) when uplift of source areas of terrigenous sediments to the east and southeast of the Appalachian basin occurred (de Witt and McGrew, 1979). Unlike the

Cincinnati Arch, the Waverly Arch does not seem to have exerted much control on sedimentation (Sable and Dever, 1990) in the study area. Structural deformation in the southern Appalachian region culminated with transport along the Pine Mountain thrust during the Late Pennsylvanian (Mitra, 1988; Andrews and Nelson, 1998).

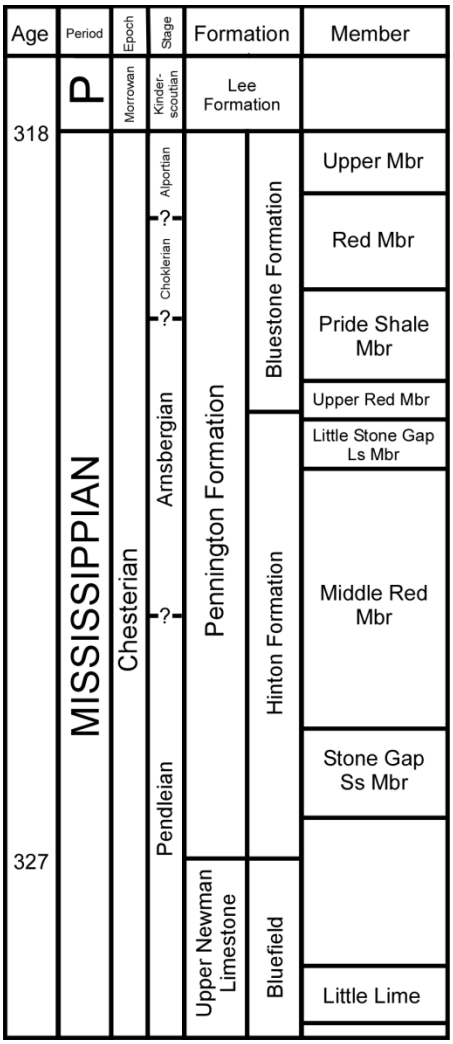

Figure 2.2 Stratigraphic nomenclature (adapted from Chesnut et al., 1998; Beuthin and Bascombe, 2004) and age assignments for upper Mississippian strata at Pound Gap, Kentucky (Al-Tawil and Read, 2003; ICS, 2004).

Over 500 m of Mississippian strata are exposed and are sharply overlain by the fluvial-dominated facies of the Pennsylvanian Lee Formation and Breathitt Group (Greb and Chestnut, 1996) (Fig. 2.2); the Mississippian-Pennsylvanian systemic boundary in this region is marked by a widespread unconformity (Chesnut, 1992). The Pennington Fm. represents the transition between open-marine depositional environments of the Newman Limestone, and the terrestrial coal swamps and fluvially dominated environments of the Pennsylvanian Breathitt Group (Greb and Eble, 1998). Pennington strata record substantial changes in base level, with punctuated and often prolonged periods of subaerial exposure resulting in soil development.

The burial history of the study area is not certain. Estimates of overburden range from 0.74 km (Harris, 1978) to 2.13 km (McKee et al., 1976). Secondary fluid inclusions in ferroan calcite cements in the underlying Newman Limestone indicate temperatures no greater than 150°C that were within a broad range, varying between 60-150°C (Niemann and Read, 1988). Vitrinite reflectance data from deeply buried Pennsylvanian strata away from the Cincinnati Arch (Fig. 2.1) suggest that burial temperatures exceeded 50°C for time intervals of up to 50 Ma (Castano and Sparks, 1974, Hower et al., 1983).

Mississippian Paleogeography and Age Constraints

During Mississippian time, eastern Kentucky was located between 5° and 10° S latitude (Ziegler et al., 1979), drifting northward into the dry latitudes (Cecil, 1990) near the boundary of the paleo-wet equatorial belt and the paleo-dry trade-wind belt (Ettensohn et al., 1988). With changing seasons, the moist and dry belts would alternately migrate toward the equator or South Pole (Strahler and Strahler, 1973) thereby forcing alternating moist and semi-arid conditions (Ettensohn et al., 1988).

Conodont biozonation indicates that the Pennington paleosols developed during the Late Chesterian stage (Fig. 2.2) (Collinson et al., 1971; Dutro, et al., 1979; Al-Tawil and Read, 2003). Miller and Eriksson (1999) report a 7.0 myr duration of deposition for the time-equivalent Hinton and Bluestone Formations (Ettensohn and Chestnut, 1998) of southern WestVirginia containing similar paleosols. Al-Tawil and Read (2003) reported an age date of 327 Ma (condont biostratigraphy Collinson et al., 1971) for the top of the Newman Limestone at Pound Gap. Given the reported Mississippian-Pennsylvanian boundary date of 318.1 Ma (International Commission on Stratigraphy, 2005), Pennington deposition might represent as much as 8.9 myr.

Methods

Field Sampling and Laboratory Analysis

Forty paleosols within the Pennington Formation were identified and logged following standards and procedures of the Soil Survey Staff (1998). Paleosol description commenced at the gradational contact between the Newman Limestone and Pennington Formation (Fig. 2.3) at Pound Gap (Nelson and Read, 1990). The stratigraphically lowest paleosol described overlies a marine brachiopod packstone identified as near the top of the Newman Limestone. Paleosols were described up to the Mississippian-Pennsylvanian boundary. Careful attention was paid to documenting pedogenic features such as redox depletions and concentrations, pedal structure, depth to Bk horizons, root traces, slickenside development and soil matrix colors. Rooting depth was determined by the deepest evidence of rhizoliths, rhizocretions, and/or drab halos. The abundance of rooting was determined by a visual percentage estimation of each soil horizon, similar to

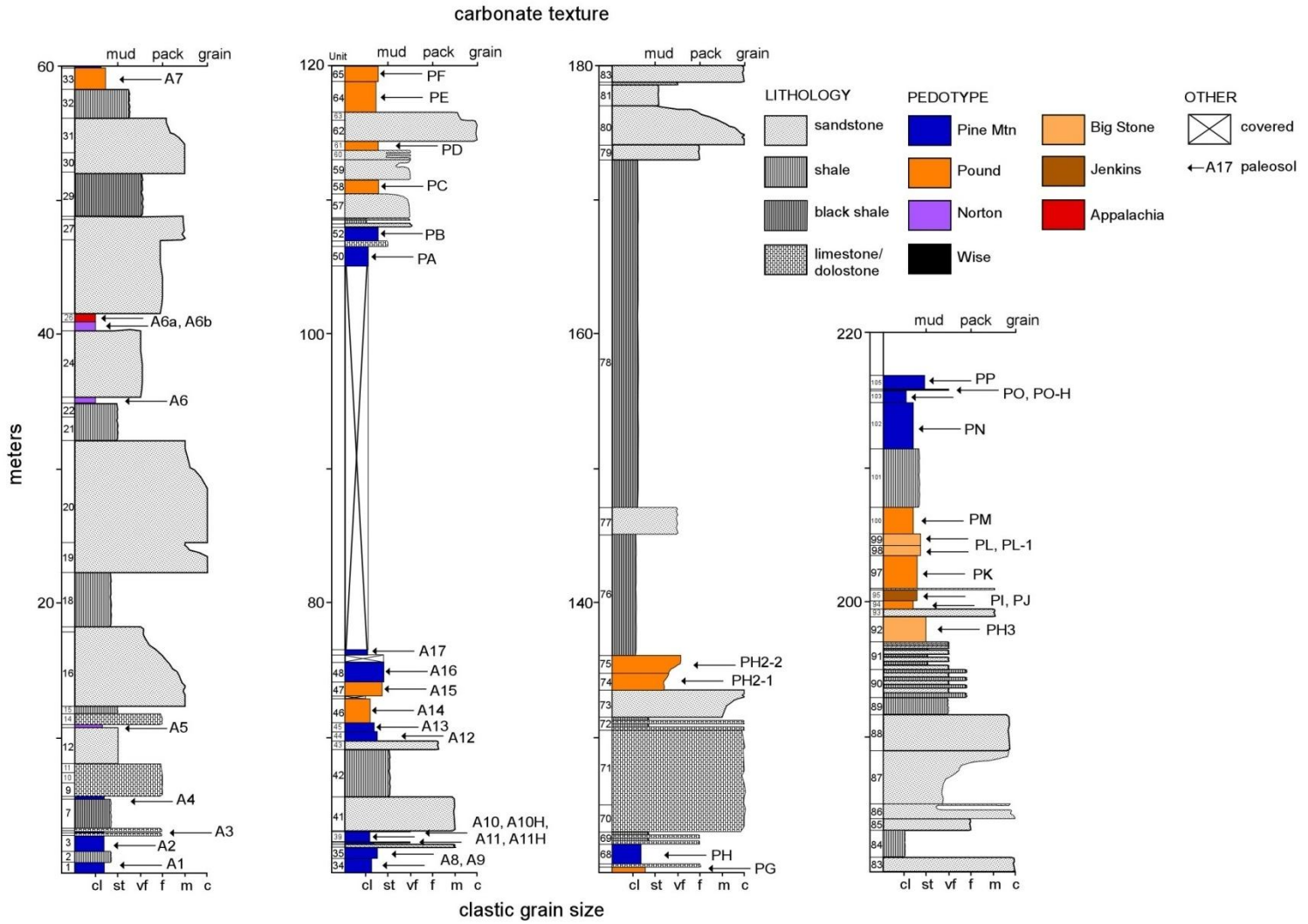

Figure 2.3 Pennington Fm. outcrop section with annotated described paleosols.

Table 2.1 Summary of description of field attributes of Pennington Fm. pedotypes at Pound Gap outcrop. Textural Class: f=fine, m=medium, c=coarse; Pedal Structure: abk=angular blocky, sbk=subangular blocky; w=wedge, pl=platey.

Pedotype description from field observation

Pedotype	Horizon	Depth	Texture	Color	Structure class/type	Rooting Abundance	Redox Color	Illuviation clay coatings	Carbonate nodules	Other	Soil Order
A. Pine Mtn	Bssg1	0-43	silty clay	3/5GY	m/w	common few	7.5YR4/6	few	-	pyrite	Vertisol
	Bssg2	43-74	silty clay	3/10GY	f/w	common few	5YR3/4	few	-		
	C	74-86	sandstone	gleyed	-	- -	-	-	-	laminated	
B. Pound	Btg1	0-5	clay	5/10Y	f/abk	few few	2.5Y6/6	few	-		Vertisol
	Btg2	5-20	clay	4/10Y	f/sbk	common common	2.5YR4/3	common	-		
	Bssg	20-65	silty clay	5/10G	c/w	few common	5/10G; 2.5YR4/6	few	-		
	Bss	65-100	silty clay	10R4/2	c/w	few few	7.5YR5/8	few			
	Bssk	100-200	silty clay	7.5R4/2	c/w	few few	5/10BG	-	common		
	Bk	200-244	silty clay	6/5G	f/sbk	- -		-	-		
C. Wise	O	0-7	coal	2.5/N	m/pl	abundant many	7.5YR5/8	-	-	pyrite	Histosol
D. Norton	Bg	0-17	silty clay	3/10Y	f/sbk-w	- -		-	-		Inceptisol
	B/C	17-26	silty clay	2.5/5GY	f/pl	- few	5YR4/6	few	-	laminated	
E. Big Stone	B/C	0-250	silty clay	3/5GY	m/pl	many common	10YR3/2	-	-	laminated	Entisol
F. Jenkins	Btg	0-16	silty clay	4/5GY	m/sbk	many common	2.5YR4/3; 7/5YR5/8	common	-		Alfisol
	Btg2	16-34	silty clay	4/10G	m/sbk	few few	7.5YR5/8	few	-		
	Btg3	34-57	silty clay	4/5GY	m/sbk	few few	4/5GY	many	few		
	BC	57-80	siltstone	4/10Y	m/pl	few few	5YR4/4	few	-		
G. Appalachia	Bo	0-15	sandy clay	7.5YR8/1	none	abundant many	2.5YR4/3; 2.5YR5/3	-	-	leaching	Oxisol
	Bts	15-66	sandy clay	7.5YR8/1	c/sbk	many common	2.5YR4/3	-	-		

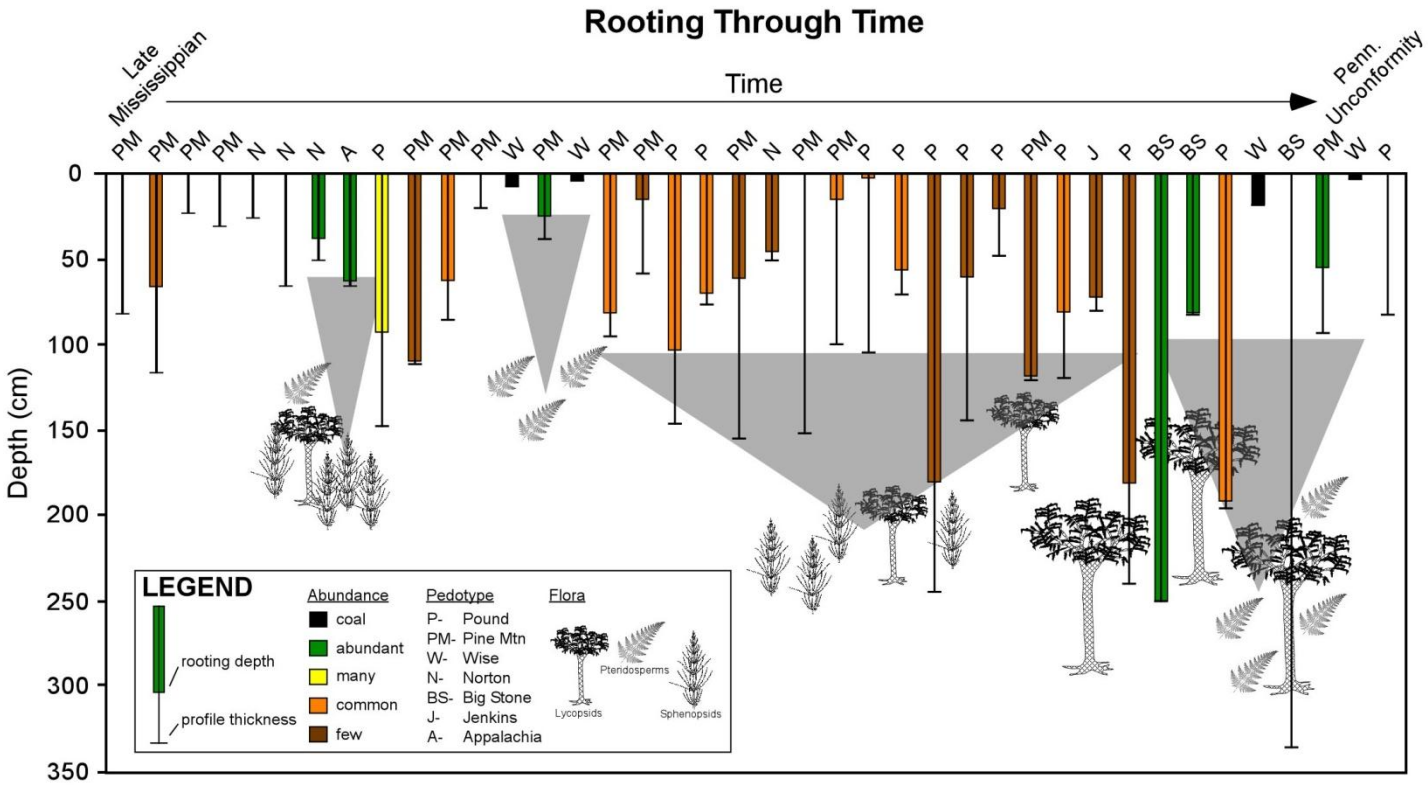

Figure 2.4 Rooting through time measure from root traces in Late Mississippian Pennington Fm. paleosols at Pound Gap, showing general transitions from smaller, shallower vegetation associations to canopy forest associations through time. Gray triangular zones represent similar floral associations and soil drainage. Floral associations are inferred from Crow and Hellquist (2000), Dunn et al. (2003), and Dunn (2004).

the description method of soil scientists, i.e., few (0-2%), common (2-20%), many (>20%). Rooting greater than 50% was given an 'abundant' descriptor (Table 2.1). Each paleosol profile was then assigned an overall rooting abundance based upon the horizon with the highest percentage of rooting (Fig. 2.4).

Bulk paleosol samples of about 200 g were collected at 10 cm intervals for geochemical and clay mineral analyses. Thin-section samples were also collected from representative paleosol profiles and horizons. All thin-section samples were dried, epoxy

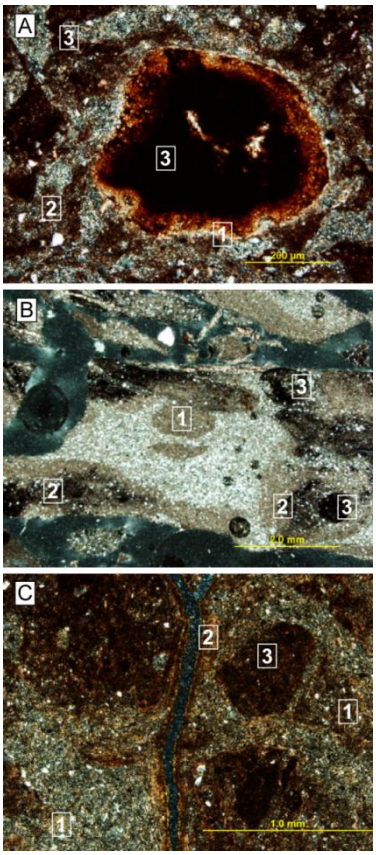

Figure 2.5 Mapping and sequencing of soil drainage features in thin-section photomicrographs using the methods of PiPujhol and Buurman, 1994. Stages of drainage are numbered from 1 to 3, oldest to youngest respectively. (A) from Paleosol E, Pound pedotype, (B) from Paleosol A, Pine Mtn. pedotype, and (C) from Paleosol A-12, Pound Pedotype.

impregnated, and commercially prepared. Micromorphological descriptions follow the nomenclature of Brewer (1976), Fitzpatrick (1993), and Stoops (2003). To better interpret the relative timing of changing soil drainage, soil features (Fe-coatings, intercalations, nodules etc.) were mapped and sequenced in thin-section photomicrographs (Fig. 2.5) according to the methods of PiPujol and Buurman (1994) for paleosols having evidence of seasonality.

Geochemical Proxies and Mass Balance Reconstruction

Soil-forming processes can be approximated using molecular ratios as indicators of the soil-forming environment (Retallack, 2001; Sheldon et al., 2002). Major, minor, and trace elements were measured commercially using ICP-MS, where samples are dried and pulverized followed by meta-borate fusion and total acid digestion (HF, HNO_3, and $HClO_4$). Data (Appendix) are reported in terms of element weight percent and/or ppm. Elemental percentages were converted to oxide weight percents. Oxide weight percents were normalized to their molecular weight and inserted into the following molecular ratios as proxies of soil-forming processes: lessivage (Al_2O_3/SiO_2); calcification ($CaO + MgO/ Al_2O_3$); base loss/lixivation ($Al_2O_3/CaO + MgO + K_2O + Na_2O$); salinization ($Na_2O/K_2O$) and leaching (Ba/Sr). The oxide percent SiO_2 was determined by a summation of all reported cations and subtracting the sum from 100% (assuming negligible loss on ignition due to low carbonate concentrations). Soil-forming process calculations for each profile were averaged and reported in this study. Oxide weight percentages were also utilized in estimating mean annual precipitation using the CIA-K (chemical index of alteration minus potash) paleoprecipitation proxy developed by

Sheldon et al. (2002). As with the soil-forming process calculations, paleoprecipitation calculations were averaged on a profile-by-profile basis and thus only averaged values are reported.

The bulk geochemical data for major elements were evaluated using a mass-balance approach, following the methodologies advanced by Chadwick et al. (1990). Parent material for each paleosol was determined by the least weathered material exhibiting primary sedimentary bedding features, commonly characterized as either a C or B/C horizon. Bulk density was measured using the paraffin-clod method of Blake and Hartge (1986). Confident parent material (C-horizon) was not associated with the Big Stone pedotype, and therefore a bulk density value was acquired from the parent material of a correlative Pennington paleosol at Sparta, TN (Robinson, 2002) to calculate strain and tau values for major cations. Calculations of strain and "transport function" values, with reference to Ti, for major cations follow the equations and methods of Driese et al. (2000).

X-Ray Diffraction Analysis

Four representative paleosol profiles were chosen for X-ray diffraction (XRD) analysis (Pine Mtn, Pound, Big Stone, and Appalachia pedotypes). The clay fraction was removed from each sample using standard centrifugation methods. To optimize diffraction peaks for kaolinite and smectite, the samples were then saturated with 10% KCl and MgCl (Moore and Reynolds, 1997), mounted on glass slides using Drever's Millipore method (1973), and glycolated for two days. The samples were then analyzed using a Siemens D5000 XRD with CuKα radiation and a step of 0.03° 2θ/min. When

kaolinite and illite peak intensities could not be confidently interpreted, samples were dried overnight at 90°C and analyzed as randomly-oriented powdered mounts. In addition, to differentiate between kaolinite and chlorite, samples were heat-treated to 550°C for 1hr and immediately measured to prevent the sample from absorbing atmospheric moisture.

Results

Pedotypes

Forty identified paleosols are organized into pedotypes following the methodology of Retallack (1998), reported in Table 2.1 and placed in stratigraphic context in Figure 2.3. Each pedotype (Fig. 2.6, Table 2.1) is based on one representative "type" profile that sufficiently captures characteristic morphologies and attributes distinguishing the pedotype from all other paleosols of other pedotypes. The name is simply descriptive, referring to geographic localities in the vicinity of the Pound Gap, VA field area. Pedotypes are described in the order of their decreasing relative abundance in the stratigraphic section.

Pine Mtn Pedotype. Sixteen of the 40 paleosols belong to the Pine Mtn (PM) pedotype, a Vertisol, with claystone to silty-claystone texture (Table 2.1). It commonly has slickensides (Bss), low chroma colors (Bg) and lacks a Bk horizon. Drab haloed root traces and Fe-Mn mottling are common (Fig. 2.6A, Table 2.1). Pine Mtn paleosols lie directly beneath Wise paleosols (Fig. 2.6C, Table 2.1). Rhizocretions of the Pine Mtn paleosols (as well as Pound and Jenkins pedotypes) exhibit overprinting of

redoximorphic features. Rhizocretions have a reduced interior with an oxidized sheath or exterior, followed by another band of reduced colors (Fig. 2.6J). Without preserved A-horizons we assume erosional truncation of the Pine Mtn paleosols. Pine Mtn paleosol thicknesses are thinner than those of the Pound, Jenkins, and Norton pedotypes (Table 2.1).

Pound Pedotype. The Pound (PD) and Pine Mtn (PM) pedotypes are similar in that they are both classified as Vertisols. Pound paleosols (eleven) are identified based upon the presence of Bss and Bk horizons (Fig. 2.6B). A Bt horizon is assigned when slickensides are not well-developed and clay skins are apparent. A-horizons are rarely preserved. Pedogenic slickensides are well-developed, and wedge pedal structure dominates. Calcium carbonate is concentrated in nodules and rhizocretions. The development of a Bk horizon can range from a Stage 2 to a Stage 4 (Retallack, 2001). Stage 4 carbonate nodules have multiple stages of growth. The nodules can be fused together forming a calcrete horizon (sensu Wright and Tucker, 1991). Between carbonate nodules the paleosol matrix is reduced with low chroma colors. Pseudo-anticlines are common and calcium carbonate occurs concentrated along the sinusoidal "boundary" of such pseudo-anticlines (cf. Fig. 2.6H).

Wise Pedotype. The Wise pedotype, comprising four paleosols, is easily identified in the field as a coal seam overlying paleosols of the Pine Mtn pedotype (Fig.

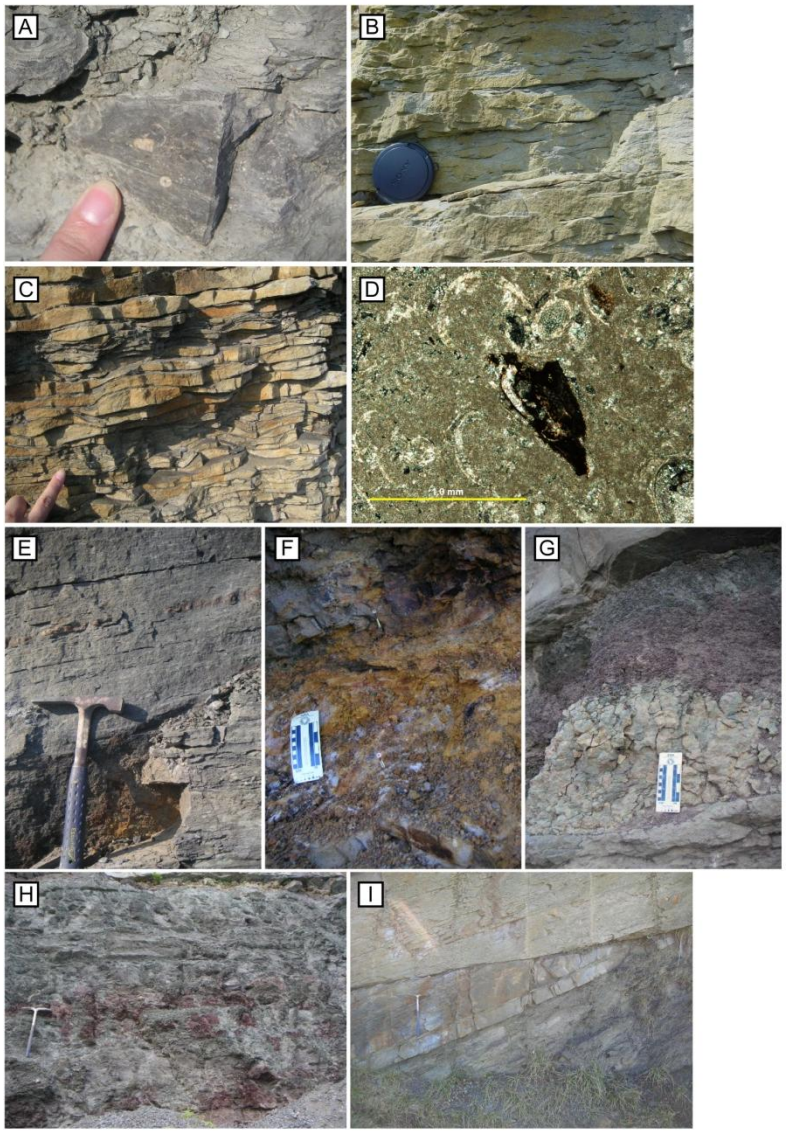

Figure 2.6 Field photos of the Pennington Formation: (A) Unit 73 - grainstone with crinoids, brachiopods and bryzoans, "Little Stone Gap"; (B) Unit 86 - representative flaser bedding formed in a tidal environment; (C) Unit 84 - tidal bundles; (D) Unit 68 - estuarine limestone (in thin-section) with ostracodes, replaced mollusk fragments and potential fish bone fragment; (E) Unit 79 - weathered outcrop photo of black, fissile shale and bedded, nodular siderite; (F) Unit 42 - Appalachia Pedotype, an Oxisol. Note the leached coloring and preserved carbonaceous material; (G) Unit 62 - Pound Pedotype, a well-drained Vertisol with a well-developed Bk (carbonate-rich) horizon; (H) Unit 99 - Big Stone Pedotype, an Entisol, showing deep taproot systems, some filled with calcium carbonate; (I) Units 28-29 - truncation of planar-tabular cross-bedded sandstone units in Unit 29.

2.6C), and in one instance a Pound paleosol (Table 2.1). Decompacted (Retallack and Sheldon, 2001) coal seams thicknesses of the Wise paleosols range from 41-247 cm. These organic-rich "horizons" are classified as Histosols. Pyrite is present in two of the four identified Histosols.

Norton and Big Stone Pedotypes. Norton (NORT) and Big Stone (BS) paleosols are weakly-developed paleosols with little to no horizon development, and are equivalent to modern Inceptisols and Entisols, respectively (Fig. 2.6D, E). The Norton pedotype includes four paleosols and the Big Stone pedotype three paleosols. B/C horizons are weakly laminated with platy pedal structure. Evidence of rooting ranges from 1-2 cm primary roots to deeply penetrating, bifurcating rhizoliths and rhizocretions extending over 2.0 m in length (Table 2.1). Reduction zones, drab halos, and mottling are also common.

Jenkins Pedotype. The Jenkins pedotype includes only one of the 40 paleosols observed in the Pennington Fm, and is classified as an Alfisol (Fig. 2.6F). Characteristic of an Alfisol is a well-developed Bt horizon (Table 2.1). In the Jenkins profile, all horizons (with the exception of the BC horizon) are classified as Bt horizons with observable clay coatings in the field. Low chroma horizons and mottling are also present. Although Bk horizons are not identified, occasional rhizocretions occur in the Btg3 horizon.

Appalachia Pedotype. One paleosol is assigned to this pedotype and is significantly different from all other identified paleosols (Fig. 2.6G). The Appalachia

Pedotype is identified by a Bo (oxic) horizon, and is highly leached and clay-rich (Fig. 2.6I, Table 2.1), suggesting the development of an Oxisol. Pedal development is non-existent, with a sandy clay texture. Red and purple mottling is prominent throughout the Bo horizon. Rooting is abundant, typified by in-situ root traces and casts in growth position. Plant remains (near charcoal) range from 3-20 cm long, and 0.5-6 mm in diameter.

Rooting Through Time

The Pennington Formation paleosols record changing floral associations through time (Fig. 2.4). Lower Pennington paleosols have few primary root traces with lengths greater than 2-4 cm. Progressing upsection, root traces penetrate more deeply and become more abundant within paleosols, to the extent that organic C content is enough to form coals. Coals occur mainly within the middle of the Pennington section. Above the interval of coal deposition, root traces in paleosols are sparse, with shallow depths of penetration. Root traces in the stratigraphically highest Pennington Fm. paleosols are denser, with deeper penetration. Just beneath the coals at the Pennsylvanian-Mississippian unconformity, root traces in an Entisol (Big Stone) include numerous bifurcating, 5-10 cm diameter traces that penetrate the paleosol to depths of 1.5 m or more.

Table 2.2 Summary of micromorphologic observations for Pennington paleosols. Color: lgg=light blue gray, gg=green gray, gb=gray blue, b=blue, bg=blue green, drb=dark reddish brown, rb=reddish brown, lyg=light yellowish gray; Nodule morphology: am=ambiodal, t=typic, c=concentric, mo=mottles, s=strongly impregnated, m=moderately impregnated, w=weakly impregnated; Rooting: ND=cannot be discerned. Thin section mircographs of Pennington Fm paleosols are presented in Figure 2.7.

Micromorphologic description

Profile	Pedotype	Horizon	Texture	Color	Matrix	Coatings			Nodules			Rooting	Other
						Type	Abundance	Morphology	Type	Abundance	Morphology		
A1	PM	Bssg	clay	lgg	sepic	-	-	-	Fe	few	c/m	common	pyrite
A2	PM	Bg	silty clay	log	bimasepic	clay	few	coating	Fe	many	t/s	many	fish bone
						Fe	few	coating					altered allochems
A2	PM	Bss2	clay	b	masepic	-	-	-	Fe	few	t/m	-	mollusc
													brachiopod
A3	PM	Bss	silty clay	lg	bimasepic	clay	few	coating	Fe	common	mo/w	few	fish bone
									Ca		ma		
A4	PM	Bss	silt loam	log	skelsepic	-	-	-	Fe	many	am/s	common	burrows
A6	NORT	Bss/BC	silty clay loam	lbg	skelsepic	clay	few	banded coatings	Fe	few	am/s	common	clay illuviation
					bimasepic	Fe	common	coatings					
					masepic								
A7	PD	Bsskg	silty clay	rb	bimasepic	Fe	many	coatings	Ca	many	t	few	Fe staining
						clay	few	coating/w	Ca	common	gla		
A7	PD	Bssg1	silty clay	lgg	bimasepic	clay	few	coatings	Ca	many	t	few	few
						Fe	few	coatings	Ca	common	gla		
									Fe	common	am, mo/s		
A8	PM	Bssg	silty clay	lbg	masepic	clay	common	coatings	Fe	common	t,am/s	common	pedorelict
A8	PM	Bg	silty clay	lgg	masepic	Fe	few-common	coatings	Ca	common	t	-	-
									Ca	common	gla		
A9	PM	Bssg	silty clay	lbg	skelsepic	-	-	-	Fe	common	am/s	-	Fe-intercalations
					masepic								
A10-O	WISE	O	coal	b	-	-	-	-	-	-	-	many	Ca-cement
A12	PM	Bssg1	clay	lyg	masepic	Fe	common	coatings	Fe	few	t,am/s,m	-	Fe staining
A12	PM	Bssg2	clay	lyg	bimasepic	clay	common	coatings	Fe	common	t/s,m	-	Fe staining
						Fe	common	banded coatings					Fe-intercalations
													clay illuviation
A13	PM	Bss	silty clay	lyg	masepic	clay	common	coatings	Fe	common	t/s	few	Fe staining
					skelsepic	Fe	few	coatings					
A14	PD	Bssk	silty clay	lyg	masepic	clay	few	coatings	Fe	common	t/s,m	common	ostracode
					bimasepic								Fe staining
A15	PD	Bss2	clay	lyg	bimasepic	clay	few	coatings	Fe	few	t/s	common	Fe staining
					masepic								
A15	PD	Bss1	silty clay	lyg	masepic	clay	few	coatings	Fe	few	t/s	few	Fe stained clay
A16	PM	Bssg2	silty clay	lbg	masepic	clay	few	coatings	Fe	few	t,am/s,w	few	-
A16	PM	Bssg1	silty clay	lbg	masepic	-	-	-	Fe	few	am/s	few	

Table 2.2 cont. Summary of micromorphologic observations

Micromorphologic description cont.

Profile	Pedotype	Horizon	Texture	Color	Matrix	Coatings			Nodules			Rooting	Other
						Type	Abundance	Morphology	Type	Abundance	Morphology		
A17	PM	Bss	silty clay	lbg	bimasepic	clay	common	coatings	Fe	common	t/m	common	plant preservation
					maspic	Fe	common	hypocoatings					
PAL-A	PM	C	silty clay	lgg	asepic	-	-	-	Fe	few	t, mot/m	-	Ca-cement
PAL-A	PM	Btg	silty clay	lgg	asepic	clay	few	coatings	Fe	many	am/m	common	fish bone
						Fe	few	coatings					pollen
PAL-A	PM	Bssg	silty clay	lgg	masepic	clay	few	coatings	Fe	many	am/s	many	fish bone
					bimasepic	Fe	few	coatings					pollen
													pyrite
PAL-B	PM	C	clay	gg	asepic	-	-	-	Fe	few	t/s	-	laminated
PAL-B	PM	Bssg1	clay	lgg	asepic	-	-	-	Ca	few	am	few	mollusc
													pyrite
PAL-B	PM	A	silty clay	lbg	masepic	-	-	-	Fe	many	am/s,m	common	pyrite
													Fe-intercalations
PAL-C	PD	Bss	silty clay	drb	masepic	clay	common	hypocoatings	Fe	many	am/m	common	Fe staining
						Fe	many	coatings					
PAL-D	PD	Bss	silty clay	drb	bimasepic	few	clay	coatings	Fe	few	t/m	common	Fe staining
													pyrite
PAL-E	PD	Bssk	silty clay	lgg	bimasepic	clay	common	coatings	Ca	many	t, gla, sep	common	pyrite
					masepic	Fe	common	coatings	Fe	many	am/s		Fe staining
													Ca-intercalations
PAL-E	PD	Bss	silty clay	lbg	masepic	Fe	common	coatings	Ca	common	t/s	ND	Fe staining
						clay	few	coatings	Fe	many	t/s,m		pyrite
PAL-E	PD	Bssg	silty clay	lgg	asepic	Fe	common	banded coatings	Fe	common	t,am/s,m	common	mollusc
					masepic	Ca	few	coatings	Ca	few	t/m		Fe staining
PAL-H	PM	BC	clay	lgg	asepic	clay	few	coatings	Fe	few	t/s	-	Ca cement
													pyrite
PAL-H	PM	Bk	clay?	lgg	ND	-	-	-	Ca	many	t, gla/s,m	few	Ca cement
PAL-I	PD	BC	silty clay	lgg	bimasepic	Fe	few	coatings	Fe	few	am/m	-	-
					masepic								
PAL-I	PD	Bsskg	silty clay	lbg	masepic	Fe	many	coatings	Fe	few	t/m	few	brachiopod
													Fe staining
													pyrite
PAL-K	PD	Bssk2	silty clay	gb	masepic	clay	few	coatings	Ca	many	t,gla, sep	few	Fe staining
						Fe	many	coatings	Fe	many	c, am/m		Ca cement
PAL-M	PD	Bssg	silty clay	bg	masepic	clay	common	coatings	Ca	few	t/m	ND	
									Fe	few	t, am/s,w		
PAL-N	BS	BC	clay	bg	masepic	-	-	-	Fe	many	am/w	-	laminated
													Fe lenses
PAL-O	PM	Bssg	silty clay	bg	masepic	Fe	few	coatings	Ca	few	t/m	few	Fe intercalations
									Fe	few	t/s		

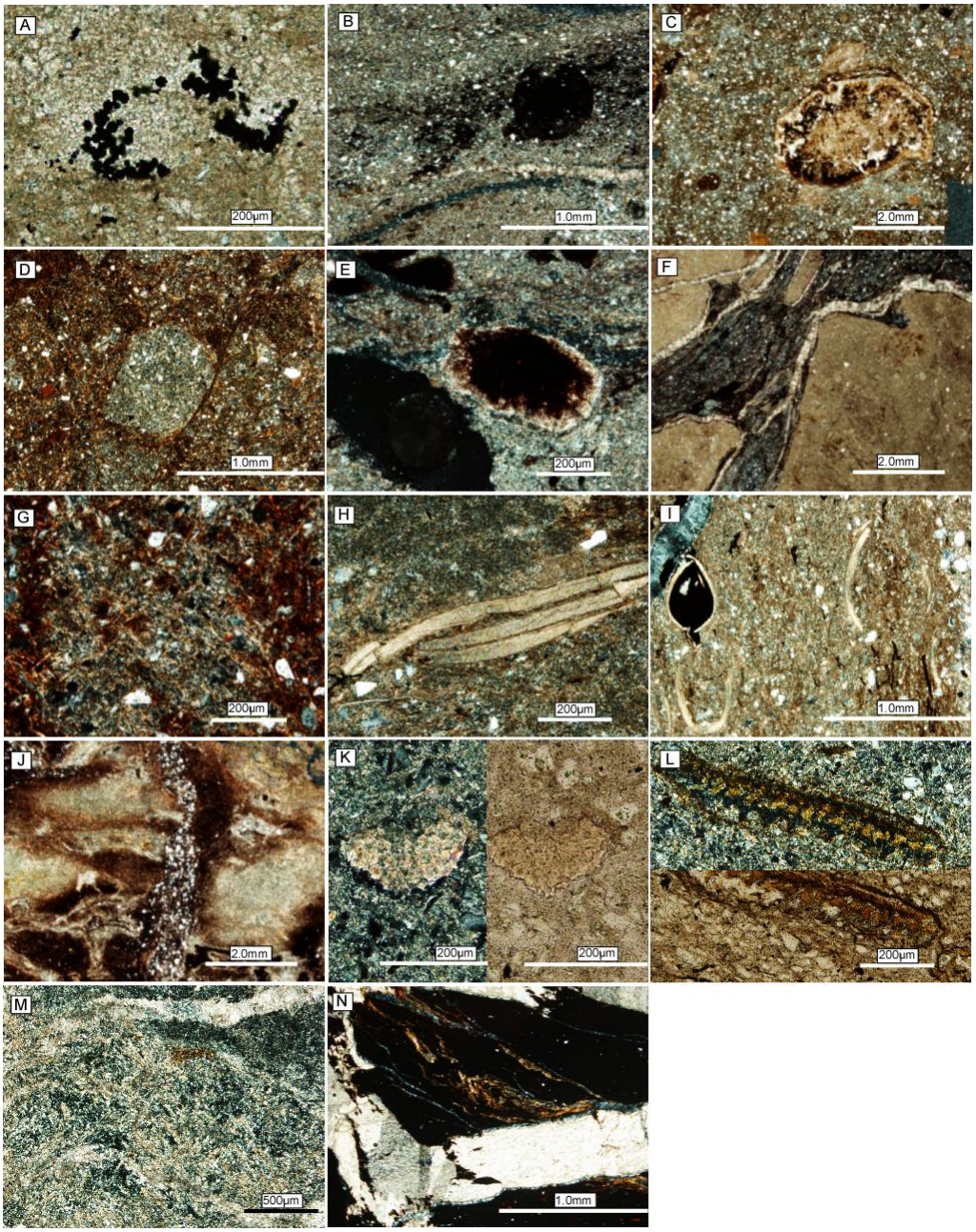

Figure 2.7 Pennington Fm paleosol micromorphology: (A) pyrite formation overprinting sparry calcite, (B) typic, strongly impregnated FeMn nodule, (C) typic micrite nodule overprinted by FeMn, (D) weak clay coat/argillan stained with Fe, (E) a typic micrite nodule by a FeMn strongly impregnated nodule, (F) alternating Fe oxide and calcite coatings, (G) light blue-green matrix overprinted by remobilized Fe (iron-staining), (H) brachiopod valves with sweeping extinction in clayey paleosol soil matrix, (I) ostracodes and mollusks in clay-rich paleosol matrix, (J) silt-filled burrows, (K) palynomorphs in both XPL and PPL light, respectively, (L) plant fragments in both XPL (top) PPL (bottom) light, (M) bimasepic plasma/matrix in a Pine Mtn. paleosol, (N) charcoal with calcite spar intercalation.

Micromorphology

The micromorphology of the Pennington paleosols supplements outcrop and field observations by providing a more detailed history of pedogenic processes (Table 2.2). We limit the discussion of micromorphology to Pound and Pine Mtn pedotypes to provide the most pertinent data to interpret soil drainage and similarly climate. Pyrite (Fig. 2.7A), iron-manganese nodules (Fig. 2.7B), and low-chroma colors are prevalent in Pine Mtn paleosols. Micritic calcium carbonate nodules (Fig. 2.7C) and clay coatings (Fig. 2.7D) are common in Pound paleosols. Clay coatings are neither well-developed nor abundant, within Pound and Pine Mtn paleosols. Overprinting and juxtaposition of redoximorphic features are common for both Pound and Pine Mtn pedotypes. Both calcite nodules and glaebules occur with strongly impregnated concentric iron-manganese nodules (Fig. 2.7E) in the same paleosol horizon. Overprinting is also manifested by alternating successive coatings of iron oxide and calcite (Fig. 2.6F), in addition to oxidized, iron-impregnated matrix in which the original matrix coating was likely bluish-grey (Fig. 2.7G). Mapping of soil features in thin-section photomicrographs suggests at least 3 stages of soil drainage in both Pound and Pine Mtn paleosols (Fig. 2.5).

Evidence of flora and fauna also occurs in thin-section. Fossil fragments of marine brachiopods (Fig. 2.7H), marine mollusk shells, and estuarine or freshwater ostracodes (Fig. 2.7I) occur in the paleosol (Pine Mtn) matrix and voids. Burrows are also apparent (Fig. 2.7J). There is exceptional preservation of macroscopic fossil plant material in Pine Mtn paleosols, and of palynomorphs (Fig. 2.6K) in what appear to be estuarine limestone. Plant material is so well-preserved that cellular structure is still

discernable (Fig. 2.7L). The best-preserved plant material generally occurs in both Pine Mtn and Appalachia paleosols.

Soil texture for all pedotypes varies little, ranging from clay to silty clay. Matrix fabrics are commonly sepic, and Pine Mtn and Pound paleosols characteristically display masepic and bimasepic (Fig. 2.7M) fabrics. Iron-staining (red/orange pigmentation) was a common feature of nearly all Pound paleosols, with common calcite spar cementation. Framboidal pyrite was also observed (although rare) in Pound paleosols. Both Pound and Pine Mtn pedotypes show evidence of multiple episodes of development of redoximorphic features.

Soil Processes and Paleoprecipitation Estimates

Proxy estimates of soil processes and paleoprecipitation vary substantially through time and are summarized in Figure 2.8. Higher base-loss estimates appear to covary (Fig. 2.8A) with higher estimates of paleoprecipitation (Fig. 2.8E). One of the highest MAP estimates (1361 mm/yr) is associated with the Appalachia (an Oxisol) pedotype and also corresponds to extreme base loss relative to the rest of the section (Fig. 2.8A). The lowest rainfall estimate (519 mm/yr) is recorded for a Pine Mtn paleosol (A4), one of the stratigraphically lower Pennington paleosols showing low base-loss. Low base- loss values are associated with Pine Mtn paleosols. CIA-K precipitation estimates were not calculated for Wise paleosols because of their high organic content and very poor drainage, making them unsuitable for this paleoclimate proxy (Sheldon et al., 2002). Trends in leaching and base-loss, for the most part, co-vary up-section and through time (Fig. 2.8A). Very high leaching is associated with high base-loss, and similarly lower leaching ratios correspond to decreased base-loss ratios.

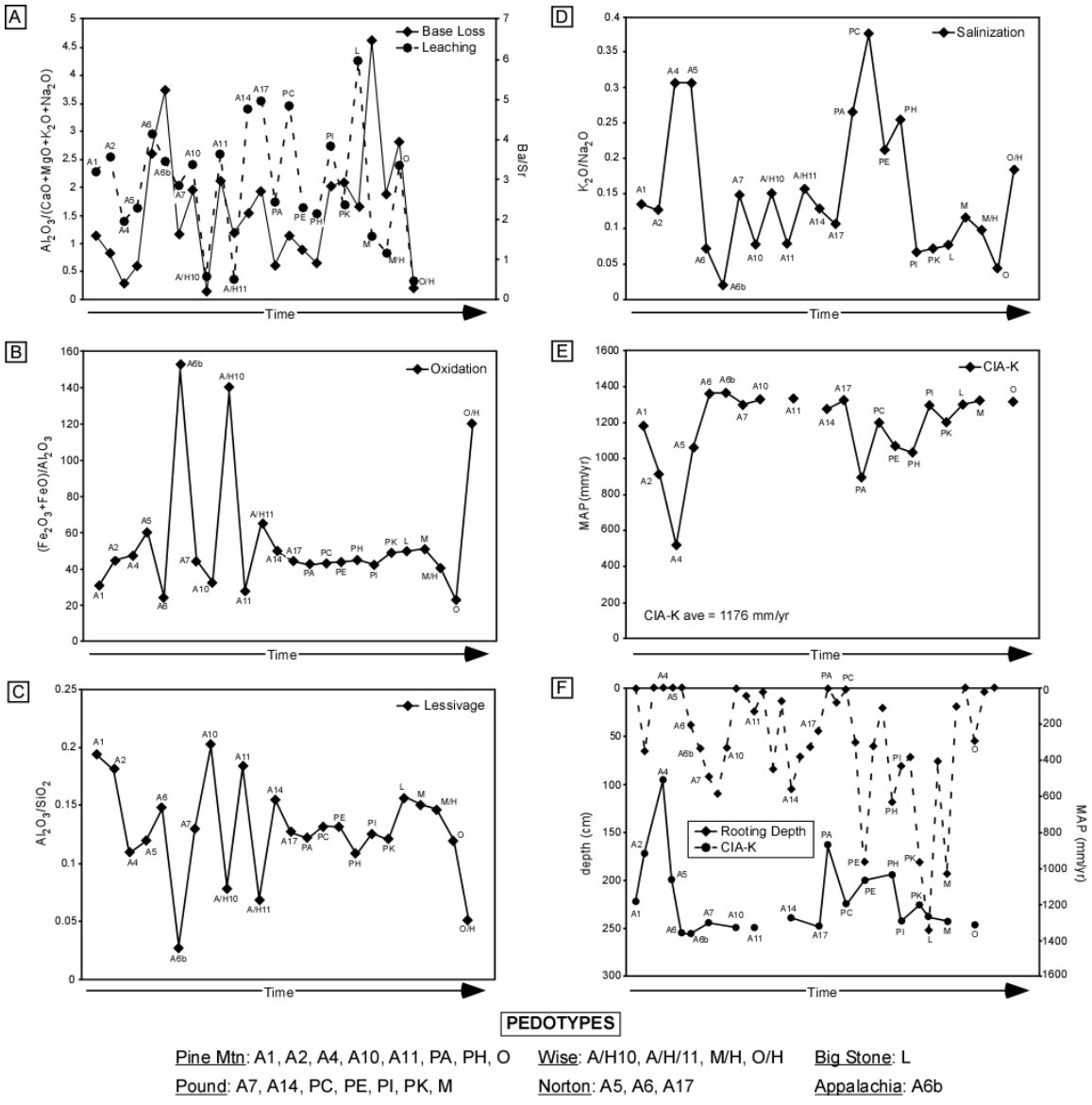

Figure 2.8 Soil process and MAP plots (profile averages) through time for select Pennington Fm paleosols representing pedotypes: (A) base loss and leaching; (B) oxidation; (C) lessivage; (D) salinazation; (E) CIA-K mean annual precipitation (MAP) estimates; and (F) MAP plotted with minimum rooting depth.

High values calculated for oxidation (Fig. 2.8B) and lessivage (Fig. 2.8C) are associated with Histosol (Wise) and Oxisol (Appalachia) formation. Oxidation of the soil profile is greatest for the Appalachia paleosols, and relatively high values are calculated for Wise pedotypes as well. Pine Mtn paleosols tend to be associated with lower oxidation values. Lessivage minimum values were calculated for Wise paleosols, and maximum values are not necessarily distinguishable by pedotype (specifically Pine Mtn and Pound). Calculations for salinization (Fig. 2.8D) do not yield any remarkable trends, except that the minimum value is associated with the Appalachia pedotype.

Mass Balance

Mass-balance calculations (Fig. 2.9) show depth distributions for strain and translocation calculated for representative pedotypes. Major oxide and trace element percentages for each sample analyzed for this study are provided in the Appendix. Paleosol parent material was assessed for its uniformity; Ti and Zr elemental concentrations were also examined throughout the profiles in order to determine the appropriate immobile element to be used in mass-balance calculations. Detrital sediment parent material was likely transported off the newly uplifted Appalachian mountain chain westward through the foothill region and deposited on the alluvial and coastal plains of the region (Craig, et al., 1979). Ti vs. Zr cross-plots (not shown) were calculated for the Pound, Pine Mtn and Appalachia pedotypes yielding r^2values ranging from 0.93-0.99, implying that Zr and Ti concentrations are highly correlated. The Ti vs. Zr cross-plots for the Big Stone pedotype yielded a statistically less significant r^2 value of 0.68, which

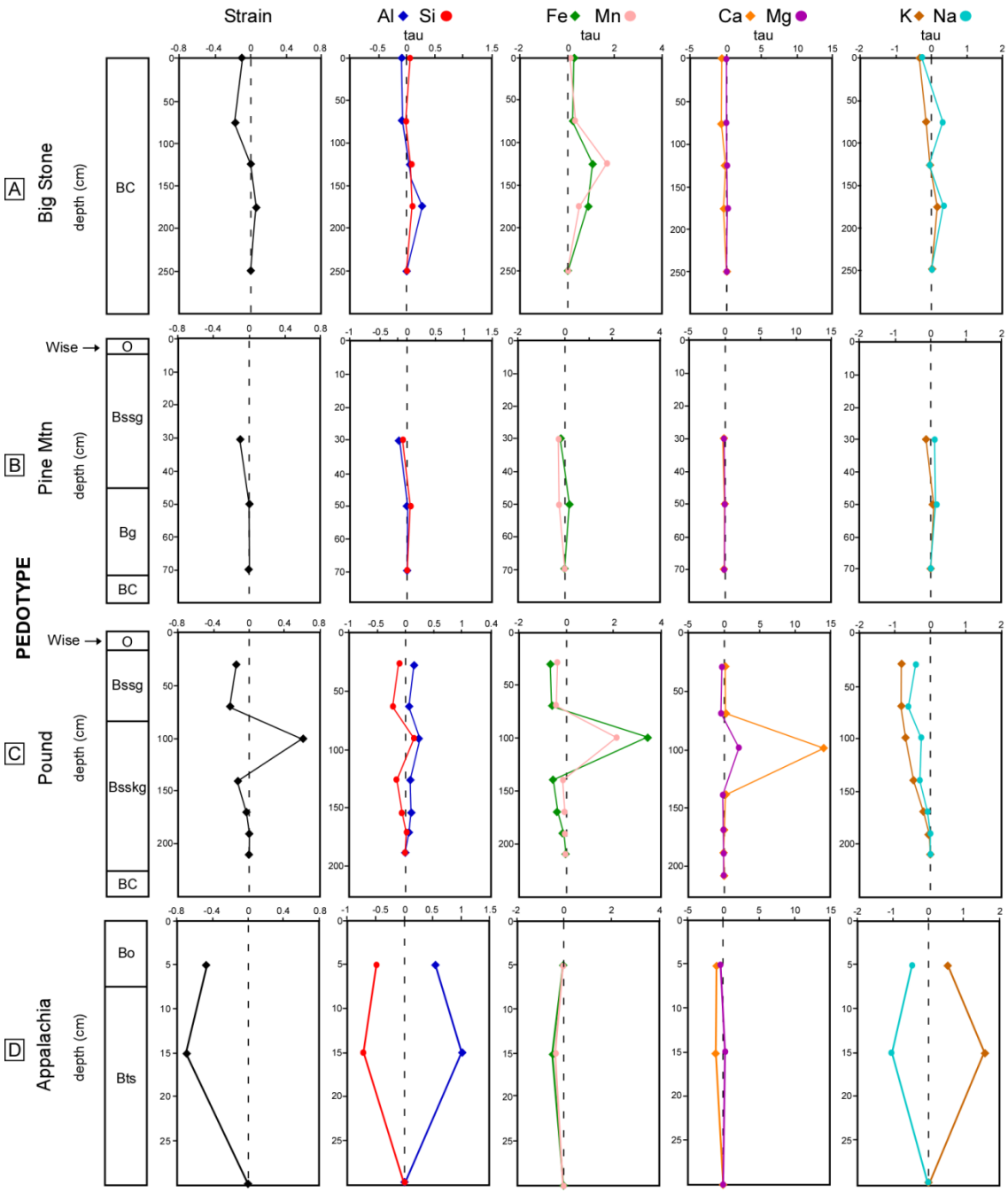

Figure 2.9 Strain (volume change during weathering) and translocation (tau) calculations, assuming immobile Ti during weathering, versus depth for representative pedotypes; (A) Big Stone pedotype; (B) Pine Mtn pedotype (note overlying Wise paleosol); (C) Pound pedotype (note overlying Wise paleosol): (D) Appalachia pedotype.

we might attribute to changing sources of parent material. Ti is used as the immobile index element in mass-balance calculations in this study because the standard deviations of strain with respect to Ti for each pedotype were <30% (Fig. 2.9), thus verifying the assumption of parent material uniformity.

Strain (volume change during weathering) calculations, assuming immobile Ti, show typical patterns for the 4 pedotypes presented in Figure 2.9, namely, volume loss during weathering, except where there are constituents added during pedogenesis (e.g., Bsskg horizon in Pound Pedotype where there is a 50% net gain in volume). Volume decreases generally range from 10-20% in most pedotypes and horizons, with the Pine Mtn pedotype showing the most conservative behavior (< 10% volume loss) and the Appalachia pedotype the least conservative (calculated 70% net loss in Bts horizon) (Fig. 2.9).

The Pine Mtn pedotype generally exhibits negative translocations (net losses) for Al, Si, and other mobile elements in the Bssg horizon, with minor net additions in the Bg horizon (Fig. 2.9B). Conversely, net additions of Al, Si, Fe, Mn, and Ca are calculated for the Bsskg horizon of the Pound pedotype, but with net losses in the Bssg horizon (Fig. 2.9C). Mass-balance calculations for the Appalachia pedotype were significantly different from those of Pine Mtn and Pound pedotypes, with net losses of Si, Fe, Mn, Ca, and Na, and net gains in Al and Mg (Fig. 2.9D). Net gains in Fe and Mn were also observed in the Bo horizon. Big Stone, Pine Mtn and Pound pedotypes all demonstrate net losses of K, whereas the Appalachia pedotype exhibits net gains.

X-Ray Diffraction Analysis

The clay mineralogy of four pedotypes was identified by XRD analysis and is summarized in Figure 2.10. XRD analysis provides an understanding of both the original clay mineralogy of the soil (related to degree of weathering associated with varying climate regimes) as well as the effects of burial diagenesis. The Big Stone pedotype (Fig. 2.10A), compared to the other 3 pedotypes, has the most intense peaks for a mixed illite/smectite clay at a d-spacing of 13.94Å. Kaolinite had stronger intensities at d-spacings of 7.0Å and 3.5Å respectively for glycolated samples. The 500°C heat-treated samples confidently determined the presence of kaolinite (as opposed to Fe-chlorite) by the disappearance of the kaolinite peak observed in the glycolated samples. Illite peaks

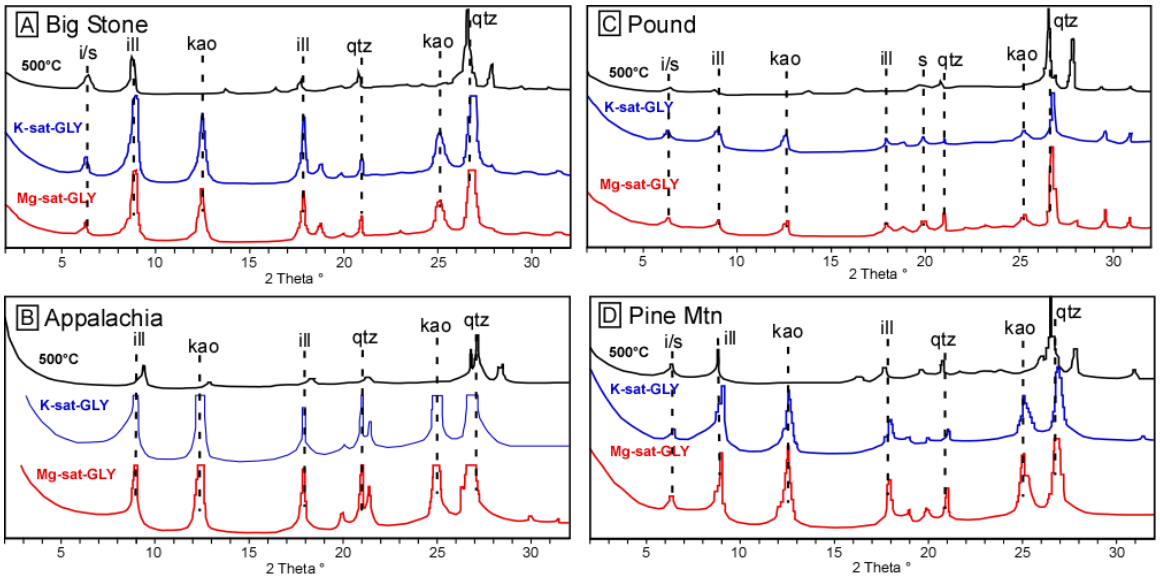

Figure 2.10 XRD clay mineral spectra for clay separates from Pennington pedotypes. All K- and Mg-saturated samples were glycolated for 2 days. The quartz peaks (for all glycolated samples of all pedotypes) at d-spacings of 3.3Å are the result of the glass mount used in XRD analysis. Heating of all samples containing kaolinite collapsed kaolinite peaks. (A) Big Stone paleosol with mixed illite and kaolinite mineralogy, with minor illite/smectite, (B) Appalachia paleosol, with a kaolinite-dominated clay mineralogy, (C) Pound paleosol, with mixed-layer clays, illite, and minor kaolinite, (D) Pine Mtn paleosol and mixed-layer clays, illite, and minor kaolinite.

in the Big Stone pedotype had even greater intensities at d-spacings of 9.90Å and 4.95Å respectively. The 060 scan of the random powdered mount (not shown in Fig. 2.10A) confirmed the presence of illite or a mixed illite/swelling clay assemblage with a d-spacing of 1.50Å. This clay association would suggest that in the pedogenic environment, smectite did once exist, but that there was later burial illitization. Kaolinite could be either depositional and/or pedogenic.

The Appalachia pedotype has a kaolinite-dominated mineralogy (Fig. 2.10B). Very intense kaolinite peaks occur with d-spacings of 7.05Å and 3.56Å, respectively, for glycolated samples. After samples were subjected to 550°C heat treatment, the kaolinite peaks collapsed. Illite peaks were only half the intensity of those in the Big Stone pedotype, with d-spacings of 9.78Å and 4.94Å, respectively. For the K- and Mg-treated samples (i.e., glycolated) a peak at ~14.0Å was not observed. This observation implies that either smectite was never present in the pedogenic environment, or smectite had experienced burial illitization.

Both Pine Mtn and Pound pedotypes have mixed clay assemblages in which illite is the dominant clay (Fig. 2.10C and 2.10D respectively). Both pedotypes have relatively low peak intensities for mixed illite/smectite clay at a d-spacing of 13.85Å in the glycolated samples. However, the Pound pedotype has another low-intensity peak at a d-spacing of 4.68Å that is interpreted as smectite. With heating this peak disappeared, which suggests that a 2:1 clay is present. Low-intensity peaks for illite for both pedotypes were observed at d-spacings between 9.78-9.81Å. Mora et al. (1998) also reported illite/smectite mineral assemblages for a time-equivalent, well-drained Pennington Vertisol from Monterey, TN, with pedogenic features similar to those of the

Pound pedotype. Kaolinite is present, but not with the intensities observed in the Big Stone and Appalachia pedotypes, with d-spacings of 7.01Å and 3.52Å, respectively. Heating of both samples collapsed the kaolinite peaks.

Discussion

Assignment of Soil Orders to Paleosols

In addition to general field observations, bulk-geochemical analysis, micromorphology and XRD-analysis were key tools in taxonomically classifying soil order (Soil Survey Staff, 1998) terms to Pennington Fm. paleosols. We recognize that there is some disagreement to this practice within the scientific community, but our intent here is to facilitate communication of paleosol properties that are most closely analogous to those required for classification of surface soils. For example, although Soil Taxonomy (Soil Survey Staff, 1998) requires surface cracking to classify a soil as a Vertisol, paleo-Vertisols were identified by B-horizons containing abundant pedogenic slickensides (Bss horizons), more than 30% clay, and a thickness greater than 50cm; two of the three criteria for Vertisols were met. Pedogenic slickensides form in clay-rich soils when the shear strength of the soil is exceeded by swelling pressure, causing expansion of clays, where vertical movement is confined (Wilding and Tessier, 1988). The observed pseudo-synclines and pseudo-anticlines (Fig. 2.6H) of the Pound paleosols are the subsurface expression of gilgai microtopography, i.e., a series of low-relief swales and hummocks (Lynn and Williams, 1992; Caudill et al., 1996; Mora and Driese, 1999; Driese and Ober, 2005). All paleosols having horizons with slickenside development and wedge-shaped pedal structure observable in the field were classified as Vertisols. In thin-section,

Vertisols (Pound and Pine Mtn) had common masepic and bimasepic matrix fabrics, indicating alternating wet-dry cycles (shrinking and swelling of clays) and seasonality that promotes Vertisol development (Brewer, 1976; Nettleton and Sleeman, 1985; Wilding and Tessier, 1988; Blokhuis et al., 1990; Fitzpatrick, 1993).

Histosol classification (Wise pedotype) was based solely upon the presence of coal. Histic epipedons are peat layers, which in paleosols are converted to coal seams (Retallack, 2001). All coals were underlain by Vertisol-like paleosols, and because Soil Taxonomy (Soil Survey Staff, 1998) does not have a classification for Vertisols in which an O-horizon is developed, we conclude that each coal represents a separate and distinct paleosol (cf. Driese and Ober, 2005). In order for a soil to be classified as a Histosol the organic layer must be more than 40 cm thick (Soil Survey Staff, 1998). Using Retallack and Sheldon's (2001) paleosol decompaction equations the decompacted thickness of the coals ranged from 41-247cm, sufficient to classify these paleosols as Histosols. In thin-section, the coals are distinctively organic-rich and carbonaceous (Fig. 2.6K). Organic matter stabilization is enhanced by the presence of clays (Shang and Tiessen, 2003; Parfitt et al., 1997); trace elements mobilized during organic maturation (Kabata-Pendias, 2001) are reflected by net gains in elements in the clay-rich Pine Mtn/Pound pedotypes, which occur directly beneath Wise paleosols (Figs. 2.9B, C).

The Appalachia pedotype, interpreted as an Oxisol, was initially identified in the field by areas of bleached soil matrix and clayey soil texture. The Bo (oxic horizon) was extremely mottled, "bleached" (Fig. 2.6I), and devoid of clay skins, despite the clay-rich texture (Table 2.1). Oxic horizons are typically kaolinite- or gibbsite-dominated (Retallack, 2001). XRD analysis of the Oxisol indicates a kaolinite-dominated

mineralogy (Fig. 2.10B), whereas the other pedotypes are dominantly illite with variable illite-smectite and kaolinite mineralogies. Oxisols, described in the Late Cretaceous, also have attributes of intense leaching, mottling, and kaolinite-dominated clay mineralogy (Pe-Piper et al., 2005). Oxidation calculations for the Appalachia pedotype (Fig. 2.8B) were the highest for any Pennington pedotype. The Oxisol exhibits net increases in Fe and Mn and net losses of the base-forming cations Ca, Mg, and Na, suggesting very intense weathering processes. Base-forming cations were leached out of the profile, whereas Fe and Mn were concentrated due to ever-wet conditions, as indicated by the intense mottling of the Bo horizon. The net gain in K likely reflects the kaolinite-rich mineralogy of the paleosol.

The Appalachia pedotype might also be interpreted as an Ultisol. Ultisols can also be extremely weathered and kaolinite-dominated (Abayneh, 2006; Trakoonyingcharoen et al., 2006). Field attributes of an Ultisol and Oxisol are quite similar (Soil Survey Staff, 1998) and would therefore be difficult to distinguish in the paleosol record. Whether an Oxisol or an Ultisol, the paleoenvironmental interpretation remains the same. The geochemistry and current modern soil research (Abayneh, 2006; Trakoonyingcharoen et al., 2006), however, is more supportive of an Oxisol interpretation rather than an Ultisol.

Both the Norton and Big Stone pedotypes are poorly-developed soils (Inceptisols and Entisols, respectively). Big Stone paleosols are essentially a BC horizon, with only rhizoliths and rhizocretions to support a paleosol interpretation Table 2.1, Fig. 2.6E). Weak pedogenesis is indicated by preserved depositional stratification. In thin-section Big Stone paleosols display features indicating poor drainage, such as FeMn coatings and

intercalations (Table 2.1). The Norton pedotype (primarily designated as a Bw in the field), in contrast, has more pedogenic features, such as weakly-developed slickensides, FeMn and clay coatings, and moderately impregnated concentric FeMn nodules.

Soil Drainage

Interpretation of temporal changes in soil drainage is integral to our hypothesis that high-frequency climate changes occurred during Pennington deposition and pedogenesis. Differences in soil drainage distinguish the Pound and Pine Mtn pedotypes interpreted as Vertisols. The Bk-horizons, as well as clay coatings and oxidized soil matrix colors, are field indicators that Pound paleosols formed during dominantly well-drained conditions (Table 2.1, Fig. 2.6B). Micromorphology likewise supports well-drained conditions for Pound paleosols, as exemplified by well-developed micrite nodules and argillans (Figs. 2.7C and D, respectively). Pine Mtn paleosols, in contrast, lack Bk horizons and clay coatings, and have drab, low-chroma matrix colors (Table 2.1, Fig. 2.6B). In addition to low-chroma soil colors, Pine Mtn paleosols have abundant concentric, strongly impregnated FeMn nodules visible in thin-section (Table 2.2; Fig. 2.7B), characteristic of poorly-drained conditions. Pyrite formation is also common (Fig. 2.7B) and similarly forms during poorly-drained conditions. Poorly-drained and well-drained features, however, are not always uniformly distributed throughout horizons.

Many of the Pound and Pine Mtn paleosols exhibit complex redoximorphic features, which indicate that they have a polygenetic soil drainage history, first noted by Greb and Caudill (1998). In the field, alternating reduced and oxidized coatings of rhizoliths suggest periodically changing drainage conditions, and it was generally difficult to identify a dominant paleosol matrix color in the field because of the

heterogeneity of redoximorphic features and low-chroma colors (Fig. 2.6H). Alternating soil drainage conditions are also very apparent in thin-section. Different stages of gley, as well as well-drained conditions are mapped in thin-section (Figure 2.5). In Pine Mtn and Pound paleosols it is apparent that Fe had been remobilized and precipitated at different stages during pedogenesis indicated by strongly impregnated concentric nodules, intercalations, and filled soil matrix voids (Figure 2.5). Weakly developed clay coatings/argillans, however, were also observed in Pine Mtn paleosols suggesting more well-drained conditions at one period of time (Table 2.1). Calcite nodules impregnated with Fe (Fig. 2.5A, 2.7A) and Fe-coatings on micrite nodules and glaebules (Figure 2.7F) in Pound paleosols are additional evidence for fluctuating drainage conditions during paleosol development.

Geochemical analysis provides additional evidence for changes in soil drainage patterns through time. For example, with increasing soil drainage, base loss, leaching, and lessivage (clay translocation) should all increase. Pound paleosols (well-drained Vertisols) have increased ratios of base loss and leaching, whereas Pine Mtn paleosols (poorly drained Vertisols) show decreased ratios (Figs. 2.8A, C). Paleosols are time-averaged and therefore analysis of bulk chemistry of paleosols typically does not allow one to distinguish details of individual phases of changing soil drainage conditions. Wise paleosols (Histosols) exhibit minimal leaching and base loss because of the clay-rich Pine Mtn and Pound paleosols underlying Wise paleosols. The underlying Pine Mtn and Pound paleosols formed aquitards and consequently retarded base-loss and leaching, thereby promoting conditions conducive to Histosol formation (and later coal development). Similar soil-drainage conditions were also inferred by Driese and Ober

(2005) for poorly-drained Pennsylvanian Vertisols in eastern Tennessee that were directly overlain by coals.

Ecosystem

The Mississippian represents a crucial time in the evolution of terrestrial ecosystems (Dunn, 2004). Plants began to spread over large parts of the Earth to produce a "tiered" plant structure similar to that of the modern (Dunn 2004; Cleal and Thomas, 1999). Studies of the Fayetteville flora (Middle Chesterian) in Arkansas suggest that lycopsids were the most numerous, and sphenopsids, although low in diversity, were also abundant (Dunn, 2004). In general, there was an increasing diversity of lycopsids, pteridosperms, and sphenopsids (Cleal and Thomas, 1999; DiMichele and Phillips, 1996). Lycopsids were likely the canopy trees (Dunn, 2004) for the Mississippian, and it is this arborescent flora that may have produced the rooting patterns and rooting morphology of Pennington paleosols.

Rooting throughout the Pennington seems strongly influenced by soil drainage and less so by precipitation variation through time (Figs. 2.4, 2.8F). Because truncation is likely for each paleosol profile, the reported depths are likely minima and roots probably penetrated much deeper than what is observed in the field. The deepest rooting occurs in Pound paleosols (Fig. 2.4: PC, PI, and M). Average MAP estimated for Pound paleosols (1234 cm/yr) is greater than the average MAP estimated for paleosols comprising the entire section (1176 cm/yr). If precipitation were the primary control on depth of rooting, increased rainfall would likely encourage shallow rooting depths, but shallow rooting depths are not characteristic of the majority of Pound paleosols. Therefore, rooting depth increases primarily with better soil drainage. Although precipitation estimates steadily

increase through time, relative minima are indicated for Pound paleosols late in Pennington deposition (Fig. 2.8E: PE, PK). In contrast, the rooting depth for the Appalachia paleosol is relatively shallow, and this soil likely records the highest rainfall for the Pennington. As mentioned previously, this Oxisol-like paleosol likely formed in an extremely wet climate characterized by intense leaching; in such a "rain forest" ecosystem plants would not have had to search very deeply for plant-available water.

Figure 2.4 thus represents our interpretation of the probable flora and floral associations that might have existed during late Mississippian time at Pound Gap. With the exception of arborescent lycopsids, the flora of the Mississippian had shallow root systems. This interpretation is not only based upon field observation, but by comparisons with modern club mosses (also lycopsids) and horsetails (sphenopsid), as well as ferns, which all exhibit shallow, laterally branching root systems (Stuzenbaker 1999; Crow and Hellquist 2000). We realize that floral associations of the modern rain forests and that of the Late Mississippian are somewhat different; however, both likely contained a canopy of larger trees and an understory of shrubby plants. During Appalachia paleosol formation seed ferns were likely the dominant floral group (Retallack and Dilcher, 1988) and were present throughout the Chesterian (Dunn et al., 2003), preferring clayey textures, but were also concentrated within swampy and/or bog soils (Crow and Hellquist, 2000). Large root traces present within a Big Stone paleosol (Entisol) strongly suggest arborescent vegetation, with root systems penetrating the soil to depths exceeding 2m. Given the clayey texture of the majority of the Pennington paleosols, the interpretations of lycopsid remains made by Dunn (2004) for the Fayetteville Formation of Arkansas, and megaspore remains from the Logan Formation in northeastern Ohio

(Arioli et al., 2007), we infer that lycopsids were the dominant arborescent flora at Pound Gap. The floral associations we have identified for the Pennington section are also consistent with the plant formations of Retallack (1992), their associated rooting depth, and characteristic paleosol features.

Climate

Climate is one of the main controls on weathering and soil formation (Cecil and Dulong, 2003). It is apparent that precipitation was variable through time, however, during middle Pennington paleosol development precipitation may have remained fairly constant, followed by a relative increase in MAP at the close of the Mississippian (Fig. 2.8E). Increasing estimated MAP, during latest Mississippian time, signals the onset of the ever-wet conditions that prevailed throughout the Early Pennsylvanian (e.g., Driese and Ober, 2005). Similarly, soil drainage also varies through time, and is strongly related to changes in MAP (Figs. 2.8E, F). Precipitation, however, was likely more seasonal because the dominant paleosols are analogous to Vertisols.

The physical, chemical and mineralogical associations of modern soil orders (with the exception of Histosols) can be associated with certain climate regimes in which they develop (Critchfield, 1974). Vertisol development requires periods of drying and wetting, and Vertisols occur mostly in humid to semiarid environments in warm regions (Nordt et al., 2004; Soil Survey Staff, 1998). Pedogenic slickensides, subsurface expression of gilgai topography, and sepic-plasmic matrix in thin-section, are all manifestations of seasonality (Soil Survey Staff, 1998). Shrinking and swelling of clays produces slickensides and preferentially aligns clays to impart a sepic-plasmic matrix fabric (Brewer, 1976; Blokhuis et al., 1990; Driese and Ober, 2005). It is also clear that

soil drainage for ancient Vertisols can vary substantially not only through time, but also within an individual profile, as evidenced by the polygenetic character of virtually all of the Pound and Pine Mtn paleosols, for which redoximorphic overprinting was common.

Early in the history of Pennington paleosol development, climatic conditions were tropical warm and wet, favoring the development of an Oxisol (Appalachia pedotype; Fig. 2.6G and Table 2.1); this was the wettest period of time during the Chesterian at Pound Gap, as indicated by intense base loss and leaching, mottling, dominant kaolinite mineralogy and high MAP estimates for this paleosol (Figs. 2.8A, E, F). Kaolinite is the dominate mineral in highly weathered soils that form in the wet tropical latitudes, which is consistent with this paleoclimate interpretation (Moore and Reynolds, 1997). In addition to conditions favorable for Oxisol development, the Pennington was punctuated by other periods of wetness (although not as severe as in the Early Chesterian) wherein Histosols developed atop clay-rich, often poorly-drained Vertisols (Fig. 2.6C).

Paleosol indicators of aridity contrast markedly with the previously described wet soil features. For example, the Pound and Jenkins paleosols have well-developed Bk-horizons, which indicate well-drained and drier conditions, as well as reddened paleosol matrix colors (10R 4/2, 7.5R 4/2) and Fe oxide staining observed in thin-section (Retallack, 2001) (Tables 2.1, 2.2; Fig. 2.6G). Cecil (1990) and Mora and Driese (1999) previously postulated similar episodes of arid to semi-arid conditions for the Appalachian Basin during latest Mississippian time.

Climate Control and Modern Analog Setting

During latest Mississippian (Chesterian) time the paleolatitude and paleotectonic setting of the Appalachian Basin were similar to that of modern-day Indonesia (Cecil et

al., 2003). The island of Timor is located between 9° and 12°S latitude and the climate of the region is dry subhumid, with four wet months and eight dry months. When the Intertropical Convergence Zone (ITCZ) passes over the island, Timor experiences its rainy season. The Arafura and Timor seas represent modern foreland basins forming astride active fold-and-thrust belts produced by tectonic collisions, which are similar to the Appalachian foreland basin during the Late Mississippian (Cecil et al., 2003; Fig. 2.1). West Timor hosts a suite of soils that are morphologically similar to the paleosols developed during Pennington time, especially clay-rich soils with a high shrink-swell potential (i.e., Vertisols). The only inconsistency with this modern analog is the absence of Histosols and Oxisols noted by Cecil et al. (2003) in West Timor.

By analogy with West Timor, we infer that contraction and expansion of a paleo-ITCZ was a likely climate driver for the formation of Pennington Formation paleosols. Morphological attributes of the paleosols (both micro- and macroscopic), as well as geochemical results, support interpretations of seasonal variations in climate. Wetter more poorly-drained periods of paleosol development occurred during times when the study area was within the influence of the paleo-ITCZ and rainfall was high, whereas drier, better-drained paleosols developed when the study area was outside of the influence of the paleo-ITCZ (Fig. 2.11). Development of Histosols and Oxisols correspond to times of more intense rainfall when the paleo-ITCZ may have experienced prolonged periods of expansion, thereby sustaining wetter conditions for longer periods of time.

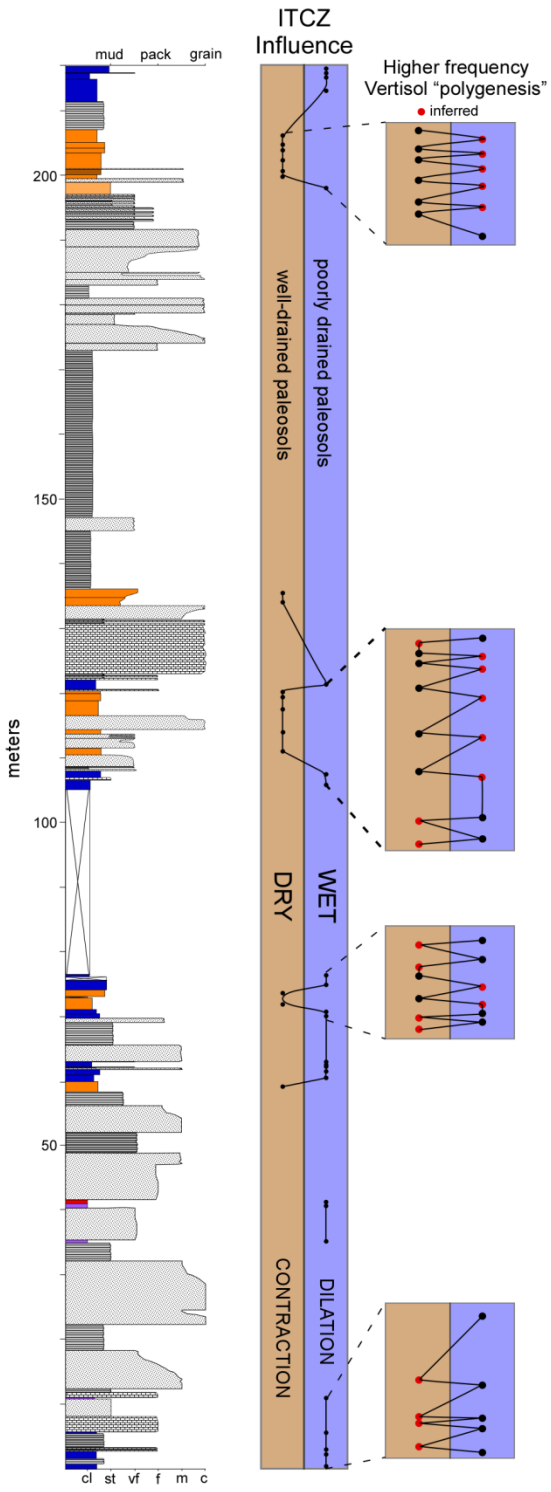

Figure 2.11 Plotted paleosol drainage through time and interpreted dilation and contraction of the paleo-Intertropical Convergence Zone (ITCZ). Black symbols are observed soil drainages, and gray symbols are inferred soil drainages from Vertisol polygenesis.

We acknowledge that there is great difficulty in determining the timing and frequency of climate changes because paleosols are records of time-averaged soil development, and we have at best coarse chronostratigraphic resolution. Although admittedly simplistic (and assuming uniform rates of pedogenesis) the development of 40 paleosols in a 8 myr time interval would suggest that each represents, on average, <200 k.y., and it is apparent that soil drainage conditions fluctuated substantially with each phase of pedogenesis as indicated by Vertisol polygenesis (Fig. 2.11). We postulate that the array of paleosols described in this study, and their documented changes in morphological, micromorphological, and geochemical properties are consistent with our initial hypothesis of high-frequency climate change.

Conclusions

The following primary conclusions can be drawn from this study:

1) Vertisol-like (Pound and Pine Mtn pedotypes) paleosols record wet-dry cycles associated with precipitation seasonality. The majority of these paleosols have a polygenetic character suggesting repeated fluctuations of soil drainage through time.

2) Wise paleosol (Histosols) formation was favored by subjacent low permeability clay-rich Vertisols that inhibited soil drainage, as indicated by low base loss and leaching ratio calculations.

3) The formation of an Oxisol-like paleosol (Appalachia pedotype) is supported by a kaolinite-dominated clay mineralogy, intense leaching, high oxidation ratios, and the highest MAP estimates for the entire Pennington Fm. Oxisol formation would have required a tropical/wet climate regime in which a rainforest might have existed.

4) Rooting through time varies with soil drainage and MAP. The abundance and depth of rooting also suggests a varying biomass through time, with increasing plant foliage toward the end of Pennington deposition and pedogenesis.

5) Mean annual precipitation (MAP) estimates using the CIA-K geochemical proxy for the Pennington range from 519 to 1361 mm/yr. MAP estimates are coincident

with calculated ratios of soil base loss and leaching. MAP increases throughout the later half of Pennington deposition, signaling the onset of the ever-wet conditions associated with development of the Pennsylvanian coal swamps.

6) Vertisol formation, the polygenetic character of Vertisols, and variation in MAP and soil processes through time are consistent with our hypothesis suggesting high-frequency climate changes as a forcing mechanism for the Late Mississippian (Chesterian) in the southern Appalachian basin region.

CHAPTER THREE

Evaluating Trace Elements as Paleoclimate Indicators: Multivariate Statistical Analysis of Late Mississippian Pennington Formation Paleosols, Kentucky, USA

Abstract

The temporal and spatial distributions of trace elements in paleosols in relation to soil-forming processes and climate have received little attention, primarily due to their generally low concentrations (< 100 ppm) and a fundamental lack of knowledge of their behavior in soil systems. Trace element concentrations of Pennington Formation paleosols, spanning an 8 Ma time interval in the late Mississippian (Chesterian), were analyzed using linear and multivariate statistics of whole-rock elemental data. Linear statistics of the elemental data set show that Ti, Zr, Nb, Cs, La, Hf, Ta, W, Ce, and Th have the highest correlation through time with r-values ≥ 0.75. Nb served as the proxy trace element for comparison. Temporal trends in Nb closely match trends in lessivage (clay formation and accumulation by feldspar weathering), mean annual precipitation (MAP), and chemical weathering. MAP effectively controls soil hydrology and organic matter accumulation, in addition to clay accumulation. MAP, in conjunction with chemical weathering, controls trace element accumulation. Fe and Mn concentrations provide conflicting evidence and question redox conditions as a fundamental control. Trace element concentrations through time support high-frequency Late Mississippian climate changes, characterized by extreme wet and dry periods. In addition, cluster analysis and discriminant analysis, using canonical variates, of trace elemental data were able to distinguish between soil order and, to a lesser degree, soil drainage. The use of

multivariate statistical analysis in a temporal study of paleosol trace element chemistry therefore provides a new tool to evaluate pedogenic processes and a means by which to draw inferences regarding intensity of chemical weathering and its relationship to climate change.

Introduction

The trace element chemistry of soils has generally been examined in relation to agricultural practices, soil sustainability, and contaminant remediation, with few applications in paleopedology (Retallack, 1986; Shotyk, et al. 2001; Sheldon , 2006). Most trace element research in sedimentary geology has been directed towards establishing sediment provenance (source areas and dispersal histories) (e.g., McLennan, 1989; Nesbitt and Markovics ,1997; Jahn et al., 2001; Dia et al., 2006) and is more spatial rather than temporal (e.g., Hieronymus et al., 2001; Brown et al., 2003, Marques et al., 2004; Tyler, 2004; Caspari et al., 2006; Scribner et al., 2006). Most prior studies of soils and paleosols examined trace element concentrations as a function of soil depth (Feakes and Retallack, 1988; Sheldon 2006), or over time periods with too few data points to constrain effects. Due to the paucity of data it is then a difficult task to interpret the controls on variability. This study, which examines over forty paleosols developed over a period of ~8 my, demonstrates that characterization of trace element chemistry in paleosols can be a powerful tool for paleoclimate analysis, provided that the following conditions are met: (1) trace element data are statistically analyzed using linear and multivariate methods, (2) data are analyzed temporally (i.e., through time) and not viewed statically, and (3) there is an understanding of the underlying controls on trace element chemistry of soils. Statistical analysis is applied here to determine the confidence

level of the trace element data for inferring changing soil drainage as related to climate changes through time.

Trace element concentrations in modern soils and sediments are fundamentally controlled by grain size, provenance, organic matter, pH, Eh, and cation exchange capacity (CEC) (Kabata-Pendias, 2001). Sediment texture has been found to be important in controlling trace element concentrations and their spatial distribution (Zhang et al., 2001). Zhang et al. (2001) observed that the majority of trace elements were associated with clays concentrated in the fine-mud fraction of intertidal flats in Bohai Bay, China. Similarly, the fine-clay fraction was found to be the most important size fraction for element (and trace elements) release in a granitic podzol (Hodsen, 2002). We therefore conclude that the fine-clay texture of the Pennington paleosols will act as a control in trace element accumulation.

The source or provenance of soil parent material determines the initial geochemical character of the sediment before pedogenesis begins. For example, the trace element content of basalt-parented soils (Stewart, 2001) is considerably different from quartz to feldspathic-parented soils of the Chinese loess plateau (eolian-transported, mainly silt-sized material) (Ding, 2001; Guo, 1998). As was the case with the fine clay fraction, trace elements also have an affinity for organic matter, which may be considered a ‘sink’ for certain trace elements (Aubert, et al. 2004; Sterckeman, 2004; Sterckeman, 2006). The organic matter can form metallo-organic complexes (Tyler and Olsson, 2002), which are variable depending upon pH and other properties of the soil (Kabata-Pendias, 2001). Therefore, the release and concentration of trace elements is largely controlled by the CEC of the soil, with both organic matter and clays contributing to high CEC.

The pH and Eh of paleosols play a role in trace element concentrations, but unfortunately these variables cannot be quantified, nor confidently interpreted within paleosols, based on direct measurements (Retallack, 2001). Although parent material is not generally considered a primary control on trace element chemistry, once the parent material undergoes pedogenesis, chemical weathering processes are the dominant mode of transport for elements within the soil profile (McLennan, 1989).

Rare earth elements (REE) are conserved in the terrigenous component during weathering, erosion, and deposition, from source to the pedogenic environment. Additionally, the fraction of REE that may be carried in solution is negligible (McLennan, 1989). Accumulation and storage of REE in weathering profiles occurs over time in mature weathered profiles (Nesbitt and Markovics, 1997). REE are mobilized during weathering, but are primarily recycled within the weathering profile rather than transported significant distances in solution. Mobilization occurs by aggressive CO_2 and organic acid-charged rainwater percolating through the soil, whereby REE are put into solution as complexes or free ions, followed by weathering reactions in which pH is increased and REE come out of solution as precipitates, or are exchanged for H+ on suitable clays or adsorbed on mineral surfaces (McLennan, 1989). It is reasonable to assume that the majority of the trace elements in the paleosols behave chemically in a manner similar to the behavior of REE in modern weathering profiles.

We hypothesize that the trace element geochemistry of paleosols is a potentially powerful, but still greatly underutilized tool for paleoclimate interpretations. The study area at Pound Gap, Letcher County Kentucky (Fig. 3.1) includes a succession of Late Mississippian age (Chesterian) paleosols in the Pennington Formation, which serve as a

case study for testing the hypothesis that trace element geochemistry can be used as a new tool in paleoclimate interpretation. As a means of testing this hypothesis we use linear and multivariate statistical techniques to evaluate trace element data from Late Mississippian Pennington Formation paleosols, and interpret differences due to variations in soil drainage, soil types, and climate change. Chemical weathering proxies for paleoclimate, established in previous basic paleopedological work by Kahmann and Driese (2008), support the interpretation of Late Mississippian climate change through temporal changes in trace element geochemistry in the Appalachian Basin region.

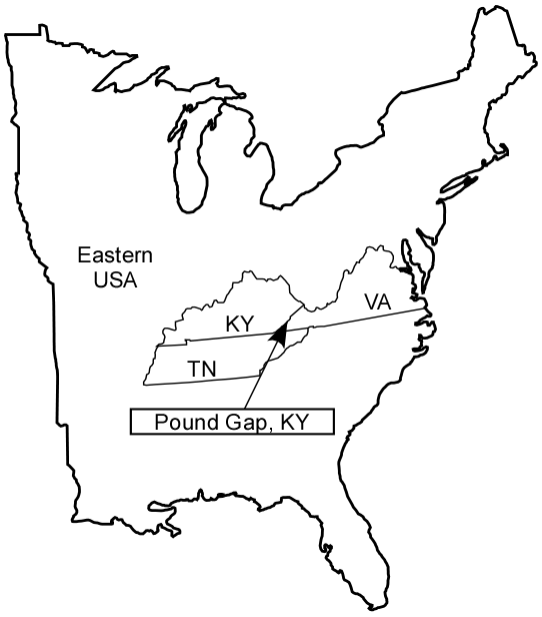

Figure 3.1 Map showing the location of the Pound Gap stratigraphic section, Jenkins County, Kentucky.

Geologic Setting

A complete stratigraphic section of the Pennington Formation (220+m) is exposed in outcrops along US Highway 58, on the Kentucky-Virginia border, near the town of Pound, Virginia, in the southeastern USA (Fig. 3.1). The Pennington Formation was deposited during the latest Chesterian (Late Mississippian) in a variety of depositional environments ranging from open-marine to rainforest environments (Kahmann and Driese, 2008). The Pound Gap study area was located between 5° and 10° S latitude during the Mississippian (Ziegler et al., 1979), near the boundary of the paleo-wet equatorial belt and the paleo-dry trade-wind belt (Ettensohn et al., 1998). Pennington strata record substantial changes in base level, with punctuated and often prolonged periods of subaerial exposure resulting in soil development. The Pennington Formation is underlain by the Newman Limestone (Mississippian) and is overlain by the fluvially-dominated facies of the Pennsylvanian Lee Formation (Greb and Chesnut, 1996). The Mississippian-Pennsylvanian systemic boundary in this region is marked by a widespread unconformity (Chesnut, 1992).

Tectonic subsidence in the study area during the latest Chesterian (Late Mississippian) influenced the distal southern Appalachian foreland (the location of the Pound Gap section) (Woodward, 1961), including uplift in highlands to the east and southeast, and in the Cincinnati Arch to the northwest (de Witt and McGrew, 1979; Sable and Dever, 1990). Structural deformation in the southern Appalachian region concluded with uplift along the Pine Mountain thrust during the Late Pennsylvanian (Mitra, 1988; Andrews and Nelson, 1998). The burial history of the study area is uncertain owing to differing estimates of overburden thickness that range from 0.74 km (Harris, 1978) to

2.13 km (McKee et al., 1976). Burial temperatures probably ranged between 60-150°C (Niemann and Read, 1988), with temperatures exceeding 50°C for time intervals of up to 50 Ma (Castano and Sparks, 1974; Hower et al., 1983).

Methods

Data Collection

Forty paleosols within the Pennington Formation were identified and logged using standards and procedures of USDA Soil Taxonomy (Soil Survey Staff, 1998). Paleosol description commenced at the Newman Limestone and Pennington Formation boundary, which is a gradational contact at Pound Gap (Nelson and Read, 1990). The stratigraphically lowest paleosol overlies a marine brachiopod packstone identified as near the top of the Newman Limestone. Paleosols were described for redoximorphic features, color, rooting depth, and pedal development, up to the Mississippian-Pennsylvanian boundary (Kahmann and Driese, 2008). The paleosols were initially grouped into 7 pedotypes and then assigned a soil order (Kahmann and Driese, 2008). Pedotype attributes and paleosols used for geochemical analysis in this study are summarized in Table 3.1. Though we recognize there is some disagreement concerning pedotype nomenclature within the scientific community, our intent in assigning these names was primarily to facilitate communication of paleosol properties that are most closely analogous to those required for classification of surface soils.

Bulk paleosol samples of about 200 g were collected at 10 cm intervals from each paleosol profile for geochemical analysis. Major, minor, and trace elements in each sample of each distinctive paleosol horizon were measured commercially using ICP-MS and ICP-AES. Samples were dried and pulverized, followed by meta-borate fusion and

total acid digestion (HF, HNO_3, and $HClO_4$). Data (Appendix) are reported in terms of element weight percent or ppm. Paleosol profiles, representative of the range of variability within each pedotype, were chosen for geochemical analysis (Table 3.1). Each reported elemental concentration is the average concentration for each paleosol profile through time, excluding C-horizon values. C-horizon values are excluded from our analysis because they were *a priori* assumed to be pedogenically unaltered to minimally weathered.

Table 3.1 Paleosol summary of paleosols used for trace element analysis (adapted from Driese and Kahmann, 2008)

Pedotype	Horizon	Depth	Texture	Drainage*	Soil Order	Included Soils
A. Pine Mtn	Bssg1	0-43	silty clay	poorly-drained	Vertisol	A1, A2, A4, A10,
	Bssg2	43-74	silty clay			A11, A17,
	C	74-86	sandstone			PA, PH, PO
B. Pound	Btg1	0-5	clay	well-drained	Vertisol	A7, A14
	Btg2	5-20	clay			PC, PE,
	Bssg	20-65	silty clay			PI, PK, PM
	Bss	65-100	silty clay			
	Bssk	100-200	silty clay			
	Bk	200-244	silty clay			
C. Wise	O	0-7	coal	poorly-drained	Histosol	A10H, A11H, MH, OH
D. Norton	Bg	0-17	silty clay	poorly-drained	Inceptisol	A5-A6,
	B/C	17-26	silty clay			
E. Big Stone	B/C	0-250	silty clay	poorly-drained	Entisol	PL
F. Appalachia	Bo	0-15	sandy clay	well-drained	Oxisol	A6b
	Bts	15-66	sandy clay			

* This is an overall drainage history, however, many soils are polygenetic with variable drainage histories

Although major oxide concentrations were used to calculate chemical weathering indices/ratios and soil-forming processes, this study primarily focuses upon trace element concentrations through time. Chemical weathering indices were calculated assuming that major cations are leached out of the weathered material, using an immobile element as reference. We applied the following chemical weathering indices: CIW ($Al_2O_3/(Al_2O_3 + CaO + Na_2O) \times 100$) (Harnois, 1988), PWI ($K_2O/0.25 + Na_2O/0.35 + CaO/0.7 + MgO/0.9$) (Parker, 1970), and WI-1 ($SiO_2 + CaO/Fe_2O_3 + TiO_2$) and WI-2 ($SiO_2 +$

$CaO/Al_2O_3 + Fe_2O_3 + TiO_2$) (Darmody, 2005). Calculations of soil-forming processes such as lessivage, base-loss, oxidation, and salinization (Retallack, 2001; Sheldon et al., 2002) provide an indication of soil drainage and can supplement conclusions drawn from chemical weathering indices in the context of climate change.

Statistical Analysis

The JMP (SAS 2007) and SAS® (SAS 2004) statistical packages were used for data analysis. The multivariate procedure in JMP was used to evaluate correlations among the trace elements. SAS procedures were employed to further analyze the data. Proc Cluster in SAS was used to perform a cluster analysis using Ward's method, after which Proc Tree was used to graph the clusters.

The SAS discriminant analysis procedure, Proc Discrim, was then used to construct a model on which subsequent classifications can be based. Using this model, theoretically other newly acquired paleosol datasets could then be classified into the particular stratum, generated from our model, based on the trace elements. The larger the separation between the categories (different soils), the more likely the procedure will correctly classify the observation. For small data sets such as ours, Proc Discrim uses all of the observations (trace element concentrations for each horizon of each paleosol profile) to construct the model, and then classifies each observation of the same data set as if it were new. Also in the case of a small sample, especially when a large number of variables are used for classification, estimation of the covariance matrix is problematic. Thus, linear instead of quadratic discriminant analysis was employed in this study. For an overview of these issues see Johnson and Wichern (2007).

A dimension-reduction strategy was needed in order to proceed with the discriminant analysis. Two common dimension-reduction techniques are Principal Components and Canonical Variates. Principal Components calculates a vector, which maximizes the associated amount of variance and typically corresponds with the eigenvector with the largest eigenvalue of the data matrix. The second principal component is orthogonal to the first and is oriented so that the resulting planar shape captures the maximum variability from the two-dimensional scatter plot or "data cloud". Principal Components is often mistakenly applied in the case of multiple populations; however, it treats all the data from the different populations as if they came from the same population. It does not attempt to separate any of the groups, and as such is not meant to be used for discriminant analysis.

Canonical Variates analysis is designed to accommodate multiple groups, such as this data set and the number of elements being evaluated. It takes the full-dimensional data and finds a lower-dimensional subspace such that the sample means of each group are maximally dispersed in the subspace relative to the covariance matrix. Canonical Variates assumes a homogeneous covariance structure for all populations. This allows a pooled estimate of the overall covariance structure. The pooling of the covariances helps when there are small sample sizes (such as in this study), in that there are fewer parameters to estimate. The dispersion is then based on the distance of the observations relative to the variances in the covariance matrix. For a more complete discussion of Principal Components and Canonical Variates, see Johnson and Wichern (2007).

The SAS procedure Proc Princomp was used to calculate principal components for the trace elements for all the paleosols using the convariance option and determining

four principal components. Next, the SAS procedure Proc Candisc was run to output five canonical variates. All other options were set to default. Proc Discrim was run on both the principal components and the canonical variates with the different paleosols as the groups for the classification, using the default settings.

Results

Trace Element Controls and Chemical Weathering

Based on a method by Gallet (1998) that can determine a sandstone or shale source rock for terrigenous materials and using a plot of weight percent SiO_2 versus Al_2O_3 and continental crustal compositions provided by Condie (1993), Pennington paleosols plot within the generalized shale field, with a few outliers within the sandstone field (Fig. 3.2*A*). Zr and Ti concentrations can also be used as a provenance indicator (McLennan, 1989). A plot of Zr vs. Ti yields an r^2 value of 0.74, which suggests relative homogeneity of source material for Pennington paleosols (Fig. 3.2*B*). Condie (1993) also published trace element concentrations for various periods of time ranging from >3.5Ga to <0.2 Ga. The average La/Th ratio for Pennington paleosols is 3.57, consistent with the findings of Condie (1993).

Grain size of the paleosols was previously determined by Kahmann and Driese (2008). All paleosols have clay or silty clay textures, with one paleosol having a rare sandy clay texture. As previously noted, variations in organic matter content are difficult to quantify through time due to generally low concentrations in paleosols, therefore, we only report the presence of Histosols (*a priori* organic-rich deposits) as an indication of times of high organic matter preservation.

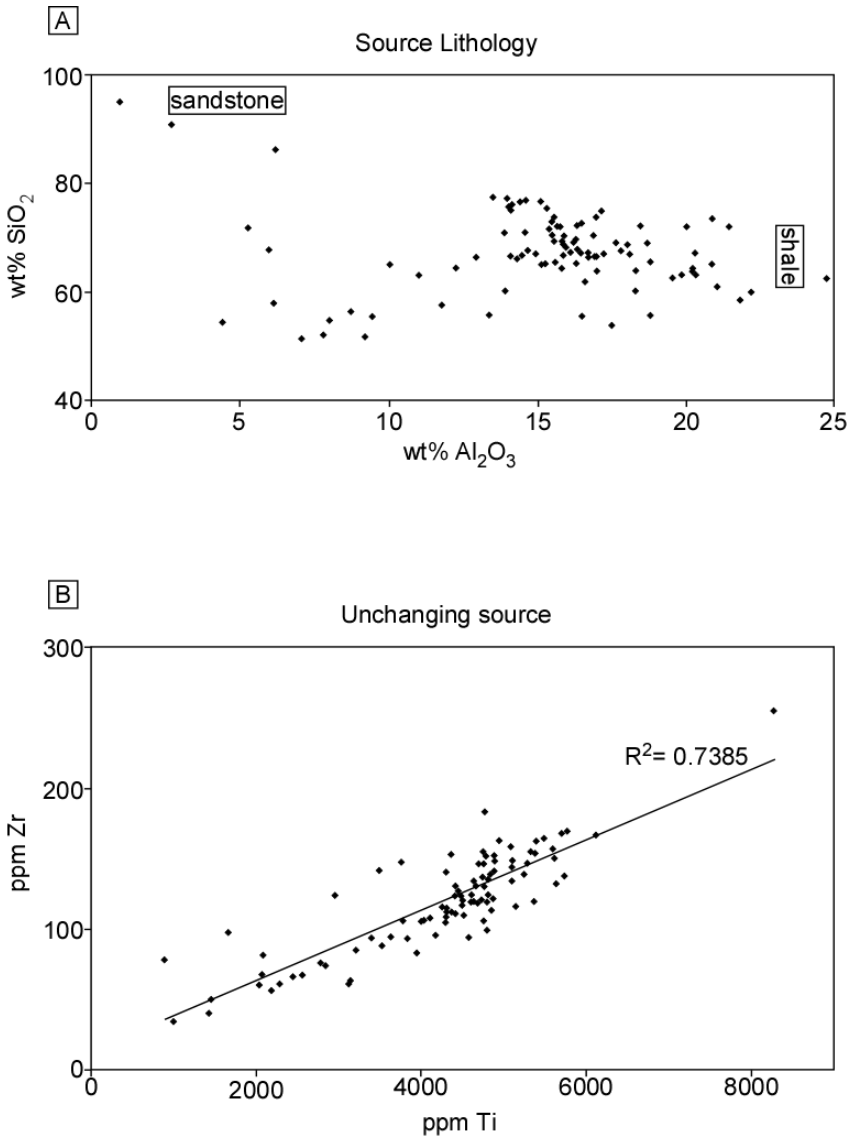

Figure 3.2 (A) Crossplot of wt %SiO_2 vs. wt %Al_2O_3 for Pennington Fm. Paleosols at Pound Gap. Sandstone and shale refer to generalized bulk compositions for these rocks types based on Condie (1993). (B) Crossplot of ppm Zr vs. ppm Ti with a calculated r^2 value. Both plots were used to determine whether or not the source areas for Pennington sediments changed during the Pennington paleosol deposition and pedogenesis.

In general, the trends observed using CWI, PWI, WI-1, and WI-2 weathering indices are in agreement with one another. Averaged values for each chemical weathering index were calculated for each soil profile and are graphically represented through time

in Figure 3.3. Although values of CWI and PWI have opposing trends (Fig. 3.3*A*), the interpretations of weathering intensity recorded by the paleosols is the same for both indices. Values for CWI vary dramatically through time and plateau towards the end of Pennington paleosol formation. Relative maxima are associated with paleosols A6b (Oxisol) and A10, A11 (poorly-drained Vertisols). Minima coincide with Histosol formation (A10-H, A11-H etc.) as well as Inceptisol formation (Fig. 3.3*A*).

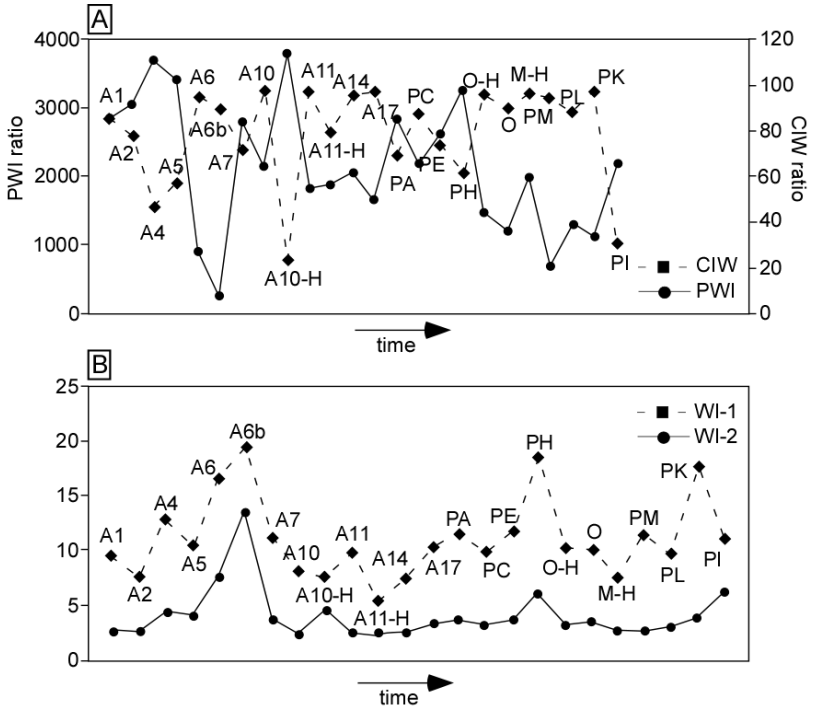

Figure 3.3 Chemical weathering indices/ratios calculated for Pennington Fm. Paleosols and plotted through relative time. (A) CWI and PWI. (B) WI-1 and WI-2. See text for discussion of indices and ratios. Note: each point on plot represents an averaged value for reach respective paleosol

The WI-1 and WI-2 indices somewhat contradict the CWI and PWI trends, although the general trends still coincide. Like CWI, the maximum value is associated with the formation of paleosol A6b, however, Histosol formation is not consistently characterized by lower values of this weathering index; in fact, by this index Histosols

record relative maxima (Fig. 3.3*B*). Overall variations in WI-1 and WI-2 persist through to the end of Pennington paleosol formation.

Statistical Analysis

Statistical analysis of trace element data began with examining the matrix of correlations among the elements. A minimum value of 0.50 for *r* was used to identify the highest correlations. All *r*-values ≥ 0.50 are highlighted in Table 3.2. For example, Ta and Th had $r = 0.81$, which suggests a strong positive covariation between the two elements (Table 3.2). More than 10 trace element pairs had positive *r* values ≥ 0.50. There were also a few cases of negative correlations, as exemplified by Cr and V. These negative correlations indicate an inverse covariation between the elements. Elements such as Nb, Ta, W, and Ti had higher correlations ($r \geq 0.75$) with eight or more elements. The elements Ce, Cs, Ga, Hf, La, Rb, Th, and Zr also had higher correlations ($r > 0.75$) with other trace elements (Table 3.2).

A dendogram was compiled using Ward's Method in cluster analysis (Proc cluster and Proc Tree) of samples, which suggests that there are relationships between the paleosols based upon their trace element chemistry (Fig. 3.4). First-order clustering indicates strong similarities in the following coupled pairs of paleosols: A2-A14; A5-A7; A6-A17; A10-A11; A10H-OH; PM-PO; PA-PE; and PI-PK (Fig. 3.4) (Table 3.3). The coupling performed by cluster analysis is related to known soil attributes described by Kahmann and Driese (2008). Four of the coupled pairs are related by both assigned modern analog soil order and soil drainage class; they are as follow: A6-A17 (poorly-drained Inceptisols), A10-A11 (poorly-drained Vertisols), A10H-OH (Histosols), and PI-

Correlation r-values

	Ba	Ce	Cr	Cs	Fe_2O_3	MnO	Mo	Ga	Ge	Hf	La	Nb	Rb	P	U	Sr	Ta	V	W	Y	Th	Ti	Zr
Ba	1.00	0.17	-0.41	0.55	0.16	-0.47	-0.45	0.66	0.15	0.13	0.18	0.46	0.70	-0.08	-0.46	0.06	0.52	0.44	0.59	-0.36	0.21	0.51	0.17
Ce	0.17	1.00	-0.33	0.49	-0.17	-0.49	-0.37	0.73	0.51	0.70	0.99	0.79	0.49	0.32	-0.08	-0.23	0.80	0.39	0.63	0.35	0.78	0.79	0.70
Cr	-0.41	-0.33	1.00	-0.28	-0.39	0.02	-0.12	-0.38	-0.45	0.18	-0.28	-0.16	-0.27	-0.12	-0.16	-0.35	-0.23	-0.58	-0.15	-0.38	-0.17	-0.15	0.21
Cs	0.55	0.49	-0.28	1.00	-0.15	-0.57	-0.41	0.81	0.06	0.44	0.53	0.79	0.92	-0.08	-0.27	-0.16	0.80	0.63	0.82	-0.22	0.66	0.79	0.41
Fe_2O_3	0.16	-0.17	-0.39	-0.15	1.00	0.24	0.49	0.00	0.26	-0.37	-0.23	-0.23	-0.21	0.06	0.28	-0.02	-0.27	0.39	-0.28	0.30	-0.25	-0.26	-0.42
MnO	-0.47	-0.49	0.02	-0.57	0.24	1.00	0.52	-0.66	-0.30	-0.51	-0.50	-0.64	-0.58	-0.07	0.26	0.16	-0.69	-0.28	-0.62	0.15	-0.56	-0.69	-0.57
Mo	-0.45	-0.37	-0.12	-0.41	0.49	0.52	1.00	-0.49	0.01	-0.49	-0.39	-0.54	-0.48	-0.03	0.49	0.14	-0.60	0.16	-0.67	0.54	-0.43	-0.63	-0.56
Ga	0.66	0.73	-0.38	0.81	0.00	-0.66	-0.49	1.00	0.37	0.54	0.72	0.88	0.81	0.17	-0.28	-0.12	0.88	0.69	0.84	-0.01	0.66	0.87	0.51
Ge	0.15	0.51	-0.45	0.06	0.26	-0.30	0.01	0.37	1.00	-0.03	0.44	0.14	0.10	0.38	0.19	-0.10	0.21	0.34	0.00	0.58	0.27	0.16	0.03
Hf	0.13	0.70	0.18	0.44	-0.37	-0.51	-0.49	0.54	-0.03	1.00	0.75	0.84	0.44	-0.09	-0.20	-0.42	0.79	0.10	0.64	-0.16	0.78	0.81	0.97
La	0.18	0.99	-0.28	0.53	-0.23	-0.50	-0.39	0.72	0.44	0.75	1.00	0.82	0.54	0.19	-0.14	-0.25	0.84	0.36	0.69	0.24	0.81	0.83	0.76
Nb	0.46	0.79	-0.16	0.79	-0.23	-0.64	-0.54	0.88	0.14	0.84	0.82	1.00	0.75	0.01	-0.24	-0.30	0.96	0.50	0.89	-0.13	0.85	0.97	0.80
Rb	0.70	0.49	-0.27	0.92	-0.21	-0.58	-0.48	0.81	0.10	0.44	0.54	0.75	1.00	0.00	-0.42	-0.17	0.79	0.54	0.83	-0.24	0.58	0.78	0.43
P	-0.08	0.32	-0.12	-0.08	0.06	-0.07	-0.03	0.17	0.38	-0.09	0.19	0.01	0.00	1.00	-0.02	-0.11	-0.10	0.03	-0.08	0.65	-0.09	-0.06	-0.14
U	-0.46	-0.08	-0.16	-0.27	0.28	0.26	0.49	-0.28	0.19	-0.20	-0.14	-0.24	-0.42	-0.02	1.00	0.14	-0.31	0.24	-0.42	0.45	0.15	-0.34	-0.29
Sr	0.06	-0.23	-0.35	-0.16	-0.02	0.16	0.14	-0.12	-0.10	-0.42	-0.25	-0.30	-0.17	-0.11	0.14	1.00	-0.22	0.11	-0.15	0.04	-0.33	-0.28	-0.42
Ta	0.52	0.80	-0.23	0.80	-0.27	-0.69	-0.60	0.88	0.21	0.79	0.84	0.96	0.79	-0.10	-0.31	-0.22	1.00	0.48	0.92	-0.20	0.84	0.99	0.80
V	0.44	0.39	-0.58	0.63	0.39	-0.28	0.16	0.69	0.34	0.10	0.36	0.50	0.54	0.03	0.24	0.11	0.48	1.00	0.46	0.26	0.44	0.45	0.02
W	0.59	0.63	-0.15	0.82	-0.28	-0.62	-0.67	0.84	0.00	0.64	0.69	0.89	0.83	-0.08	-0.42	-0.15	0.92	0.46	1.00	-0.37	0.70	0.94	0.66
Y	-0.36	0.35	-0.38	-0.22	0.30	0.15	0.54	-0.01	0.58	-0.16	0.24	-0.13	-0.24	0.65	0.45	0.04	-0.20	0.26	-0.37	1.00	0.00	-0.23	-0.23
Th	0.21	0.78	-0.17	0.66	-0.25	-0.56	-0.43	0.66	0.27	0.78	0.81	0.85	0.58	-0.09	0.15	-0.33	0.84	0.44	0.70	0.00	1.00	0.83	0.76
Ti	0.51	0.79	-0.15	0.79	-0.26	-0.69	-0.63	0.87	0.16	0.81	0.83	0.97	0.78	-0.06	-0.34	-0.28	0.99	0.45	0.94	-0.23	0.83	1.00	0.82
Zr	0.17	0.70	0.21	0.41	-0.42	-0.57	-0.56	0.51	0.03	0.97	0.76	0.80	0.43	-0.14	-0.29	-0.42	0.80	0.02	0.66	-0.23	0.76	0.82	1.00

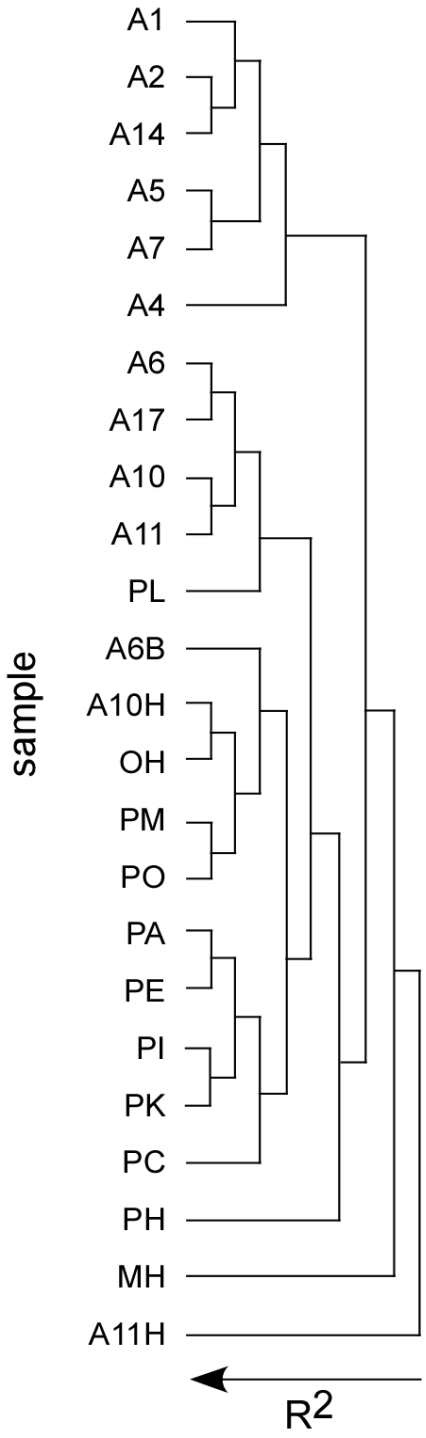

Figure 3.4 Dendogram compiled with SAS program using cluster analysis. See text for discussion.

Table 3.3 Summary of paleosols grouped by cluster analysis (and represented as a dendogram in Figure 3.6 and their associated soil attributes. RSQ= r-squared value, MAP= mean annual precipitation estimated using CIA-K geochemical proxy of Sheldon et al. (2002). Thickness refers to paleosol thickness without decompaction. Soil drainage class and orders are reported in Kahmann and Driese (2008). See text for discussion.

Cluster Pair	RSQ	MAP	Thickness	Rooting Depth	Drainage	Soil Order
PA	1.00	884.03	152	0	poor	Vertisol
PE		1067.80	244	180	very well	Vertisol
A5	1.00	1063.60	26	0	poor	Inceptisol
A7		1303.01	147	92	well	Vertisol
A2	1.00	918.42	116	65	poor	Vertisol
A14		1276.73	146	103	well	Vertisol
PI	0.999	1293.16	120	80	well	Vertisol
PK		1203.49	240	180	well	Vertisol
A10	0.998	1326.67	20	0	poor	Vertisol
A11		1331.28	38	25	poor	Vertisol
A6	0.998	1362.49	66	0	poor	Inceptisol
A17		1321.19	50	45	poor	Inceptisol
A10H	0.992	n/a	7	7	poor	Histosol
OH			3	3	poor	Histosol
PM	0.990	1320.99	196	191	well	Vertisol
PO		1313.89	93	55	poor?	Vertisol

PK (well-drained Vertisols) (Table 3.3). Other paired paleosols are simply related by their soil order, e.g., pairings of Vertisols: A2-A14, PM-PO, and PA-PE. Second-order clustering indicates chemical similarity between the Histosols and the Oxisol relating A6b (Oxisol) to the Histosol first-order couple: A10H-OH. Two other pairs are related on the second-order level by soil drainage: A10-A11 and A6-A17.

The first four principal components were extracted from the matrix of correlations. A total of 99.73% of the variance in the data set was taken into account using these first four principal components. Discriminant analysis, based upon these principal components, resulted in high error rates due to

misclassification. Whereas the lowest observed error was 20% misclassification, most of the error rates, however, were above 50%.

A total of 94.26% of the variance in the data was taken into account based upon the first five canonical variates. The error rates based upon the canonical discriminant procedure are lower than those based on the principal components, with seventeen of the error rates below 33%. Only paleosol A17 has a higher misclassification rate for canonical variates than for principal components. All other error rates are less than, or equal to, their counterparts in principal components.

Canonical analysis established similar relationships between the paleosols made apparent in the cluster analysis discussed previously. In a plot of Canonical variable1 vs. Canonical variable 2, the trace element chemistry distinguishes between soil orders, and to some degree soil drainage (Fig. 3.5). The crossplot shows a distinct swath of data points, as well as "outliers" distinctly plotted apart from the swath. Only the paleosols separable using canonical variates were plotted on this graph. A region of indiscernible paleosols in canonical variate space is outlined in Figure 3.5. Data points overlap as a consequence of similar soil orders and soil drainage. Outlier paleosols include A10H, A11H, MH, A6b, and OH. With the exception of paleosol A6b, all outliers are Histosols. The swath can be separated into two clusters. Cluster one includes paleosols PH, A10, and PO, all poorly drained Vertisols. Cluster two includes paleosols PC, PE, and PM (well-drained Vertisols), and A4, PA, and A1 (poorly-drained Vertisols).

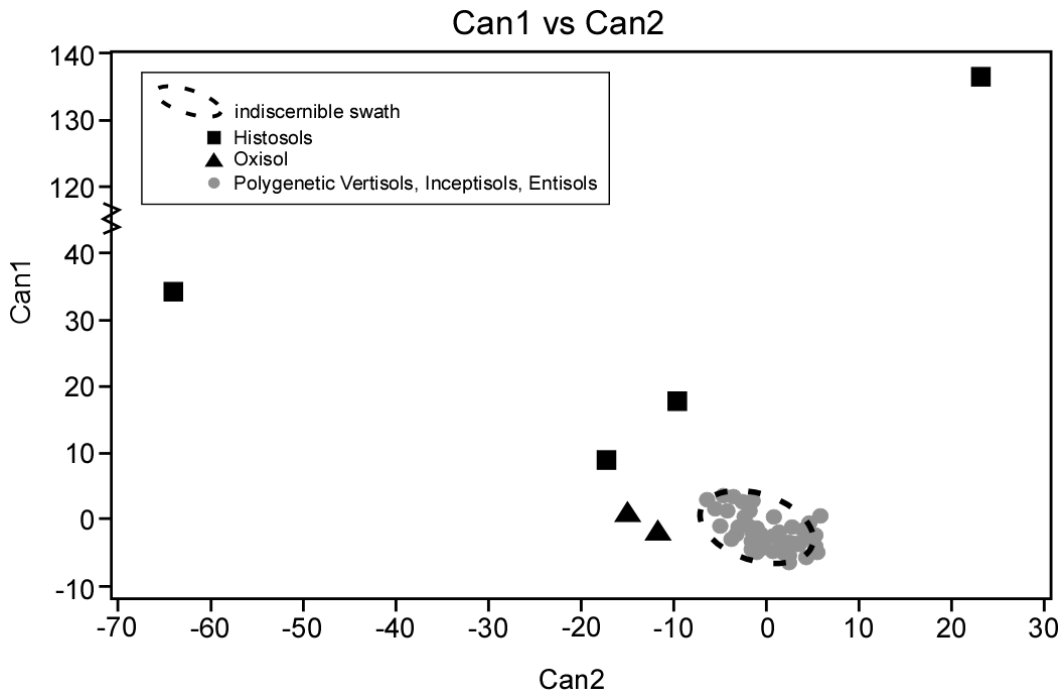

Figure 3.5 Crossplot of Canonical variate 1 vs. Canonical variate 2 for statistical differentiation of soil orders for Pennington Fm. paleosols. Note presence of several paleosol "outliers" as well as considerable overlap for some paleosols. See text for discussion.

Temporal Relationships

Temporal relationships were examined in the context of the matrix of correlations and the dendogram-based couples established by statistical analysis. Trace elements such as Nb, Ta, W, and Ti had strong temporal relationships as manifested by their high values in the correlation matrix (Table 3.2). Given their >0.75 *r*-values, these elements were plotted versus time, showing trends that covary, with little to no variation (Fig. 3.6*A*). Prominent peaks in trace element concentrations are associated with paleosols A6, A10, A11, PL and PO, whereas notable troughs/minima are associated with paleosols A6B, A10H, PH, and OH. Although the trace elements Ce, Hf, La, Th, and Zr had smaller *r*-values ($0.50 < r < 0.75$) than those of Nb, Ta, W and Ti, the correlations through time are still

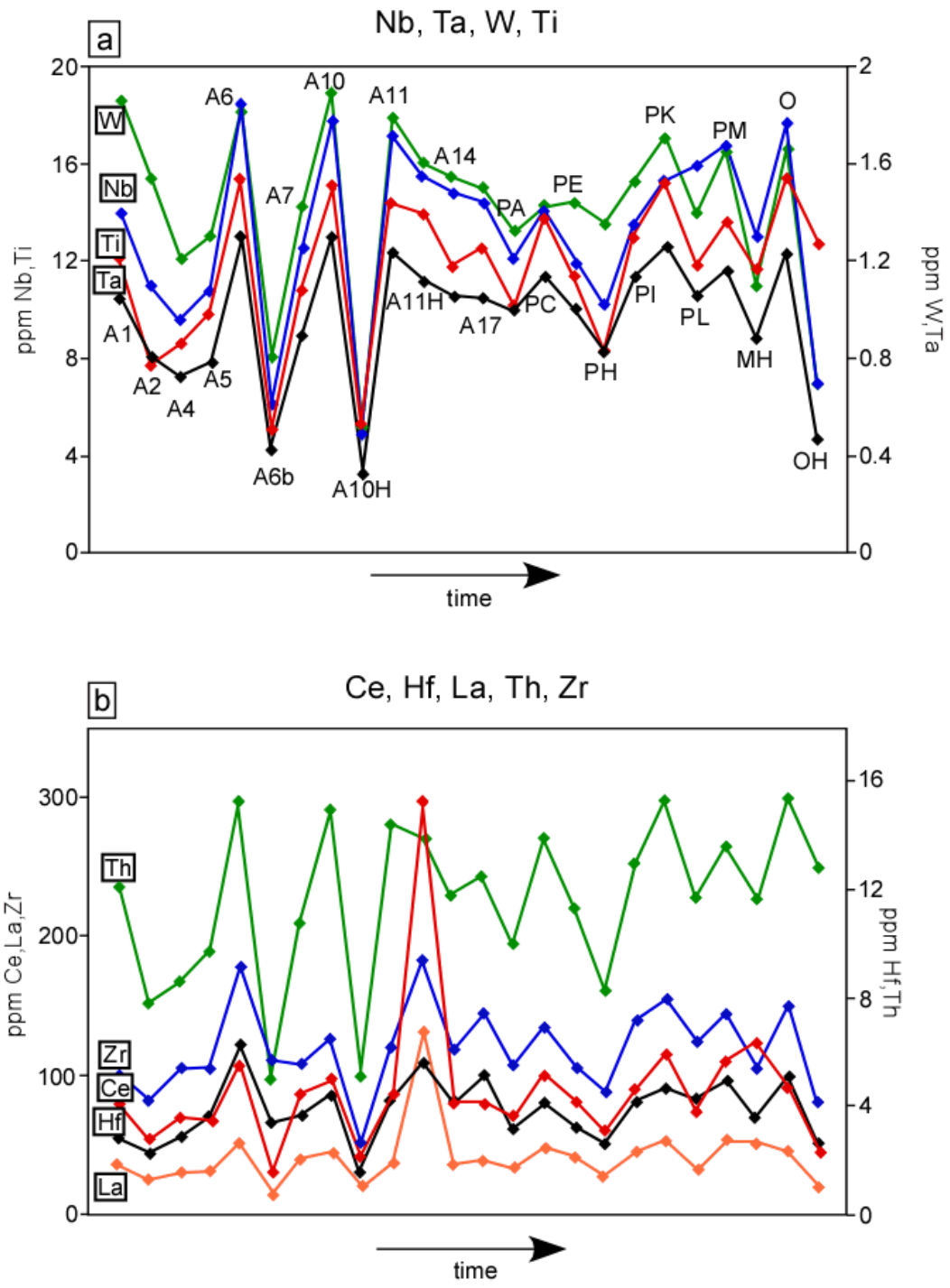

Figure 3.6 Trace element concentrations through relative time for Pennington Fm. paleosols. (a) Trace elements Nb, Ta, W, and Ti with correlations (*r*-value) >0.75 with 8 or more other trace elements. b. Trace elements Ce, Hf, La, Th, Zr with correlations (*r*-value) >0.75 with 8 or less other trace elements. See text for discussion.

tightly covarying, and the same relative minima and maxima hold true for these elements through time, although with slightly more variance (Fig. 3.6*B*).

Niobium (Nb), the element with the highest *r*-values, was chosen as the proxy with which to evaluate controls on trace element variability through time. Nb was chosen on the following basis: (1) its chemical behavior is similar to that of Ti, but avoids the risk of *a priori* assumptions of chemical behavior that would be introduced by using an established "immobile" element such as Ti or Zr, which is routinely used in mass-balance calculations for soils and paleosols (e.g., Chadwick et al., 1990; Driese et al., 2000), (2) Nb *r*-values are the highest and correspondingly have the highest number of correlations ($r > 0.50$) with other trace elements and therefore, (3) represents a typical response of trace elements to interpreted trace element controls. Nb concentrations through time co-vary with lessivage (Al_2O_3/SiO_2), a measure of clay production by feldspar weathering as well as clay translocation (Fig. 3.7*A*). Relative maxima and minima are as follow: maxima are recorded by paleosols A6, A10, and A11; minima are indicated for paleosols A6b, A10H, A11H, and OH. Although not shown here, the relationships of Nb to leaching (Ba/Sr) and base loss ($Al_2O_3/ (CaO + MgO + K_2O + Na_2O)$) through time are similar to those depicted for lessivage (Fig. 3.7*A*). Nb was plotted with mean annual precipitation (MAP) versus time in order to address the influence of paleoprecipitation; MAP for the Pennington paleosols was estimated using the CIA-K ($Al_2O_3/ (Al_2O_3 + CaO+Na_2O)$) paleoprecipitation proxy of Sheldon et al. (2002) and was reported in Kahmann and Driese (2008). The maxima observed in the Nb-lessivage plot are also apparent for the Nb-MAP plot

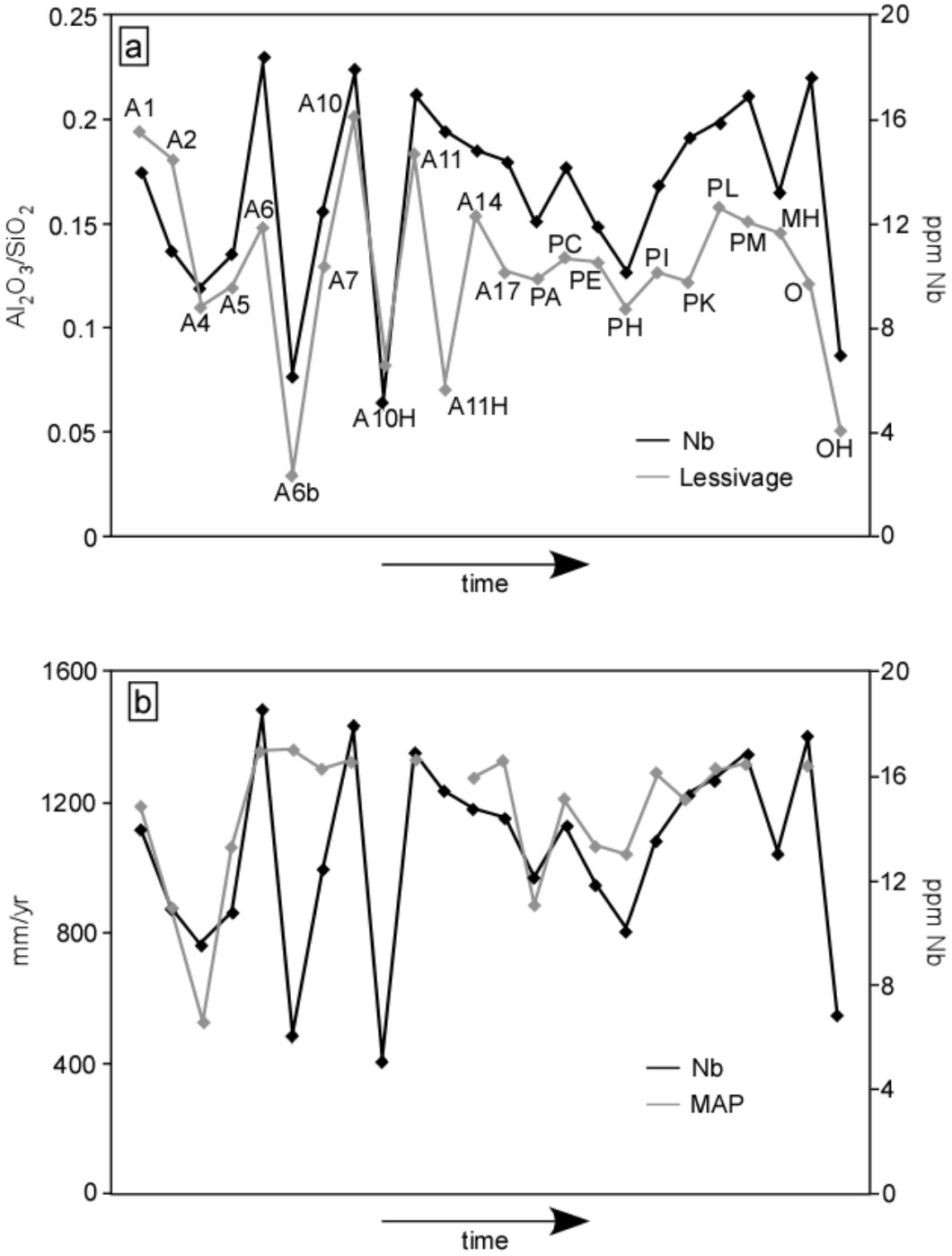

Figure 3.7 Niobium (Nb) concentrations (ppm) through relative time for Pennington Fm. paleosols. (a) Comparison with Al_2O_3/ SiO_2 (lessivage). (b) Comparison with mean annual precipitation (MAP) in mm/yr estimated using CIA-K geochemical proxy of Sheldon et al. (2002). See text for discussion.

(Fig. 3.7*B*), however, the minima are not apparent due to limitations of the CIA-K proxy in evaluating MAP for poorly drained, organic rich-soils represented by paleosols A10H, A11H and OH.

Many of the trace elements in soils and paleosols are metals, and susceptible to changing soil hydrology and redox conditions, as well as the presence of organic matter (Kabata-Pendias, 2001). Both Mo and MnO were plotted against lessivage and MAP. Mo was chosen because of its relatively high *r*-values and known chemical affinity for sorbing with organic matter and different mobilities under variable redox conditions. MnO was chosen for similar chemical behavior and as a comparison with Mo, even though it occurs in concentrations greater than 100 ppm and thus is technically not a trace element. Generally speaking, Mo and lessivage values have opposing trends, i.e., when Mo concentrations are high for paleosols A6b, A10H, A11H, MH, and OH, lessivage values are relative minima (Fig. 3.8*A*). The opposite is also true when concentrations for Mo are extremely low. As mentioned previously, paleosols A10H, A11H, MH and OH are Histosols and therefore characteristically organic-rich. Although the trends between Mo and MAP are not coupled through time, a few maxima/minima are related, as is the case for paleosols PK and PE (Fig. 3.8*B*). The trends in MnO and lessivage are likewise decoupled throughout Pennington paleosol formation (Fig. 3.9*A*). As with Mo, the temporal trends between MnO and MAP are not conclusive, although some weak covariation such that a few MAP maxima are associated the high MnO concentrations is suggested (Fig. 3.9*B*).

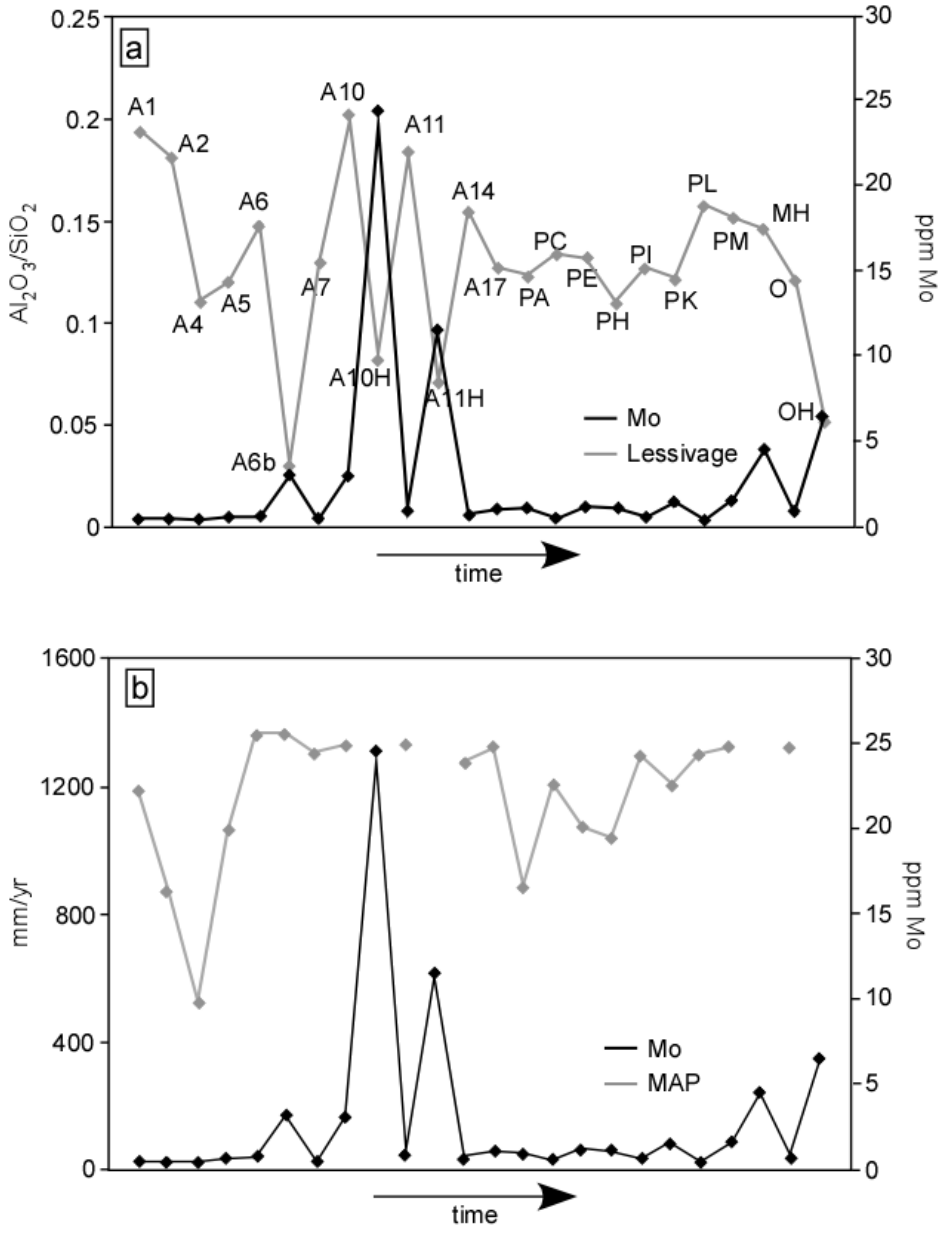

Figure 3.8 Molybdenum (Mo) ppm concentrations through relative time for Pennington Fm. paleosols. (a) Comparison with Al_2O_3/ SiO_2 (lessivage).(b) Comparison with mean annual precipitation (MAP) in mm/yr estimated using CIA-K geochemical proxy of Sheldon et al. (2002). See text for discussion.

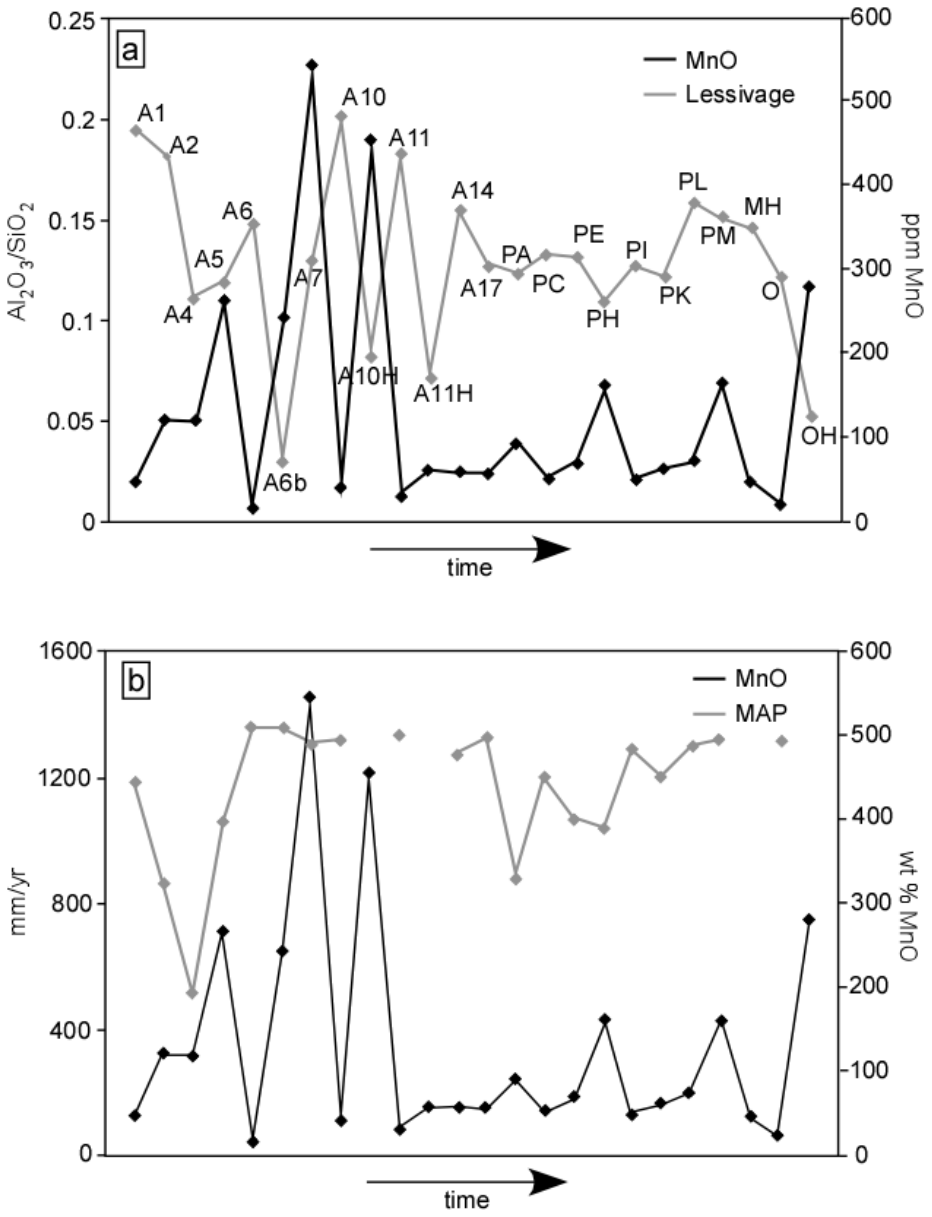

Figure 3.9 Manganese oxide (MnO) wt % concentrations through relative time for Pennington Fm. paleosols. (a) Comparison with Al_2O_3/ SiO_2 (lessivage).(b) Comparison with mean annual precipitation (MAP) in mm/yr estimated using CIA-K geochemical proxy of Sheldon et al. (2002). See text for discussion.

Discussion

Statistical Significance and Discrimination of Soil Attributes

Discriminant analysis of the paleosols based upon five canonical variates was clearly superior over the principal components-based discriminant analysis for all but one group of paleosols, as previously reported. The canonical variates methodology maximally separates the group means, which naturally lends itself to discriminant analysis. We therefore rely upon the discriminant analysis of canonical variates to confidently model associations between the Pennington paleosols, in tandem with the cluster analysis. Simple linear analysis, in the form of a correlation matrix (Table 3.2), was sufficient to interpret variance-covariance relationships between various trace elements.

Oxisol and Histosols are clearly distinguishable from the Pennington paleosol suite based upon both cluster (Fig. 3.4) and canonical variates analysis (Fig. 3.5). Both Oxisols and Histosols are unique in their formation and pedogenic environment: Oxisols require intense leaching and long periods of formation (Retallack, 2001) resulting in major losses of trace elements as well as major elements, with the exception of Si-, Al-, and Fe- and Mn-oxides. The Histosols have a chemical behavior similar to that of Oxisols as indicated by their second-order tiering in the dendogram (Fig. 3.4, Table 3.3), but with some significant deviations from the general Oxisol trend (Fig. 3.8*A*, 3.9*A*).

Both Vertisols and Inceptisols/Entisols tend to show similar statistical behavior, however, the dendogram does differentiate between a few of the Vertisols (Fig. 3.4). Kahmann and Driese (2008) documented variations in soil

drainage within the Pennington Fm.Vertisols, which were significant enough to separate these paleosols into well-drained and poorly-drained pedotypes formed under different hydrologic conditions. Both field and micromorphologic observations support an interpretation of changing soil drainage conditions as well during the formation of Pennington Inceptisols and Entisols. It is therefore reasonable to conclude that variations in soil drainage conditions are responsible for the differentiation of Vertisols in the statistical analysis of trace elements reported here.

Trace Element Controls

Clay translocation (lessivage) and organic matter accumulation, within the larger context of chemical weathering, are responsible for trace element trends through time, as well as the statistical discrimination of soil orders for the Pennington paleosols. The concentrations of Nb, Ta, W, Zr, Ti, Ce, Hf, La, and Th covary with lessivage/clay translocation through time (Fig. 3.6*A*, 3.6*B*). Many trace elements, and especially the REE's, are strongly sorbed to clays (Caspari et al., 2006; Marques et. al., 2004; Brown et al., 2003; Kabata-Pendias, 2001; Zhang et al., 2001), therefore greater intensities of clay production by feldspar weathering and clay concentration (lessivage) would result in corresponding trace element accumulation (Fig. 3.7*A*). Maximum trace element accumulation also occurs in association with poor soil drainage in both Vertisols and Inceptisols. The previously documented polygenetic character of Pennington Vertisols (Kahmann and Driese, 2008), however, complicates simple interpretations of trace element distributions. For example, the overall character of Vertisol soil

drainage attributes (slickensides, sepic-plasmic microfabrics, pedogenic carbonates) may indicate well-drained conditions with higher ratios of lessivage, but the history of Pennington Vertisol genesis apparently included alternating periods of poor soil drainage during which lessivage (clay translocation) may have been inhibited. Therefore, the overall patterns of trace element distributions reflect an "average" of good and poor drainage.

Statistical analysis determined that the Histosols and Oxisol had trace element concentrations significantly different from those of Vertisols and Inceptisols (Fig. 3.6; referring to Fig. 3.5). The high concentrations of Mo (corresponding to Histosol formation) and other trace metals suggest that organic matter is a primary control (Fig. 3.8). Histosols are organic-rich, and are derived from the accumulation of decaying flora as opposed to mineral soils composed of transported sediments from a source area. Trace metals such as Mo form organic ligands (Olivie-Lauquet, 2001) and their concentrations are thus greatly influenced by the presence of organic matter (Kabata-Pendias, 2001). La and Th concentrations co-vary with lessivage, and this variation can be attributed to organic matter content because La and Th also form organic-ligands (Olivie-Lauquet, 2001) (Fig. 3.6). REE, such as La, Th, and Ce are also mobilized by organic acids in the soil environment (Caspari, 2006).

Not only does organic matter content play a role, but the presence of redox-sensitive elements and variable redox conditions during pedogenesis can also exert a minor control upon trace element accumulation in paleosols. The Pennington Oxisol was interpreted to have formed in a wet/humid environment

where weathering rates were high with significant vegetative cover (Kahmann and Driese, 2008). Trace metals such as Mo are highly redox-sensitive (Kabata-Pendias, 2001; Olivie-Lauquet, 2001) and are associated with elevated Fe and Mn concentrations. Elevated Fe concentrations of the Pennington Oxisol are typical of ancient Oxisols (Pe-Piper, 2005). Trace element accumulation in the Oxisol would therefore suggest that trace elements are depleted during oxidizing conditions, whereas poorly-drained, reducing paleosols A10 and A11 show trace element accumulation. Although Mn and Mo have strong correlations, Fe concentrations do not have any *r*-values ≥ 0.50 (Table 3.2) and may not influence trace element accumulation. Thus, not only is there an organic matter influence upon the concentration of trace elements, but potentially the influence of redox conditions and presence of redox-sensitive elements.

Chemical Weathering

Weathering, soil formation, and abundance of trace element concentrations are clearly linked (Caspari, 2006). Sheldon (2006) interpreted the trace element and REE chemistry of Triassic-Permian paleosols as an indication of a rapid climatic shift accompanied by increased intensity of chemical weathering. Similarly, the formation of the Pennington Formation Oxisol is associated with the highest degree of chemical weathering (Fig. 3.3). Due to increased rates of chemical weathering, trace element concentrations consequently decrease (Fig. 3.6). Oxisols have very long periods of soil formation and are characterized by kaolinite and gibbsite clay mineralogies and concentrations of hematite and/or goethite suggesting high rates of chemical

weathering in oxidizing conditions (Muggler and Buurman, 2000). The Oxisol in this study has a kaolinite-dominated mineralogy (Kahmann and Driese, 2008). Canonical analysis and clustering both record the highly decreased nature of trace element concentrations for the Oxisol as compared with all other paleosol types (Figs. 3.4, 3.5).

Whereas Oxisols represent maximum chemical weathering intensities, Histosols conversely record greatly decreased weathering intensities, with the Vertisols reflecting highly variable weathering intensity. The susceptibility of the Histosols to chemical weathering is likely decreased due to poor soil drainage coupled with reducing conditions (Kahmann and Driese, 2008). Vertisols, by virtue of high clay contents, are especially susceptible to changing soil drainage conditions (Wilding and Tessier, 1988). The variations in chemical weathering indices, and trace element concentrations in Oxisols, Histosols and Vertisols through time, record changes in weathering intensities (Figs. 3.3, 3.6).

MAP estimates trend closely with trace element concentrations through time as well as chemical weathering and lessivage through time (Fig. 3.7B). The paleoenvironmental conditions of Oxisol and Histosol formations were very wet. MAP estimates are high for formation of the Oxisol, as well as chemical weathering intensity. Trace element concentrations subsequently fall due to high precipitation and chemical weathering rates. MAP estimates for the Vertisols are highly variable as a consequence of changing soil drainage. Vertisols are characterized and identified by their shrink-swell features generally associated with seasonality of climate or seasonal soil-moisture deficits (Wilding and

Tessier, 1988; Lynn and Williams, 1992). The clustering of Vertisols in both the dendogram and the Canonical Variates crossplot likely records the effects of seasonality on trace element distributions (Figs. 3.4, 3.5). The variability of Vertisol trace element chemistry is a consequence of a wet-dry climate for the Late Mississippian, which was characterized by high-frequency climate changes.

Conclusions

The application of linear and multi-variate statistics to the trace element geochemistry of Pennington Formation paleosols indicates the following:

1. Correlation matrices suggest chemical similarity between Nb, Ta, W, Zr, Ti, Ce, Hf, La, and Th with *r*-values greater than 0.50, the majority of which exceed 0.75.

2. The discriminant procedure run using a canonical analysis for the dataset is confidently modeled and suggests a robust dataset with which to study trace elements through time.

3. Cluster and canonical variates analysis differentiate paleosols based upon previously assigned soil orders (Kahmann and Driese, 2008) and less confidently upon inferred soil drainage class.

4. Trace element concentrations through time are controlled by clay production by feldspar weathering and clay translocation (lessivage), as well as by the presence of organic matter.

5. Trace element concentrations are broadly reflective of variations in the intensity of weathering experienced over time during the Late Mississippian and similarly correspond to changes in mean annual precipitation (MAP) estimated using other geochemical proxy indicators.

6. A high-frequency Late Mississippian climate characterized by extreme wet and dry periods can be inferred from trace element concentrations through time.

This work serves as a “pilot-study” that introduces trace element chemistry in conjunction with statistical analysis as potentially useful, but

currently underutilized paleoclimate indicators. Further investigations are essential to develop a more quantitative application of this paleoclimate tool. From a statistical standpoint a larger sample size (i.e., more stratigraphic sections and paleosols) is needed to validate these statistical procedures, and other methods might be tested that account for the individual covariance matrices. In addition, only high *r*-value correlations were investigated in association with soil processes. A comprehensive study needs to be conducted concerning other highly correlative trace elements, specifically those with high negative correlations. The application of multivariate statistics to trace element data from paleosols is especially useful in supporting paleoclimate interpretations, when paleosol attributes are confidently known using other established methodologies. Trace element characterization of modern soils, as it relates to soil order and soil drainage, must also be carried out in a variety of climate regimes, in order to better understand trace element behavior in lithified paleosols. Geochemical investigations of younger Tertiary-Quaternary paleosol-loess sequences of China (Guo et al., 1998; Jahn et al., 2001; Yin and Guo, 2006), and of modern Vertisols in Texas (e.g., Stiles et al., 2001, 2003; Driese et al., 2005), will also serve to test the procedures and methods applied in this Late Mississippian paleosol case-study.

CHAPTER FOUR

Sequence Stratigraphy of the Chesterian Pennington Formation, Pound Gap, KY, USA: An Intertonguing Marine-Terrestrial Succesion

Abstract

A sequence-stratigraphic analysis of the Pennington Formation (latest Chesterian), Pound Gap outcrop section identifies eustatic controls on sedimentation, in response to both tectonic and climate forcing. The Pennington was deposited within the tropics and sub-tropics and records the effects of icehouse conditions of the Late Mississippian. Outcrop description and facies stacking patterns suggest a variety of depositional environments ranging from rainforest, coal swamp, tidal-estuarine, and open-marine carbonate-ramp systems. Although the Pennington is dominated by siliciclastic deposits, there were intermittent periods of marine carbonate sediment production induced by a decline in terrestrial sediment input associated with regional uplift. Three tiers of stratal cyclicity have been identified within the Pennington: composite sequences, sequences, and cycles. Composite sequences are controlled by Gondwana glaciations and represent the longest period of geologic time. Generally speaking, the Pennington became more clastic-dominated due to Mississippian icehouse conditions. Sequence development is controlled by both tectonics and climate, and within each sequence, systems tracts (both marine and alluvial) are proposed where preserved. Individual cycles within sequences may reflect both tectonism and climate, however, paleosol development and the nature of fluvial cyclicity

would suggest the latter. High-frequency climate change is recorded by paleosol formation, possibly associated with seasonal migration of the paleo-Intertropical Convergence Zone.

Introduction

The Mississippian was a period of dynamic climate change, and in the Appalachian Basin, records icehouse climate conditions associated with the buildup of Gondwana continental glaciers in the southern hemisphere (Maynard et al., 2006; Miller and Eriksson, 2000; Smith and Read, 2000). We propose that the Pennington Formation (Upper Chesterian) at Pound Gap has evidence for higher frequency climate change; however, other controls on sedimentation and cyclicity overprint the high-frequency climate signal that should be represented in the Pennington Formation. In order to determine controls on cyclicity and sedimentation in the Pennington, a sequence-stratigraphic study is necessary to evaluate composite base level fluctuation and its response to reported variations in glaciation, tectonic processes, and climate.

Several orders of cyclicity for Upper Mississippian rocks in the Appalachian Basin have been previously reported. Third-order cyclicity, controlled by both eustatic and tectonic forcing are recorded in West Virginia (Maynard et al., 2006; Al-Tawil et al., 2003) as well as in the vicinity of the field area of this study in southwestern Virginia (Al-Tawil and Read 2003). However the study by Al-Tawil and Read (2003) did not include the Pennington Formation. Fourth-order cyclicity has also been suggested by (1) Wynn and Read (2007) in ramp-slope mudstones of Virginia, Kentucky, and West Virginia, (2) ramp

carbonates of a similar geographic area of study including the Pound Gap exposure (Al-Tawil and Read, 2003), and (3) in terrestrial siliciclastic deposits of West Virginia (Miller and Eriksson, 2000). The majority of these authors postulated even higher orders of cyclicity but could not demonstrate their lateral continuity from one geographic area to another.

These higher orders of cyclicity within the Appalachian Basin were initially proposed to be the result of climate-forcing (Cecil, 1990). The ability to identify high-frequency climate change is enhanced by recognition of paleosols including coals in the Late Mississippian. Paleosols within Paleozoic and Mesozoic stratigraphic sections have proven to be valuable tools in the interpretation of paleoclimate and paleoenvironments (e.g., McCarthy et al., 1998; Mora and Driese, 1999; Driese et al., 2000; McCarthy, 2002; Sheldon et al., 2002; Driese et al., 2005). Paleosols developed in the Pennington Formation at Pound Gap were first identified and reported by Greb and Caudill (1998) and subsequently were evaluated in greater detail by Kahmann and Driese (2008). A number of related paleosol studies involving climate change have been completed within coeval deposits of the Appalachian Basin (Caudill et al., 1996; Mora et al., 1998; Miller and Eriksson, 1999; Driese et al., 2000; Robinson, 2002; Driese et al., 2005). This study, however, utilizes modern sequence-stratigraphic concepts as well as the most recent study of Pennington Formation paleosols by Kahmann and Driese (2008) and Kahmann et al. (2008) to evaluate the control of high-frequency climate variation on sedimentation.

Back ground Information

Tectonic Setting

During latest Mississippian time the study area at Pound Gap, currently located on the border of eastern Kentucky and southwestern Virginia, Fig. 4.1),

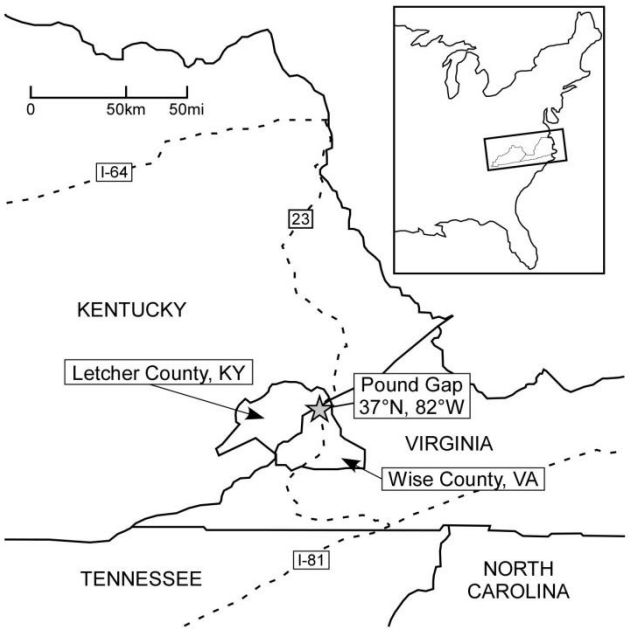

Figure 4.1 Location of the Pound Gap study area on the Kentucky-Virginia border. GPS coordinates: 37° 09′ 18” N, 082° 37′ 58” W.

was located between 5° and 10° S latitude (Ziegler et al., 1979; Scotese and McKerrow, 1990). Subsidence dominated much of the Appalachian Basin during the early part of the Chesterian, with maximum subsidence taking place before the mid-Chesterian (deWitt and McGrew, 1979). Structural features of importance included the Cincinnati Arch to the west, the Waverly Arch to the north-northwest (Woodward, 1961), and the Pine Mountain thrust to the east. During the Late

Chesterian, the Cincinnati Arch became active, and areas east of the Appalachian Basin were uplifted (Dever, 1999) and delivered sediments into the distal foreland basin (de Witt and McGrew, 1979). Uplift of the Waverly Arch appears to have had minor effects on sedimentation in the basin (Sable and Dever, 1990). The Waverly Arch, however, continued to experience uplift and remained a positive paleotopographic feature throughout the Chesterian and into the Pennsylvanian (Dever, 1999). Uplift of source areas contiguous to the eastern side of the basin continued throughout the Late Chesterian at an accelerated pace (deWitt and McGrew, 1979). Lithospheric flexure, the development of a peripheral bulge, and subsequent bulge migration were suggested as a potential driver of uplift for both the Cincinnati Arch (Dever, 1999; Chestnut, 1991; Tankard, 1986; Quinlan and Beaumont, 1984) and the Waverly Arch (Dever, 1999; Ettensohn, 1998).

The final tectonic event to influence sedimentation in the eastern portion of the Appalachian Basin occurred during the Late Pennsylvanian with emplacement of the Pine Mountain Thrust (Andrews and Nelson, 1998; Mitra, 1988). The Mississippian-Pennsylvanian unconformity at Pound Gap is a prominent erosional surface. This surface is inferred to record Late Mississippian visco-elastic relaxation after loading, prior to the beginning of the main Alleghanian orogenic processes associated with the initial collision of the Gondwanan and North American continents (Ettensohn, 1998).

Stratigraphic Setting

The Pennington Formation was deposited during the latest Mississippian (Chesterian) in coastal-plain to transitional-marine environments after shallow-marine seas deposited the Newman Limestone (Greb and Eble, 1988; Al-Tawil and Read, 2003) (Fig. 4.2). Conodont zonations for the Chesterian stage are inconsistent within the literature, therefore, the conodont zone boundaries annotated on Figure 4.2 represent approximations (Collinson et al., 1971; Dutro et al., 1979; Miller and Eriksson, 1999; Al-Tawil and Read, 2003; Al-Tawil et al., 2003; Maynard et al., 2006). The Chesterian stage within the study area defined by the following zones (in ascending order): *Gnathodus bilineatus- Kladognathus mehli, Kladognathus primus, Kladognathus-Cavusgnathus naviculus* and *Adetognathus unicornis* (Fig. 4.2). Pennington deposition was terminated by development of the Mississippian-Pennsylvanian unconformity, the Kaskaskia-Absaroka supersequence boundary of Sloss (1963). Upon this surface Pennington terrigenous clastic deposits were likely removed by Pennsylvanian fluvial downcutting and valley incision. The Pennsylvanian fluvial deposits of the Lee Formation overlie the Mississippian-Pennsylvanian unconformity (Greb, 1998a). Despite the uncertainty in both the biostratigraphy and chronostratigraphy at Pound Gap, the Pennington Formation likely spans approximately 8-9 Myr (Fig. 4.2)

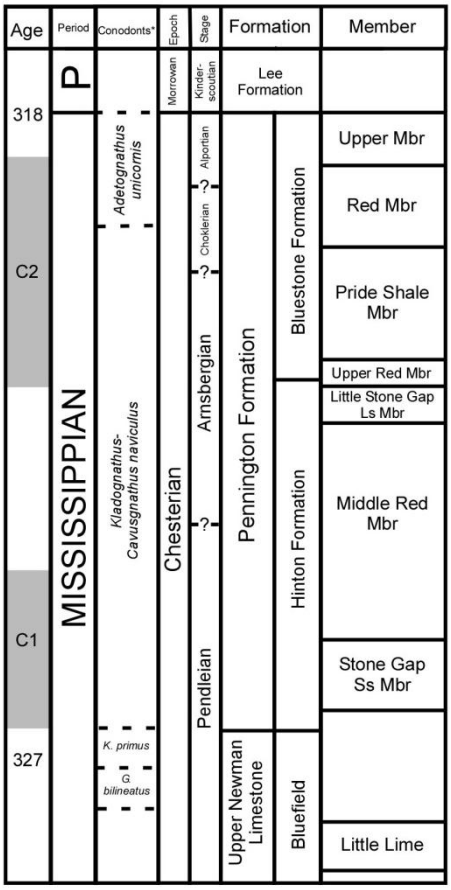

Figure 4.2 Stratigraphic nomenclature for the Late Mississippian in Virginia, Kentucky, and West Virginia. Conodont zones are tentatively drawn from multiple (and somewhat inconsistent) sources. See text for discussion. Stratigraphic nomenclature is based upon Al-Tawil and Read (2003) and Ettensohn et al. (1998). Glacial zones C1 and C2 are adapted from Fielding et al. (2008) and Menning et al. (2000).

Methods

Field and Laboratory Methods

The Pennington Formation was logged and measured in detail from the top of the Newman Limestone to the Mississippian-Pennsylvanian unconformity. The precise location of the boundary between the Newman Limestone and Pennington Formation, at Pound Gap, is not certain (Nelson and Read, 1990). The stratigraphically lowest unit described is a paleosol overlying an articulate-

brachiopod packstone that approximates the location of the top of the Newman Limestone. Depositional units were described based upon grain size and texture, sedimentary structures, trace fossils, and allochems (in the case of limestone and dolostone) observed. Samples of Units 77 and 79, which are black shale (Fig. 4.3), were collected at approximately 5 m intervals (spanning the entire two units) for subsequent geochemical analysis.

Twenty-four facies were described including clastic, carbonate, and pedogenic (Table 4.1). The measured section and associated facies were compiled into a stratigraphic column (Fig. 4.3). Clastic facies were classified based upon texture, sedimentary structures, and bedforms. Designations for the clastic alluvial facies are modified from Miall (1978), and take into account grain size and dominant sedimentary structures. Carbonate strata were classified according to the Dunham (1962) scheme. Carbonate facies were described in detail, paying particular attention to allochems, texture and sedimentary structures.

Forty paleosols were identified, described using USDA Soil Taxonomy (Soil Survey Staff, 1998), and organized into pedotypes (*sensu* Retallack, 1988) by Kahmann and Driese (2008). Each pedotype (Table 4.1) is based on one representative profile that sufficiently captures characteristic morphologies and attributes distinguishing that pedotype from other paleosols.

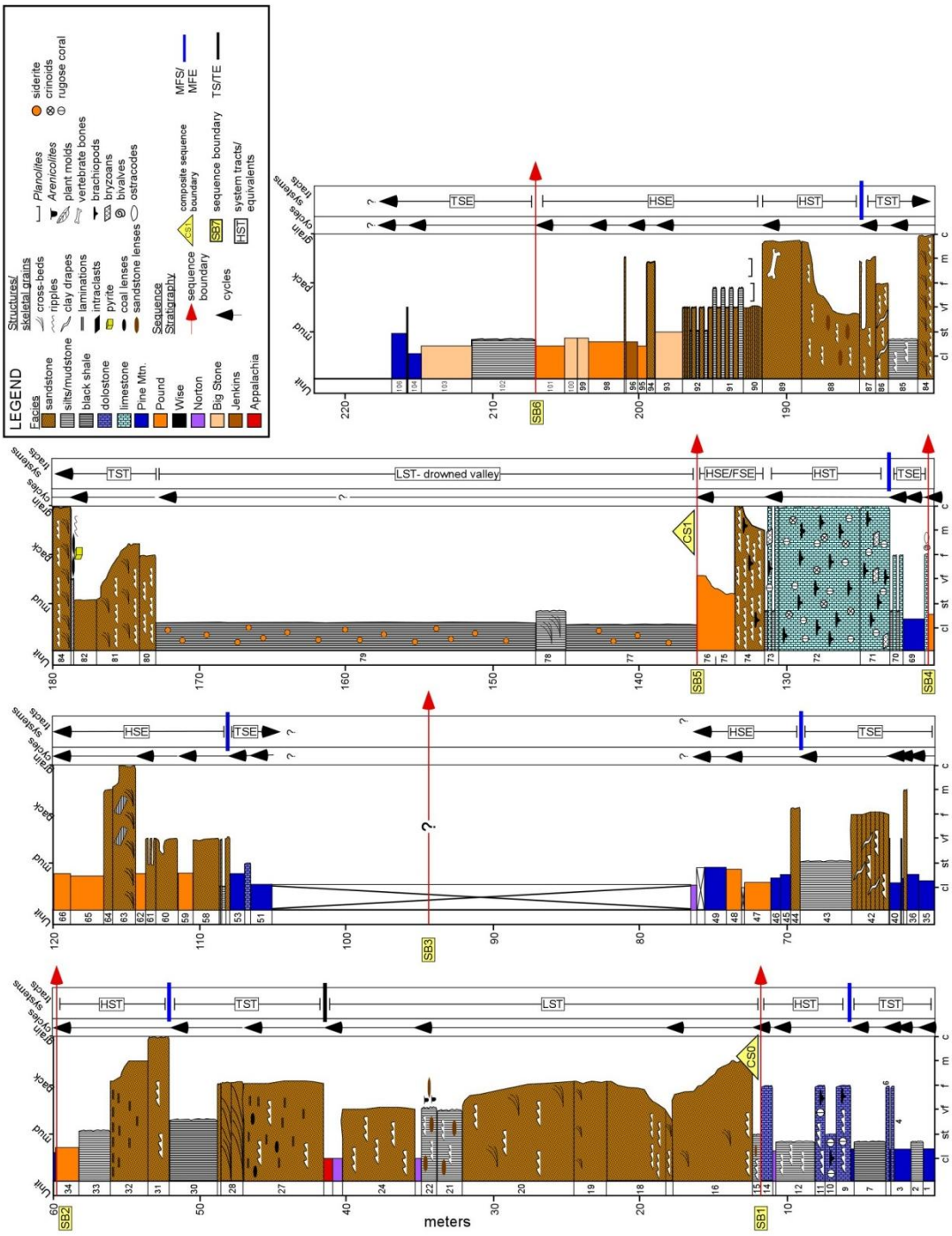

Figure 4.3 Pennington Formation stratigraphic section. Refer to figure legend for explanation of symbols.

Table 4.1 Description for clastic, carbonate, and pedogenic facies, including the frequency observed in the Pennington as well as percent thickness of the Pennington.

Designation	Description	Environment	frequency	%thickness
Clastic				
Shb	black shale to black silty claystone	incised valley fill	3	20.33
Shg	gray fissile shale to claystone	deltaic/estuarine	8	5.27
Vfx	very fine sandstone, cross trough bedding	deltaic	1	0.32
Frx	fine sandstone, 0.5-2cm bedded, rippled, cross trough bedding	deltaic	1	0.28
Frcl	fine sandstone, rippled, clay drapes	tidal	1	0.86
Fr	fine sandstone, rippled	deltaic	3	3.88
Fm	fine sandstone, massive	fluvial	4	3.32
Ftb	fine sandstone, 5-10cm beds	fluvial	2	0.64
FMr	fine-medium sandstone, 5-10cm rippled beds	deltaic	4	4.56
FSi	fine sandstone, interbedded w/ siltstone	tidal	1	1.02
Mu	medium sandstone, fining-upward	fluvial, marine	2	3.65
Mtb	medium sandstone, 5-10cm beds	fluvial	1	1.24
Mx	medium sandstone, cross trough bedding, may be rippled	deltaic	5	7.26
Mm	medium sandstone, massive	fluvial	8	3.01
Cx	coarse sandstone, cross trough bedding	deltaic	1	1.08
SiCl	interbedded siltstone/claystone	tidal	1	0.32
Shrss	shale, ripple-laminated w/ interbedded sandstone lenses	tidal	3	1.76
SiShr	silty shale, ribbon rock, ripple laminated	tidal	2	1.38
Carbonate				
Dp	dolomitized packstone massive	open marine	4	0.87
Dpr	dolomitized packstone, rippled	open marine	2	0.65
Dm	dolomitized mudstone	open marine	1	0.19
Pa	packstone	estuarine	1	0.06
PaSh	packstone interbedded w/ shale	estuarine	1	0.70
Ga	grainstone	open marine	3	3.70
Pedogenic				
PD	Pound pedotype: well-drained Vertisol, pedogenic carbonate	well-drained soil	13	7.88
PM	PineMtn pedotype: poorly-drained Vertisol, FeMn nodules	poorly-drained soil	17	6.61
JE	Jenkins pedotype: Alfisol, illuviated clay	well-drained soil	1	0.37
NT	Norton pedotype: Inceptisol	stable overbank	3	0.92
BS	Big Stone pedotype: Entisol	forest	4	3.85
AP	Appalachia pedotype: Oxisol, dense rooting	rain forest	1	0.03
WI	Wise pedotype: Histosol, coal	swamp	3	0.48
Covered		covered		13.51

Geochemical analysis was required to assist in determining the environment of deposition for Units 77 and 79, which are black shale. Samples were prepared, decarbonated with HCl, and analyzed by the University of Kansas W.M. Keck Paleoenvironmental and Environmental Stable Isotope Laboratory (KPESIL) for % total N, % total organic C, $\delta^{13}C$, and $\delta^{15}N$ (both delta values are expressed in the standard per mil (‰) notation using the PDB and N_2 of air standards, respectively) using a Costech ECS 4010 Elemental Combustion System in conjunction with a Finnigan MAT 253 isotope ratio mass spectrometer.

Sequence- Stratigraphic Nomenclature

The dynamic, changing depositional environments interpreted for thePennington Formation range from open-marine to subaerial exposure and pedogenesis. As such, the complex nature of the deposits poses a formidable task in unraveling sequence- stratigraphic relationships. To clarify, we define the nomenclature used, and the inferences drawn from that nomenclature. The lack of chronostratigraphic constraints within the Pennington necessitates a nomenclature that makes no assumptions as to the duration of deposition, such as 3rd order sequences/cycles (Van Wagoner, 1995) or high-frequency sequences (Mitchum and Van Wagoner, 1991; Tinker, 1998). The terminology used must therefore rely upon physical relationships alone.

Although absolute time spans are not known, a three-tier hierarchy of stratal units documented in this study is suggestive of varying accommodation frequencies. For example, a composite sequence is of longer duration in geologic time than that of a sequence. Similarly, a cycle accumulated in response to a higher frequency accommodation episode than a sequence. The term *unit* is defined by a facies change (beds or bedsets) where the lithology, type or suite of sedimentary structures and/or allochems changes. Units are subdivisions of cycles. Similar to a parasequence (Van Wagoner et al., 1988; 1995), cycles are genetically related beds or bedsets bound at their base and top by a surface of rapid environmental change. This surface of rapid environmental change can be created by a flooding event within the marine realm, or channel avulsion within the terrestrial realm. Sequences are composed of cycles, and their boundaries are

identified by one or more of the following criteria: subaerial exposure, a basinward shift in facies (Van Wagoner et al., 1988), abnormal facies successions, and/or a surface associated with erosional truncation of underlying units. Sequence boundaries are always associated with a cycle boundary and most often with pedogenesis. Sequences stack into composite sequences. The composite sequence boundary is coincident with a sequence boundary, however, with greater geologic significance manifested by reciprocal sedimentation (Van Siclen, 1958; Wilson, 1965) or truncation of prolonged periods of landscape stability.

Systems tract terminology is applied to better understand sequence development and cyclical hierarchy. In marine successions we refer to the terminology and nomenclature defined by Van Wagoner et al. (1988). Wright and Marriott (1993) suggested that accommodation and systems tract concepts, as used in marine sequence stratigraphy (Sarg, 1988; Van Wagoner et al., 1988), also transfer to sediment accumulation on a terrestrial floodplain. This concept has been used in a number of investigations of alluvial successions (Bown and Kraus, 1987; Kraus, 1987; Atchley et al., 2004; Prochnow et al., 2006, Cleveland et al., 2007). Base level is the surface of equilibrium between erosion and deposition within both marine and continental areas (Catuneanu, 2002).

Systems tracts are identified based upon the following facies attributes and stratal stacking patterns. For both marine (LST) and terrestrial (LSE) successions the lowstand systems tract (LST) is recognized by a coarsening sediment fraction, includes aggradational fill of incised valleys, and is capped by the transgressive surface (TS) or maximum regressive surface (*sensu* Van Wagoner et al., 1988).

The transgressive systems tract in marine (TST) and terrestrial deposits (TSE) both exhibit fining-upward profiles and it is bound by the TS/TE at its base and by the maximum flooding surface (MFS/MFE; marine/terrestrial) at its top. The MFS/MFE is recognized by a basinward shift in facies (shift towards the channel in terrestrial deposits), the abrupt increase in water depth / accommodation, or a coarser sediment fraction overlying a finer sediment fraction. In terrestrial successions the high-stand systems tract (HSE) is recognized by upward-fining in fluvial grain size, whereas in marine successions (HST) it is recognized by coarsening-upward successions. The HSE/HST is bound at its base by the MFE/MFS and at its top by a sequence boundary. Other evidence for systems tract assignments, particularly with regard to pedogenic facies, will be discussed further on a sequence-by- sequence basis.

Results

Changes in grain size, texture and sedimentary structures are depicted in the stratigraphic section shown in Figure 4.3. Table 4.1 summarizes the observed facies represented in the stratigraphic section (Fig. 4.3), as well as their number of occurrences in the Pound Gap section, percent of total thickness in section, their designation as clastic, carbonate, or pedogenic, and probable environment of deposition. Figure 4.4 shows a comparative relationship between facies, depositional environments, and percent section of each facies. Examples of facies in outcrop are provided in Figure 4.5.

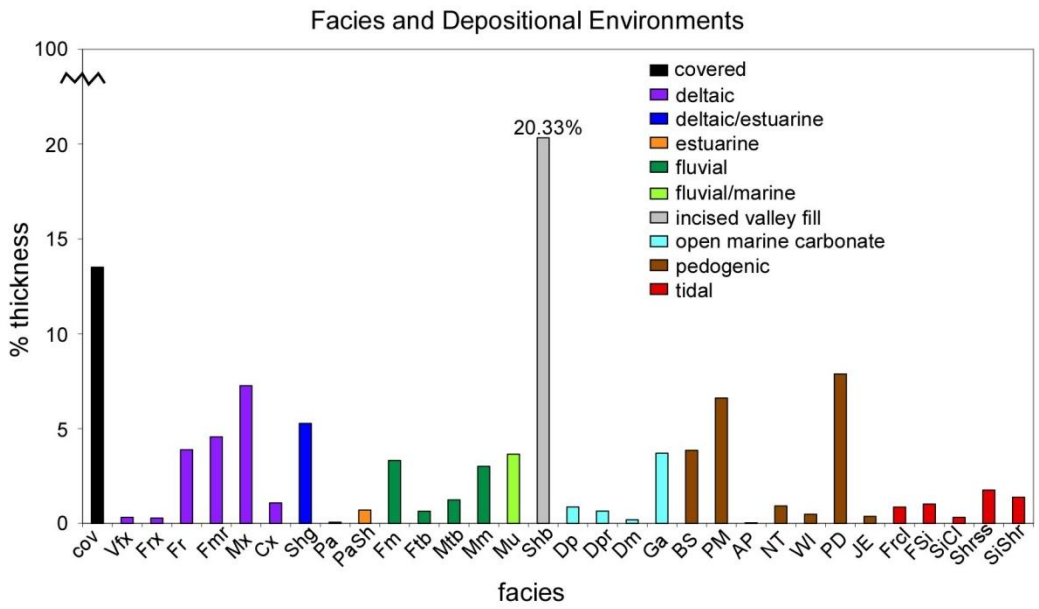

Figure 4.4 Relationships between facies, depositional environments, and percent (%) thickness that each facies represents in the Pennington section.

Facies and Pedotypes

Clastic facies do not display a high degree of variability. The dominant clastic facies (Fig. 4.4, Table 4.1) includes massive medium-grained sandstone (*Mm*), gray fissile shale to claystone (*Shg*), and medium-grained sandstone with trough cross-bedding and current ripples (*Mx*). With the exception of the trace fossil *Arenicolites*, trace fossils are rare. Because of the absence of trace fossils and other diagnostic sedimentary structures, depositional environments for the clastic facies are difficult to determine, hence we emphasize facies successions as "clues" for interpreting individual facies.

Successions of carbonate facies are much less abundant than clastic facies, and account for only ~6% (Fig. 4.4) of the entire section. The most common carbonate facies is a massive dolomitized packstone (*Dp*). Because of the distinctive origin of skeletal grains in carbonate rocks, environments of deposition

can be more easily determined. Dominant skeletal grains include an open-marine assemblage of brachiopods, fenestrate bryozoans, crinoids, rugose coral, and less commonly, mollusk fragments in association with ostracodes (Fig. 4.5A).

Paleosols, classified into pedotypes, account for 20% of the observed facies in the Pound Gap outcrop section. Each pedotype is based on one representative "type" paleosol that sufficiently captures characteristic morphologies and attributes distinguishing the pedotype from all other paleosols of other pedotypes. The majority of paleosols observed in the Pennington belong to the Pound (*PD*) and Pine Mtn (*PM*) pedotypes, which are both classified as Vertisols, with differing soil drainage histories (Table 4.1). Less common are paleosols belonging to the Appalachia (*AP*) and Wise (*WI*) pedotypes, classified as an Oxisol and Histosol respectively (Table 4.1). For a thorough description of paleosol attributes and related paleoenvironmental/paleoclimatological conditions within the Pennington Formation please see Kahmann and Driese (2008).

Geochemistry of Black Shale

The geochemical data for Units 77 and 79, laminated fissile shale, are summarized in Table 4.2. Due to a lack of conodont material, and to better determine the depositional environment for Units 77-79, samples were also collected from an older marine black shale unit within the Newman Limestone for comparison (New 1a-1c in Table 4.2). The $\delta^{13}C$ values of bulk organic matter in shale samples ranged from -22.93 to -23.13 ‰ PDB and from -23.50 to -22.66 ‰ PDB, for the Newman and Pennington shales, respectively. Generally speaking, both units become isotopically "more enriched" in ^{13}C through time. The ranges

of C/N ratios are 13.5 to 13.6 for Newman shale samples and 13.4 to 18.3 for the Pennington samples. The Pennington shows a steady increase in the C/N ratio up-section. A plot of ^{13}C values versus C/N ratios (Fig. 4.6) graphically represents the sources of organic carbon (Meyers, 1994) for these samples. Values for both the Pennington and Newman plot within the range of $\delta^{13}C$ values for marine algae, but are skewed towards the field of C3 land plants due to their increased C/N ratios.

Interpretations

Depositional Environments

Depositional environments of the Pennington Formation range from open-marine ramp carbonates to terrestrial landscapes. The block diagram in Figure 4.7 represents our interpretation for the majority of the Pennington. With the diversity of environments and sediment controls, however, this diagram does not represent completely the characteristics of each environment. For instance, during transgressive to highstand clastic-lean periods of deposition, the open-marine carbonate ramp would replace the deltaic environment and parts of the estuarine environment. This block diagram and its inherent interpretations were strongly influenced by the depositional models of Horne et al. (1978) for the Appalachian Basin during the Carboniferous.

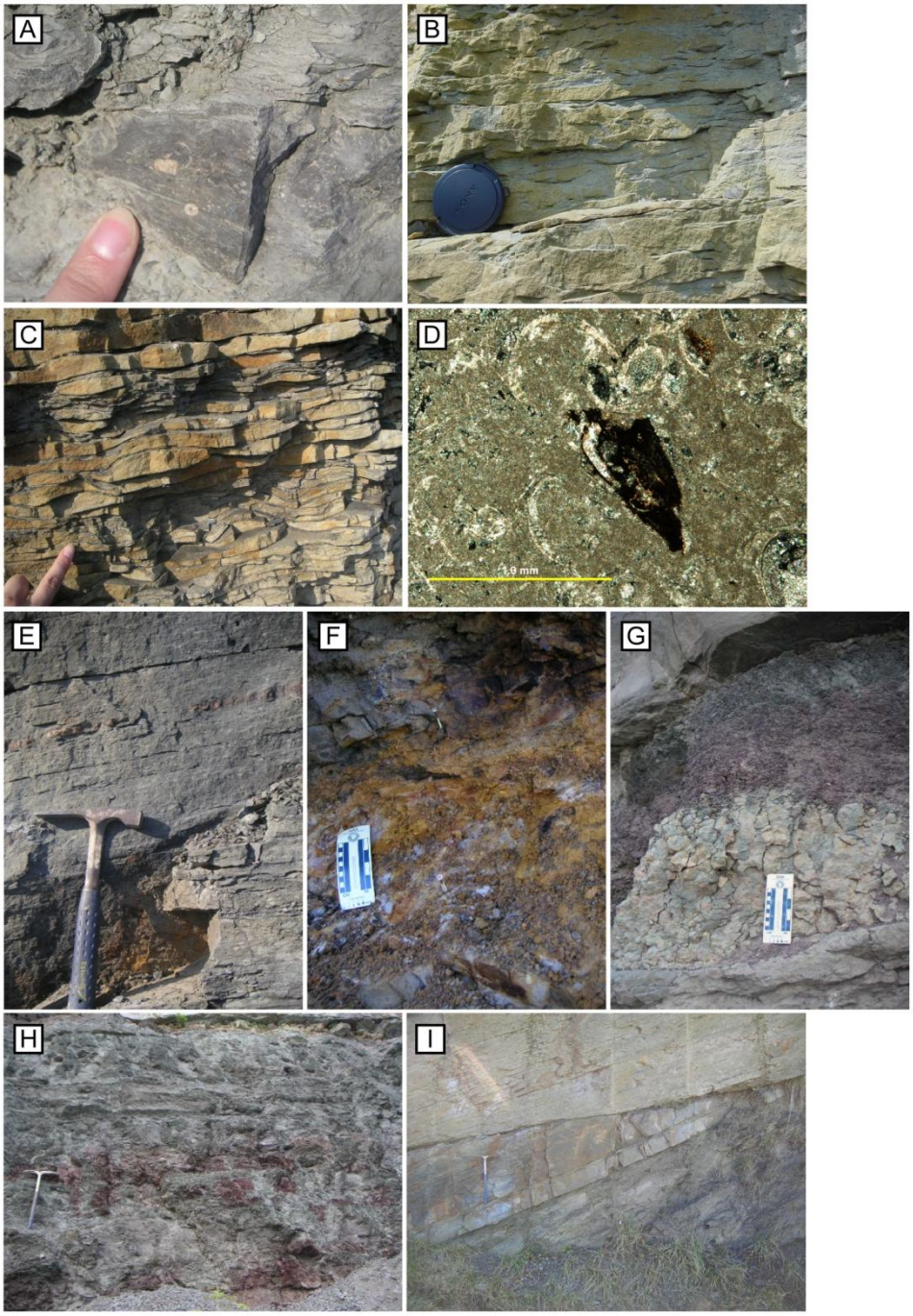

Figure 4.5 Field photos of the Pennington Formation: (A) Unit 73 - grainstone with crinoids, brachiopods and bryzoans, "Little Stone Gap"; (B) Unit 86 - representative flaser bedding formed in a tidal environment; (C) Unit 84 - tidal bundles; (D) Unit 68 - estuarine limestone (in thin-section) with ostracodes, replaced mollusk fragments and potential fish bone fragment; (E) Unit 79 - weathered outcrop photo of black, fissile shale and bedded, nodular siderite; (F) Unit 42 - Appalachia Pedotype, an Oxisol. Note the leached coloring and preserved carbonaceous material; (G) Unit 62 - Pound Pedotype, a well-drained Vertisol with a well-developed Bk (carbonate-rich) horizon; (H) Unit 99 - Big Stone Pedotype, an Entisol, showing deep taproot systems, some filled with calcium carbonate; (I) Units 28-29 - truncation of planar-tabular cross-bedded sandstone units in Unit 29.

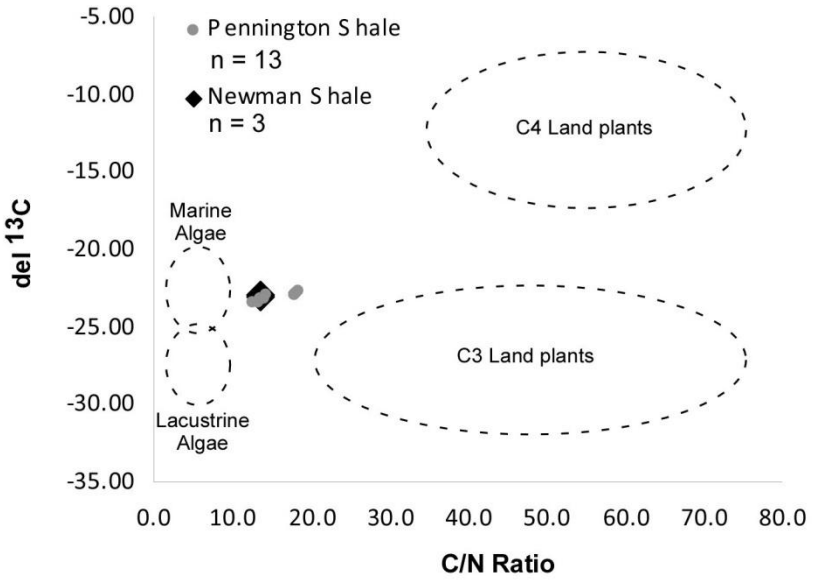

Figure 4.6 Plot of $\delta^{13}C$ values (‰ PDB) versus C/N ratio, adapted from Meyers (1994). Samples were collected from both Pennington and Newman black shales for comparison.

Table 4.2 Carbon and nitrogen data for the Pennington Formation (Penn, Units 77 and 79) and Newman Limestone (New; stratigraphically older, see Fig.2) samples for comparison.

SAMPLE	^{15}N	^{13}C	N%	C%	C/N
New 1a	4.52	-23.13	0.07	1.00	13.6
New 1b	4.56	-23.00	0.07	1.00	13.6
New 1c	4.57	-22.93	0.07	1.00	13.5
Penn 1a	3.09	-23.42	0.07	1.00	13.4
Penn 1a-R	3.36	-23.21	0.08	1.03	13.6
Penn 1b	3.26	-23.50	0.08	1.01	13.3
Penn 1c	3.08	-23.44	0.08	0.96	12.7
Penn 2a	3.05	-23.01	0.08	1.15	14.4
Penn 2b	3.09	-23.17	0.08	1.13	14.1
Penn 2c	3.14	-23.20	0.08	1.14	14.1
Penn 3a	3.10	-22.94	0.07	1.21	18.0
Penn 3b	3.07	-22.94	0.07	1.25	18.0
Penn 3c	3.16	-22.80	0.07	1.30	18.2
Penn 4a	3.07	-22.90	0.07	1.19	17.9
Penn 4b	3.10	-22.80	0.07	1.19	18.2
Penn 4c	2.96	-22.66	0.07	1.22	18.3

Marine ramp. The open-marine ramp environment is characterized by massive grainstones composed of the following skeletal grains: bryozoans, horn corals, brachiopods and crinoids (Units 70-71; "Little Stone Gap Limestone"; Figs. 4.3, 4.5A). This skeletal grain assemblage is classified by Lees and Buller (1972) as a chlorozoan grain association characteristic of warm, normal-marine waters between 30°S and 30°N present-day latitude, and is consistent with the paleogeographic reconstructions for this time period and area. The carbonate build-up style of a ramp is based upon studies of the underlying Newman Limestone by Al-Tawil and Read (2003) for the Pound Gap exposure. Al-Tawil and Read (2003) interpreted a similar facies association as having been deposited in high-energy, open-marine carbonate sand-sheet environments. Because of the absence of physical sedimentary structures such as cross-bedding, Pennington carbonate facies were likely deposited within an open-marine environment, below fair-weather wave base.

Tidal. Weak sigmoidal bedsets are observed in Unit 82, and are suggestive of a tidal environment (Nio and Yang, 1991). Additional "tidal" sedimentary structures observed include flaser and lenticular bedding in Units 28, 42, 80-81, 91 (Fig. 4.5B), lenticular bedding, and tidal bundles in Unit 86 (Fig. 4.5C), recognized by their diagnostic double clay drapes (Driese, 1987). The cyclicity of Pennington tidal rhythmites has been studied previously by Greb (1998b) and was interpreted as orbitally-forced based tidal bundling ratios.

Estuarine. Estuaries are characterized by a semi-enclosed body of water with free access to the ocean such that marine saline water is diluted by freshwater input (Pritchard, 1967; Schroeder-Adams, 2006). Like deltas, the estuary may be influenced by tidal, fluvial, and marine processes, making it difficult to equivocally classify an estuarine environment in the ancient rock record (Rosetti, 2000). Thus geological context (stratigraphic relationships) may provide important clues to the existence of estuarine facies. As examples, Units 68 and 70 (both limestones) contain a skeletal grain assemblage vastly different from the marine skeletal assemblage of Units 71 and 72. The main skeletal grains are mollusks, ostracodes, rare brachiopods and fish bone fragments (Fig. 4.5D). Unit 70 directly overlies Unit 69, a poorly-drained Vertisol (PM), and lies stratigraphically beneath an open-marine limestone (Unit 71). Unit 70, dominantly limestone, also has interbedded siltstone suggesting a potential tidal influence. The facies succession would indicate both marine and freshwater influences, thus making Unit 70 a good candidate for an estuarine paleoenvironment.

Fluvial and pedogenic. Massive sandstone units (*Mm*) tend to be concentrated between Units 44 to 67 and 88 to 97. These are fine- to medium-grained massive sandstones (*Mm*) that, in some instances, also pinch and swell. Units within intervals 43-66 and 88-105 are interpreted to be channel sandstones deposited in a low-energy, low-gradient fluvial system.

Pedogenic facies consist of pedogenically modified fluvial overbank deposits and/or delta lobes formed during periods of subaerial exposure and

periods of long-term geomorphic stability. Three pedotypes have direct paleoenvironmental and paleoclimatological significance. The PM and PD pedotypes, both Vertisols, developed under seasonal climate conditions (Fig. 4.5G). Both AP and WI pedotypes, an Oxisol and Histosol respectively, suggest very wet climates and/or poorly-drained conditions. The Oxisol (Unit 26) formed in rain forest-like environments (Fig. 4.5F), and Histosols in ever-wet swamp or bog environments. Unit 103 has additional paleoenvironmental significance not associated with its soil order, but rather, with its extraordinary rooting density and habit. Unit 103, an Entisol (BS, Fig. 4.3), has 2 m vertically penetrating root traces through the profile; bifurcating root traces and laterally spreading forms are also present. Some of these traces exhibit calcite rhizocretions (Fig. 4.5H). These features in Unit 103 are evidence of a dense, forest-like environment that developed nearing the close of Pennington deposition.

Drowned river valley. Units 77 to 79 likely represent an incised-valley fill. Both Miller and Erikkson (2000) and Reed et al. (2005) made the same interpretation for time-equivalent facies in the Hinton-Princeton and Mauch Chunk Formations, respectively. This interval is also known as the Pride Shale, and is regionally extensive, with outcrops in West Virginia, Virginia, Kentucky, and Tennessee (Miller and Eriksson, 1997). In West Virginia, the Pride Shale is interpreted to have been deposited in a prodeltaic environment recording hundreds of years of tidal rhythmite deposition (Miller and Eriksson, 1997). In the Pound Gap exposure, the Pride Shale lacks diagnostic tidal sedimentary structures as well as sand/silt input, thereby suggesting that it was deposited outside the

influence of tidal processes. Our geochemical analysis of these black shales additionally indicates that the organic carbon sources were from marine algae (Fig. 4.5). Also noteworthy is an increase in the C/N ratio (Fig. 4.6) for a few of the Pennington Shale samples (within Units 77 to 79). Although this shift might be attributable to terrestrial C3 plant carbon input, during anoxic conditions nitrogen-bearing compounds degrade at higher rates than pure carbon compounds (Hoefs, 2004), therefore the % C can become elevated relative to % N by early diagenetic processes.

Early diagenetic siderite is ubiquitous throughout the black shale Units 77 to 79. Siderite can form in brackish waters during the filling of incised valleys (Bhattacharya and Walker, 1992), and is an early-diagenetic mineral that requires conditions that are: (1) anoxic, (2) non-sulfidic, and (3) have low concentrations of organic matter (Berner, 1981). In most cases, siderite formation requires a meteoric water influence to avoid having high sulfate concentrations that would promote pyrite formation, rather than siderite formation (Berner, 1981; Kim at al., 2007). El-ghali et al. (2006) reported higher concentrations of siderite in highstand tidal flats, as opposed to fluvial highstand deposits where prolonged residence time of marine sediments under suboxic conditions and slow sedimentation rates are required. Depositional conditions of Units 77 to 79 were clearly anoxic because the shale is black, organic-rich, and devoid of any trace fossils or body fossils. Sedimentation rates were likely slower given the absence of any tractive transport structures. Assuming the incised-valley fill interpretation, pore waters would have been brackish with periodic freshwater input.

Delta. There are many clastic facies common throughout the Pennington that exhibit evidence for deposition by unidirectional flow, including asymmetrical current ripples (e.g., Units 42, 74, and 86) and planar-tabular cross-beds (e.g., Units 20, 28, and 81). Units that contain unidirectional flow-related structures could have been deposited in a wide-range of environments ranging from tidal channels, delta fronts, and/or estuaries, all of which are compatible with the mixed fluvial and nearshore-marine setting envisioned for the Pennington at the study site. However, given the facies stacking patterns and sedimentary structures, we propose an upper delta-plain environment for sandstone Units 16-34. Units 28-29 suggest lobe switching with the observation of reactivation surfaces (Fig. 4.5I). The tidal facies of Units 80-87 may have formed in a tidally-influenced deltaic environment. Soil formation (Units 23, 25-26) occurred on stabilized lobes during lowstand and or/ falling stage systems tracts.

Sequence-Stratigraphic Framework

The sequence-stratigraphic architecture is discussed in terms of base level change and systems tracts. Facies, systems tracts and cyclicity are presented on a sequence-by- sequence basis. Seven sequences, composed of one or more cycles, are interpreted for the Pennington outcrop section (Fig. 4.3), and were deposited within a span of 8-9 Myr as determined by conodont zonations and the ICS (2004)

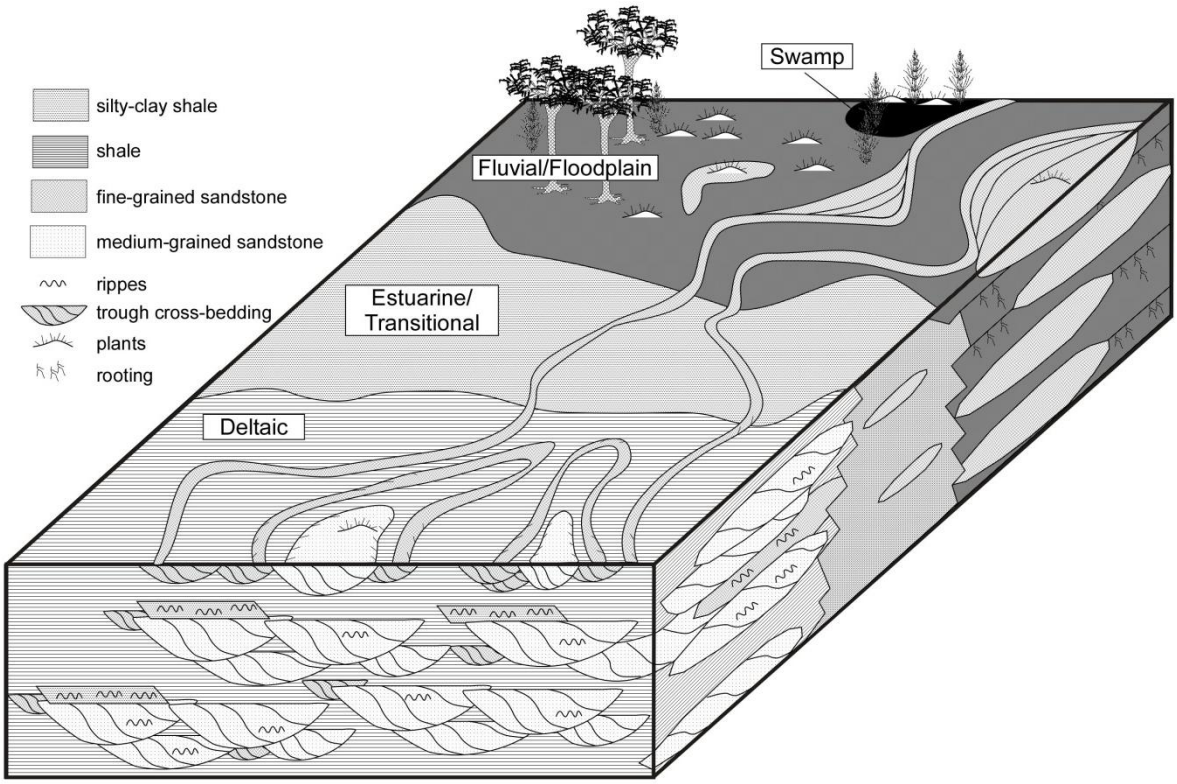

Figure 4.7 Block diagram of interpreted Pennington depositional environments for Sequences 2 and 3. Note that during optimum conditions for carbonate deposition, the marine ramp would have replaced deltaic and estuarine depositional systems. Diagram is not drawn to scale.

age determined for the Mississippian/Pennsylvanian systematic boundary (Fig. 4.2). Not all systems tracts are preserved, particularly the lowstand systems tract (LST). Figure 4.3 interprets the following: cycle boundaries, sequence boundaries, composite sequence boundaries, and systems tracts. Figure 4.8 is a summary of the sequence stratigraphic hierarchy for the Pennington outcrop section.

Sequence 1. (Units 1 through 14), comprised of 6 cycles, preserves both part of, or possibly the entire transgressive systems tract (TST), and the highstand systems tract (HST). Sequence boundary 1 (SB1) also marks the beginning of composite sequence 0 (CS0). TST cycles fine upward and thicken (Fig. 4.3). The HST is dominated by carbonate production in a clastic-poor phase of Sequence 1. Paleosols are poorly-drained and poorly-developed (Kahmann and Driese, 2008) in the TST, and are abruptly overlain by open-marine dolomitized carbonates, marking the maximum flooding surface (MFS). Poor drainage of Sequence 1

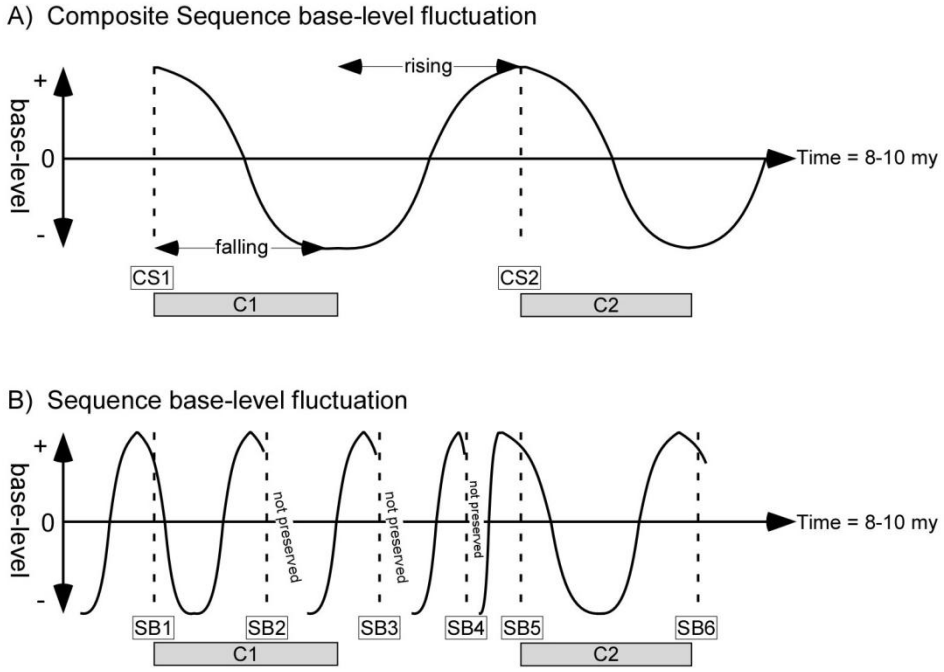

Figure 4.8 General overview of cyclicity for the Pennington Formation and associated composite base-level fluctuation through time. Composite sequences (A) and sequences (B) are shown only. It is assumed that cycles are higher in frequency than that of sequences. Both C1 and C2 glaciations of Fielding et al. (2008) are annotated for reference.

paleosols (and others of the PM pedotype throughout the Pennington) can be attributed to higher water tables, or higher base level. A less stable landscape will also inhibit the formation of well-developed paleosols. The sequence terminated with an influx of clastic sediments from the succeeding lowstand, increasing water turbidity and thereby shutting off carbonate production. This interpretation is consistent with the cyclic and reciprocal model of mixed carbonate and clastic sedimentation (Van Siclen, 1958; Wilson, 1965; 1975).

Sequence 2. (Units 16 to 34), composed of 6 cycles, is entirely clastic, with no carbonate deposition. Although identification of the depositional system is ambiguous, we suggest a deltaic environment as illustrated in Figure 4.7, in which delta lobes became exposed, stabilized, and soils developed. The LST is characterized by the coarsest sediment fraction of the sequence, whereas the TST fines upward (Fig. 4.3) to the MFS between Units 30 and 31. During the lowstand systems tract (LST) soils developed. A cycle boundary marks the transgressive surface (TS, cycle boundary between Units 26 and 27) where a paleosol of the AP pedotype is truncated by ripple cross-bedded sandstone (Fig. 4.3). Unit 27 also contains one of the few examples of trace fossils observed within the Pound Gap outcrop section. The trace fossil *Arenicolites*, as part of a *Glossifungites* ichnofacies association, (Pemberton and MacEachern, 1995) was excavated into an erosional surface separating Units 27 and 28. This substrate-controlled ichnofacies indicates a bounding discontinuity (Pemberton et al., 1992), or in our model, a cycle boundary (Fig. 4.3). The HST fines upward, ending in paleosol formation.

The AP paleosol, part of the LST, is considered the best-developed soil within the entire stratigraphic section and likely represents the longest period of geomorphic stability (Kahmann and Driese, 2008). Although Units 23 and 25 are poorly-developed soils in comparison to the AP paleosol, the instability of the landscape is consistent with a dynamic delta environment. With base-level rise and instability of the landscape, the TST could not support soil development. During the HST, base-level rise was either negligible or in its falling stages, thus promoting the development of mature well-drained paleosols of the PD pedotype.

Sequence 3. (Units 35 to 50) developed within a fluvial environment, preserving the transgressive equivalent systems tract (TSE) and the highstand equivalent systems tract (HSE) (Fig. 4.3). We interpret a sequence boundary within the covered interval due to the interpreted HSE of the preceeding sequence and what we observe to be a TSE in Sequence 3. Sequence 3 is composed of at least 6 cycles with potentially more undetected in a covered interval. TSE cycles fine upward (Fig. 4.3) and coal formation (Units 39 and 41) within the TSE indicates rising base level. The HSE fines upward and the formation of well-drained, mature (PM pedotype) paleosols indicate lower base-level and stability of the landscape. Not all paleosols of the HSE, however, are well-drained. The paleosols of Units 45 and 46 belong to the PM pedotype. The poor drainage of these paleosols might signal the onset of a late lowstand and/or early transgression of the next sequence. Another mechanism, and potentially more likely, is the influence of climate change.

Sequence 4. (Units 51 to 66), begins within a covered interval and only a TSE and HSE are preserved. Fluvial deposition continues with 5 cycles, all capped by paleosols and abruptly overlain by structureless channel/sheet sands (*Mm*). The TSE is indicated by fining-upward successions, poorly-drained PM paleosols and a dolostone. The HE is represented by well-drained, well-developed PD paleosols. The sequence terminates with brackish-water flooding in an estuarine environment (Unit 68).

Sequence 5. (Units 68 to 76) is the thinnest of the sequences and includes only 4 cycles (Fig. 4.3). Composite base-level rise during TSE/TST is indicated by both poorly-drained Vertisols and estuarine facies. The marine carbonate grainstone facies is the dominant facies in this sequence, indicating open-marine environments ("Little Stone Gap" shown in Fig. 4.2) during HST. Marine facies only exist because erosion ceased and clastics were not deposited. Otherwise, the HST would be more similar to the facies succession of the Sequence 2 HST. Erosion continued again with clastics filling accommodation to form another estuary in Unit 73. Carbonate deposition at this site did not resume for the rest of the Mississippian. The sequence ends with composite paleosol development in the PD pedotype during late HST to falling stages of base-level fluctuation.

Sequence 6. (Units 77 to 101) is the thickest of the Pennington sequences and is composed of nine cycles. Sequence 9 is unusual in that the LST is dominated by a black, fissile shale facies with ubiquitous bedded nodular siderite (Fig. 4.3). As an incised valley-fill or drowned river valley, the black shale

environment was anoxic, with poor circulation, low-energy, and outside the influence of terrigenous-derived sands. In time-equivalent sections a pro-deltaic environment of deposition has been suggested for the Pride Shale (Miller and Eriksson, 1999). This brackish, low-energy environment is somewhat analogous (with the exception of grain size) to the modern Chesapeake Bay estuaries where brackish, poorly-circulated waters exist, yet are fed by fluvial systems (Bratton et al., 2003). Sequence boundary six (SB 6) also marks composite sequence boundary 1 (CS 1). Units 80-87 were deposited in a tidal-fluvial environment, and likely represent a TST (Fig. 4.3) with observations of fining-upward cycles (Fig. 4.3). The cycle boundary between Units 83 and 84 is marked by minor scour, plant preservation and pyrite formation. Although soil formation did not occur (or is not preserved), there may have been periods of stability and subaerial exposure as indicated by plant preservation. Following this stability, the environment became tidally influenced, as evidenced by tidal bundling (Greb 1998b), clay drapes (Unit 86, Fig. 4.5C), and by flaser and lenticular bedding (Units 84 and 85, Fig. 4.5B). This facies succession is similar to the conceptual trangressive systems-tract model suggested by Dalrymple et al. (1992) in which following transgression, fluvial sediments are initially deposited and followed by estuarine and tidal flat deposition. Greb (1998b) reported the presence of *Arenicolites* in Units 80-89, and interpreted this trace fossil as associated with tidal-estuarine deposits. The HSE is characterized by early coarsening-upward fluvial channel sands (88-89), overbank deposits (Units 90-92), and mature, well-drained, and stacked paleosols of the PD pedotype (Units 95-96; 99-101). Only

the TSE of *Sequence 7* is preserved, where fluvial deposition continued with associated soil formation during periods of geomorphic stability. A TSE is interpreted due to WI (coal) and PM paleosol (poorly-drained soil) formation that suggest rising composite base-level.

Discussion

Controls on Sedimentation and Cyclicity

Although cyclicity is typically described in terms of base-level and accommodation change, the controls on cyclicity are not limited to eustasy or channel avulsion on a floodplain. Tectonic and climatic controls must also be considered (Sarg, 1988; Van Wagoner et al., 1988; Wright and Marriott, 1993; Atchley at al., 2004). Eustasy or base-level fluctuation controls Pennington cyclicity, but is the corresponding symptom of global ice, tectonics, and/or climate change. Milankovitch scales of cyclicity are not ruled out, however, due to a lack of chronostratigraphic constraints the discussion of this topic would be purely speculative. Figure 4.8 represents a summary of the hierarchy of cyclicity for the Pennington Formation.

To assess eustatic control upon fluvial/terrestrial cyclicity, the Late Mississippian shoreline must have been close enough to the study area to have influenced terrestrial deposition. Blum and Tornqvist (2000) have shown that the Mississippi River, a low-gradient, high-sediment-supply fluvial system, has an updip limit of fluvial onlap extending at least 300-400 km landward of the shoreline. Although the Pennington might not have had such high sedimentation rates, we do assume a low-gradient fluvial system. From paleogeographic

reconstructions (Ziegler et al., 1979; Scotese and McKerrow, 1990) of the Late Mississippian and the alternating episodes of clastic/carbonate deposition within the 200 m thick Pennington section, we assume that the shoreline existed within this 300-400 km threshold.

Global ice sheets. Waxing and waning of global ice sheets likely controlled the development of Pennington composite sequences (Fig. 4.3). Overall, the Pennington depositional environments became more terrestrially dominated over time (Kahmann and Driese, 2008), which is consistent with interpreted Late Mississippian icehouse conditions and interpreted depositional environments (Miller and Eriksson, 1999; Miller and Eriksson, 2000; Maynard et al., 2006; Fielding et al., 2008). Icehouse conditions effectively locked seawater in ice, thereby lowering global sea levels. Evidence suggests that global ice sheet advance and retreat controlled composite sequence cyclicity (CS0/CS1; Fig. 4.8). Influences of these glacial events are also suggested by other studies of Carboniferous strata within the Appalachian basin (Miller and Eriksson, 1999; Al-Tawil and Read, 2003; Wynn and Read, 2007), and of a time-equivalent section in the Askyn River, Southern Urals, Russia (Brand and Bruckschen, 2002).

Fielding et al. (2008) reported two episodes of glaciations for Gondwana that occurred during Pennington deposition. C1 (Fig. 4.2) glaciation began at 326.5 Ma and ended at 325.5 Ma, and C2 glaciation began at 322.5 Ma and ended at 319.5 Ma, near the recorded date for the Mississippian-Pennsylvanian unconformity of 318.1 Ma established by the ICS (2004). C1 glaciation was likely recorded with SB1 (Fig. 4.3) where clastic deposition began and dominated due to

a long-term fall in composite base level. The onset of the C2 glaciation might coincide with SB5/CS1, or at the cycle boundary between Units 76 and 77 (Fig. 4.3). This interpretation is strictly based upon stacking patterns of facies successions. SB5 records the "turn around" from what appears to be a highstand- to lowstand- facies succession suggested by a drowned-river valley (previously lowstand valley incision). During glaciations, sea level lowers and erosion increases, initiating and/or enhancing clastic deposition.

Tectonics. Uplift and erosional unloading during Pennington deposition is associated with closure of the Iapetus seaway (proto-Atlantic prior to Pangean supercontinent formation) (Ettensohn, 1998). The increase in clastic deposition during the Chesterian is suggestive of a regional tectonic control on Pennington sequence development.

The success of the carbonate factory is commonly associated with variation in accommodation/base level. Water turbidity, however, as a function of clastic input is the main control upon sequence development. The carbonate factory was rarely active in the Pennington with the exception of Units 71 and 72- "Little Stone Gap" (Fig. 4.2). This carbonate facies is similar to the facies interpreted by Al-Tawil and Read (2003) in the Newman Limestone (Figs. 4.2, 4.3). This facies developed below fair-weather wave base and above storm wave base (Al-Tawil and Read, 2003), with no substantial gains in accommodation beyond the rate of sediment production. Erosion likely ceased during this highstand phase of deposition, decreasing clastic input (turbidity) into the basin and allowing for carbonate sedimentation to resume. Units 71-73 were then

inundated by an influx of clastics during lowstand valley incision, which terminated carbonate sedimentation for the remainder of the Mississippian. Given the rather abrupt "turn off" of carbonate production with subsequent clastic deposition, regional uplift and subsequent erosion would seem the likely candidate. If erosion had not ceased (a period of tectonic quiescence) the facies succession would likely be similar to Sequence 1(Fig. 4.3). By the Pennsylvanian, the seaway had closed (Ziegler et al., 1979; Scotese and McKerrow, 1990). Timing of that closure could easily coincide with SB5/CS1 with cessation of carbonate production and fully terrestrial conditions by SB6.

The successions in which paleosols developed are within fluvially-dominated or influenced environments that are autocyclic in nature. Observed cyclicity in the fluvial system is likely the result of channel avulsion in response to base- level changes (Wright and Marriott, 1993; Atchley et al., 2004). Thickening and thinning of these cycles are related to sedimentation and erosion rates, as well as accommodation. Higher rates of erosion, associated with regional uplift, promoted higher sedimentation rates and potentially less stability. Less stable landscape promoted the development of BS and NO paleosols, observed in Sequences 1 and 5. More mature paleosols (PM, PD, JE, and/or AP pedotypes) suggest greater stability of the floodplain allowing for longer durations of soil genesis.

Climate change. Climate control of Carboniferous cyclicity and sedimentation within the Appalachian Basin was first suggested by Cecil (1990) whereby periods of wet-dry seasonality enhanced siliciclastic input, represented

by the clastic-dominated Pennington. Further study of the Pennington paleosols (Kahmann et al., 2008; Kahmann and Driese, 2008) suggested high-frequency climate shifts, possibly related to seasonal migration of the paleo-Intertropical Convergence Zone (Cecil et al., 2003; Kahmann et al., 2008; Kahmann and Driese, 2008). These-high frequency climate shifts, or monsoons, have also been suggested for the British Isles for this time period and similar paleo-latitude (Falcon-Lang, 1999). The fluvial-pedogenic cycles of Sequence 2 and 3 have a climatic overprint that may exert control upon their cyclicity.

Paleosol morphology is extremely climate-sensitive. Dry conditions and higher sedimentation rates are suggested by the JE (Alfisol) and PD (well-drained Vertisol) pedotypes, dominating Sequences 2 and 3. Both pedotypes are characteristically thicker and bear calcium carbonate nodules, and/or rhizocretions. Calcium carbonate forms in response to drier climate, promoting better soil drainage. Wet/humid conditions favor the formation of WI (Histosol/coal), AP (Oxisol/ rain forest soil) and PM (poorly-drained Vertisols) pedotypes present in Sequences 2, 3 and 7. Histosol or coal formation requires a high water table with thick vegetative cover in a humid environment (Cecil, 1990; Kahmann and Driese, 2008). The AP Pedotype, in Sequence 1, is characterized by intense leaching and kaolinite formation as well as thick vegetative cover (Kahmann and Driese, 2008). The change from humid to dry conditions, as manifested by paleosol attributes, causes channel avulsion and changes in landscape stability, thereby influencing fluvial cyclicity.

With greater seasonality, and wetting and drying cycles, erosion increases and clastics dominate. (Cecil, 1990). Seasonal climate is also manifested by the Vertisols of the PD and PM Pedotypes. The formation of Vertisols is the result of seasonal precipitation or seasonal soil-moisture deficits with 4-8 dry months per year (Coulombe et al., 1996; Cecil et al., 2003). The shrink and swell nature of the clay-rich Vertisols promotes slickenside formation (Wilding and Tessier, 1988); a diagnostic indicator of seasonality, or wet/dry climates. By the end of Pennington deposition it is evident that conditions were becoming more wet with the development of PM (poorly-drained soils) and coals, signaling the onset of the ever-wet conditions of the Pennsylvanian (Kahmann and Driese, 2008; Kahmann et al., 2008).

Conclusions

This sequence-stratigraphic study of the Late Mississippian/Chesterian Pennington Formations indicates the following:

1. The Pennington Formation hosts a variety of depositional environments ranging from open-marine carbonate ramp deposits, to terrestrial coal swamps and forests.

2. Composite sequences of the Pennington were controlled by Gondwana glaciations- effectively eustasy.

3. Sequence development was controlled by both tectonics and climate, overprinting the eustatic signature, as a function of uplift and erosional unloading.
4. Cycle development, particularly in the fluvial/pedogenic environment was strongly influenced by high-frequency climate change like associated with fluctuation of the paleo-ITCZ.

This sequence-stratigraphic study of the Pennington has shown that multiple mechanisms exert a control upon cyclicity. For the most part, any one mechanism

is not mutually exclusive of the others. The Pennington also marks the closure of the Iapetus Ocean. Although an unconformity is present at the Mississippian-Pennsylvanian boundary, this closure likely sutured within 1-2 my of this unconformity. Given the crude nature of our age constraints, greater study should be applied to the Pennington section, as well as to other time-equivalent terrestrially-dominated sections to further investigate this closure. The results of this closure significantly altered ocean and atmospheric circulation (Parrish, 1993), the understanding of which would enhance paleoclimatic reconstructions of the Late Paleozoic.

CHAPTER FIVE

Conclusions

The Pennington Formation at Pound Gap has provided a robust case study for Late Mississippian climate change. Paleosol study confidently supports high-frequency climate change associated with seasonal migration of the Paleo-ITCZ. Vertisol-like paleosols confirm seasonal precipitation variation. This variation is manifested by their polygenetic character resulting from fluctuation of soil drainage through time. The Late Mississippian experienced both aridity and extreme humidity with the formation of well-drained Vertisols (aridity) and Oxisols (humidity). MAP ranged from 519 mm/yr during dry periods, to 1362 mm/yr during wet/humid periods. Other geochemical proxies support this high-frequency climate fluctuation. Paleo-ecosystems also responded to climate fluctuations, as evidenced by changes in the density of rooting and rooting depth through time.

Trace element chemistry, in conjunction with statistical analysis, has proven to be a potentially useful tool to evaluate climate change. Positive correlations between trace element concentrations with known climate variation, provided by paleosol study, were established with remarkable results. It is apparent that the trace element chemistry of the paleosols is controlled by clay translocation (lessivage) and is broadly reflective of variations in the intensity of weathering. Furthermore, variations in the rate of chemical weathering can be correlated to changing climate conditions. However, these results serve as a "pilot

study". Further investigations are essential to develop a more quantitative application of this paleoclimate tool involving characterization of modern soils, and a more comprehensive study of those elements with high negative correlations.

Sequence-stratigraphic study of the Pennington Fm. has shown that multiple mechanisms exerted a control upon cyclicity. Changing climate was not the only control upon Pennington cyclicity. Published data suggests that Pennington deposition responded to both the waxing and waning of global ice, as well as to regional tectonic processes. At the close of Pennington deposition, evidence such as the lack of carbonate sediment production and increased occurrences of well-developed paleosols suggest final closure of the Iapetus Ocean, which likely sutured within 1-2 my of the Mississippian-Pennsylvanian unconformity. Given the coarse nature of Pennington Fm. age constraints, greater biostratigraphic study should be applied to the Pennington section, as well as other time-equivalent terrestrially-dominated sections to further investigate this closure. The results of this closure significantly altered ocean and atmospheric circulation (Parrish, 1993), the understanding of which would enhance paleoclimatic reconstructions of the Late Paleozoic. With the combined evidence provided by paleosol, geochemical, and sequence-stratigraphic study, it is apparent that the Late Mississippian was a time of a high-frequency climate change.

APPENDIX

Appendix

Elemental concentrations used in statistical analysis

SAMPLE DESCRIPTION	Ba ppm	Ce ppm	Cr ppm	Cs ppm	Fe2O3 %	MnO %	Mo ppm	Ga ppm	Ge ppm	Hf ppm	La ppm	Nb ppm	Rb ppm	P ppm	U ppm	Sr ppm	Ta ppm	V ppm	W ppm	Y ppm	Th ppm	Ti %	Zr ppm
A1 AVERAGE	530.00	79.83	185.33	9.15	6.43	0.04	0.38	27.87	0.22	2.80	37.43	14.00	195.33	876.67	2.73	165.67	1.04	135.33	1.87	21.43	12.13	0.46	100.73
A2 AVERAGE	507.50	53.28	144.75	7.18	8.02	0.09	0.44	22.23	0.20	2.25	24.98	11.00	122.03	742.50	1.40	146.25	0.81	109.50	1.55	15.80	7.75	0.37	81.43
A4 AVERAGE	286.67	69.10	156.00	4.48	5.06	0.09	0.41	12.78	0.18	2.87	31.17	9.53	94.37	1093.33	2.23	150.33	0.72	63.33	1.20	23.70	8.57	0.34	104.80
A5 AVERAGE	300.00	67.40	168.50	4.92	6.13	0.20	0.62	16.28	0.14	3.50	32.20	10.80	104.85	660.00	2.75	145.75	0.78	77.50	1.30	21.05	9.80	0.34	104.00
A6 AVERAGE	380.00	108.23	258.75	6.11	4.13	0.02	0.63	24.69	0.18	6.20	51.90	18.43	137.93	422.50	3.38	94.45	1.30	103.50	1.83	27.15	15.30	0.56	180.50
A6B AVERAGE	90.00	30.48	544.00	1.52	5.59	0.18	3.16	7.04	0.15	3.30	15.75	6.10	31.50	150.00	1.25	28.15	0.43	45.50	0.80	6.05	5.00	0.23	110.80
A7 AVERAGE	287.14	86.10	131.86	6.44	5.84	0.41	0.37	18.62	0.19	3.63	40.33	12.51	125.97	705.71	2.33	138.21	0.89	94.43	1.43	28.89	10.80	0.39	106.94
A10 AVERAGE	425.00	96.15	159.50	11.25	6.87	0.03	2.99	31.55	0.20	4.45	45.75	17.85	195.00	195.00	5.15	126.75	1.30	141.00	1.90	21.90	14.95	0.55	126.25
A10H-0 AVERAGE	150.00	41.60	80.00	3.18	9.62	0.34	24.50	8.47	0.19	1.50	19.60	5.10	51.00	130.00	6.20	282.00	0.33	124.00	0.50	59.90	5.20	0.15	50.00
A11 AVERAGE	386.67	85.80	137.67	9.58	5.79	0.02	0.89	29.47	0.18	4.27	39.17	17.00	158.17	280.00	3.20	108.17	1.23	140.67	1.80	22.13	14.43	0.52	122.50
A11H-0 AVERAGE	170.00	296.00	148.00	6.23	10.49	0.05	11.60	23.20	0.55	5.60	132.00	15.50	123.00	>10000	95.60	348.00	1.11	176.00	1.60	298.00	13.90	0.48	183.50
A14 AVERAGE	462.00	78.76	157.00	7.82	8.42	0.04	0.62	24.22	0.20	4.12	35.78	14.80	143.80	724.00	2.12	97.10	1.05	103.40	1.54	24.64	11.84	0.46	118.00
A17 AVERAGE	386.67	80.73	173.67	7.27	6.67	0.04	1.04	21.17	0.19	5.10	39.47	14.40	149.17	363.33	2.47	78.00	1.04	101.00	1.50	21.97	12.50	0.46	145.50
PA AVERAGE	394.00	69.10	110.00	6.21	5.60	0.07	1.03	21.76	0.25	3.18	33.42	12.08	118.22	0.09	2.44	170.00	1.00	98.60	1.32	19.72	9.92	0.40	105.88
PC AVERAGE	495.00	101.18	105.75	5.96	6.47	0.04	0.53	24.80	0.29	4.08	47.73	14.15	142.75	0.06	2.60	116.75	1.14	97.50	1.43	28.10	13.85	0.47	134.63
PE AVERAGE	402.86	82.19	121.14	7.85	6.32	0.05	1.22	22.62	0.23	3.26	40.63	11.89	143.44	0.08	2.61	204.43	1.01	105.00	1.44	26.37	11.41	0.40	106.44
PH AVERAGE	388.33	59.52	97.50	5.52	5.38	0.12	1.04	19.33	0.17	2.63	27.50	10.12	97.83	0.05	3.83	863.75	0.83	105.33	1.35	18.83	8.22	0.34	87.15
PI AVERAGE	388.33	90.35	123.50	8.37	6.47	0.04	0.64	23.18	0.22	4.22	44.55	13.52	159.33	0.02	2.87	103.72	1.14	111.33	1.53	21.33	13.07	0.47	138.00
PK AVERAGE	314.29	114.99	133.00	6.92	7.13	0.05	1.50	22.67	0.24	4.63	54.04	15.30	102.76	0.07	3.31	135.64	1.26	110.71	1.71	31.99	15.34	0.52	155.64
PL AVERAGE	654.00	75.12	116.60	7.67	8.55	0.06	0.31	28.60	0.21	4.22	32.62	15.86	140.10	478.00	3.34	114.00	1.06	126.00	1.40	21.32	11.70	0.45	124.10
PM AVERAGE	172.86	110.37	156.00	5.71	7.82	0.12	1.55	26.43	0.21	4.93	51.66	16.84	79.19	272.86	5.06	109.07	1.16	112.86	1.66	29.04	13.66	0.50	144.59
MH-0 AVERAGE	180.00	125.00	107.00	5.42	6.76	0.04	4.55	26.70	0.32	3.60	52.10	13.00	102.00	3100.00	5.00	155.50	0.88	115.00	1.10	87.60	11.60	0.38	106.00
PO AVERAGE	180.00	91.77	278.00	10.87	3.49	0.02	0.70	22.33	0.16	5.13	45.30	17.60	169.67	133.33	2.57	54.07	1.23	95.67	1.67	22.13	15.47	0.51	151.00
OH-0 AVERAGE	70.00	47.10	208.00	3.08	7.02	0.21	6.56	6.85	0.22	2.60	20.20	6.90	31.20	70.00	11.60	153.50	0.46	95.00	0.70	35.30	12.80	0.21	81.50

REFERENCES

Abayneh, E., Zauyah, S., Hanafi, M., and Rosenani, A.B., 2006, Genesis and classification of sesquioxidic soils from volcanic rocks in sub-humid tropical highlands of Ethiopia: Geoderma, v. 136, 682-695.

Al-Tawil, A., and Read, J.R., 2003, Late Mississippian (Late Meramecian-Chesterian), glacio-eustatic sequence development on an active distal foreland ramp, Kentucky, U.S.A: Society for Sedimentary Geology v. 78, p. 35-55.

Al-Tawil, A., Wynn, T.C., and Read, J.R., 2003, Sequence response of a distal-to-proximal foreland ramp to glacio-eustasy and tectonics: Mississippian, Appalachian Basin, West Virginia-Virginia,USA: Society for Sedimentary Geology Special Publication, v. 78, p. 11-34.

Andrews, W.M., and Nelson, W.J., 1998, Overview of the Structural Geology Around Pound Gap, Letcher County, Kentucky *in* Geology of the Pound Gap Roadcut, Letcher County, Kentucky: Kentucky Society of Professional Geologists, 169 pp.

Arioli, C., Wellman, C.H., Lugardon, B., and Servais, T., 2007, Morphology and wall ultrastructure of the megaspore Lagenicula (Triletes) variables (Winslow, 1962) Arioli et al. (2004) from the Lower Carboniferous of Ohio, USA: Review of Palaeobotany and Palynology, v. 144, p. 231-248.

Atchley, S.A., Nordt, L.C., and Dworkin, S.I., 2004, Eustatic control on alluvial sequence stratigraphy: A possible example from the Cretaceous-Tertiary transition of the Tornillo Basin, Big Bend National Park, West Texas, U.S.A.: Journal of Sedimentary Research, V. 74, p. 391-404.

Aubert, D.; Probst, A., and Stille, P. 2004, Distribution and origin of major and trace elements (particuarly REE, U and Th) into labile and residual phases in an acid soil profile (Vosges Mountains, France): Applied Geochemistry, v. 19, p. 899- 916.

Berner, R.A., 1981, A new geochemical classification of sedimentary environments: Journal of Sedimentary Petrology, v. 51, p. 359-365.

Beuthin, J.D., 1997, Paleopedological evidence for a eustatic Mississippian-Pennsylvanian (Mid-Carboniferous) unconformity in Southern West Virginia:Southeastern Geology, v. 37, p. 25-37.

Beuthin, J.D., and Bascombe, M.B. Jr., 2002, Scrutiny of a global climate model for Upper Mississippian depositional sequences in the Central Appalachian foreland basin, USA: Journal of Geology, v. 110, p. 739-747.

Beuthin, J.D., and Bascombe, M.B. Jr., 2004, Revised stratigraphy and nomenclature for the Upper Hinton Formation (Upper Mississippian) based on recognition of regional marine zones, Southern West Virginia: Southeastern Geology, p. 42, p. 165-178.

Bhattacharya, J.P., and Walker, R.G., 1992, Deltas *in* Walker, R.G., James, N.P., eds., Facies Models: Response to sea level change: Geological Association of Canada, p. 157-177.

Blake, G.R., and Hartge, R.H., 1986, Bulk Density, in A. Klute, ed., Methods of Soil Analysis, Part I. Physical and Mineralogical Methods, 2nd ed: Agronomy Monograph 9. American Society of Agronomy, Madison, WI, p. 363-375.

Blokhius, W.A., Kooistra, M.J., and Wilding, L.P., 1990, Micromorphology of cracking clayey soils (Vertisols) *in* Douglas, L.A.., ed., Soil Micromorphology: A Basic and Applied Science: New York, Elsevier: Developments in Soil Science, v. 19, p. 123-148.

Blum, M. D., and Tornqvist, T.E., 2000, Fluvial responses to climate and sea-level change: a review and look forward: Sedimentology, v. 47 (Suppl. 1), p. 2-48.

Bown, T.M., and Kraus, M.J., 1987, Integration of channel and floodplain suites, I. Development of sequence and lateral relations of alluvial paleosols: Journal of Sedimentary Research, v. 57, p. 587-601.

Brady, N.C., and Weil, R.R., 2002, The nature and properties of soils, 13ed. New Jersey, Prentice Hall. 960 pp.

Brand, U., and Bruckschen, P., 2002, Correlation of the Askyn River section, Southern Urals, Russia, with the Mid-Carboniferous Boundary GSSP, Bird Spring Formation, Arrow Canyon, Nevada, USA: implications for global paleoceanography: Palaeogeography, Palaeoclimatology, Palaeoecology, v. 184, p. 177-193.

Bratton, J.F., Colman, S.M., Thieler, E.R., Seal, R.R., 2003, Birth of the modern Chesapeake Bay estuary between 7.4 and 8.2 ka and implications for global sea-level rise: Geo-Mar Letters, v. 22, p. 188-197.

Brewer, R., 1976, Fabric and Mineral Analysis of Soils, 2nd edition. Krieger Pub., New York. 482 pp.

Brown, D.J.; Helmke, P.A.; and Clayton, M. K. 2003, Chemical indices for redox and weathering on a granitic laterite landscape in Central Uganda: Geochimica et Cosmochimica Acta, v. 67, p. 2711-2723.

Caspari, T.; Baumler, R.; Norbu, C.; Tshering, K.; and Baillie, I. 2006, Geochemical investigation of soils developed in different lithologies in Bhutan, Eastern Himalayas: Geoderma, v. 136, p. 436-458.

Castano. J.R., and Sparks, D.M., 1974, Interpretation of vitrinite reflectance measurements in sedimentary rocks and determination of burial history using vitrinite reflectance and authigenic minerals: Geological Society of America Special Paper, v. 153, p. 31-52.

Catuneanu, O., 2002, Sequence stratigraphy of clastic systems: concepts, merits, and pitfalls: Journal of African Earth Sciences, v. 35, p. 1-43.

Caudill, M.R., Driese, S.G., and Mora, C.I., 1996, Preservation of a paleo-Vertisol and an estimate of Late Mississippian paleoprecipitation: Journal of Sedimentary Research, v. 66, p. 58-70.

Cecil, C.B., 1990, Paleoclimate controls on stratigraphic repetition of chemical and siliciclastic rocks: Geology, v.18, p. 533-536.

Cecil, C.B., Dulong, F.T., Harris, R.A., Cobb, J.C., Gluskoter, H.G., and Nughroho, H., 2003, Observations on climate and sediment discharge in selected tropical rivers, Indonesia: Society for Sedimentary Geology Special Publication, v. 77, p. 29-50

.

Chadwick, O.A.; Brimhall, G.H., and Hendricks, D.M. 1990, From a black to a gray box- a mass balance interpretation of pedogenesis: Geomorphology v. 3, p. 369- 390.

Chesnut, D.R., Jr., Eble, C.F., Greb, S.F., and Dever, G.R., 1988, Geology of Pound Gap Roadcut, Letcher County, Kentucky: Kentucky Society of Professional Geologists, 169 pp.

Chesnut, D.R., Jr., 1991, Timing of Alleghanian tectonics determined by central Appalachian foreland basin analysis: Southeastern Geology, v.31, p. 203-221.

Chesnut, D.R., Jr., 1992, Stratigraphic and structural framework of the Carboniferous rocks of the Central Appalachian Basin in Kentucky. Kentucky Geological Survey, v. 3, 42 pp.

Cleal, C.J., and Thomas, B.A., 1999, Plant Fossils; The history of land plant vegetation: he Boydell Press, Suffolk, 128 pp.

Cleveland, D.M., Atchley, S.A., and Nordt, L.C., 2007, Continental Sequence Stratigraphy of the Upper Triassic (Norian-Rhaetian) Chinle Strata, Northern New Mexico, U.S.A.: Allocyclic and Autocyclic Origins of paleosol-bearing alluvial successions, v. 77, p. 909-924.

Collinson, C.W., Rexroad, C.B., and Thompson, T.L., 1971, Conodont zonation of the North American Mississippian, *in* Sweet, W.C., Bergstrom, S.M., eds., Symposium on Conodont Biostratigraphy: Geological Society of America Memoir, v. 127, p. 353-394.

Condie, K.C. 1993, Chemical composition and evolution of the upper continental crust: Contrasting results from surface samples and shales: Chemical Geology, v. 104, p.1-37.

Coulombe, C.E., Wilding, L.P., and Dixon, J.B., 1996, Overview of Vertisols: Characteristics and impacts on society: Advances in Agronomy, v. 57, p. 289-375.

Craig, L.C., and others, 1979, Paleotectonic investigations of the Mississippian System of the United States: U.S. Geological Survey Professional Paper 1010, Part I, II, and III, 529 pp.

Critchfield, H.L., 1974, General Climatology, Englewood Cliffs, New Jersey, Prentice-Hall, 446p.

Crow, G.E., and Hellquist, C.B., 2000, Aquatic and Wetland Plants of Northeastern North America: University of Wisconsin Press, 480 pp.

Dalrymple, R.W., Zaitlan, B.A., Boyd, R., 1992, Estuarine facies models: Conceptual basis and stratigraphic implications: Journal of Sedimentary Petrology, v. 62, p. 1130-1146.

Darmody, R.G., and Thorn, C.E. 2005, Chemical weathering and boulder mantles, Kärkevagge, Swedish Lapland: Geomorphology, v. 67, v. 159-170.

Dever, G.R., Jr., 1999, Tectonic implications of erosional and depositional features in Upper Meramecian and Lower Chesterian (Mississippian rocks) of South-Central and East-Central Kentucky: Kentucky Geological Survey, University of Kentucky, v.5, 67p.

Dia, A.; Chauvel, C.; Bulourde, M.; and Gerard, M. 2006, Eolian contribution to soils on Mount Cameroon: isotopic and trace element records: Chemical Geology, v. 226, p.232-252.

DiMichele, W.A., and Phillips, T.L., 1996, Clades, ecological amplitudes, and ecomorphs: phylogenetic effects and persistence of primitive plant communities in the Pennsylvanian-age tropical wetlands: Palaeogeography, Palaeoclimatology, Palaeoecology, v. 127, p. 83-105.

Ding, Z.L.; Sun, J.M.; Yang, S.L.; and Liu, T.S. 2001, Geochemistry of the Pliocene red clay formation in the Chinese Loess Plateau and implications for its origins, source provenance and paleoclimate change: Geochimica et Cosmochimica Acta, v. 65, p. 901-913.

Drever, J.I., 1973, The preparation of oriented clay mineral specimens for X-ray diffraction analysis by a filter-membrane peel technique: American Mineralogist, v. 58, p. 553-554.

Driese, S.G., 1987, An analysis of large scale ebb-dominated tidal bedforms: evidence for tidal bundles in the Lower Silurian Clinch Sandstone of East Tennessee: Southeastern Geology, v. 27, p. 121-140.

Driese, S.G., Ashley, G.M., Li, Z., Hover, V.C., and Owen, R., 2004, Possible Late Holocene equatorial paleaoclimate record based upon soils spanning the Medieval Warm Period and Little Ice Ag, Loboi Plain, Kenya: Palaeogeography, Palaeoclimatology, Palaeoecology, v. 213, v. 231-250.

Driese, S.G., Mora, C.I., Stiles, C.A., Joeckel, R.M., and Nordt, L.C., 2000, Mass-balance reconstruction of a modern Vertisol: implications for interpreting the geochemistry and burial alteration of paleo-Vertisols: Geoderma, v. 95, p. 179-204.

Driese, S.G., Nordt, L.C., Lynn, W.C., Stiles, C.A., Mora, C.I., and Wilding, L.P., 2005, Distinguishing climate in the soil recorded using chemical trends in a vertisol climosequence from the Texas Coast Prairie, and application to interpreting Paleozoic paleosols in the Appalachian Basin, U.S.A.: Journal of SedimentaryResearch, v. 75, p. 339-349.

Driese, S.G., and Ober, E.G., 2005, Paleopedologic and paleohydrologic records of precipitation seasonality from Early Pennsylvanian "Underclay" paleosols, USA: Journal of Sedimentary Research, v. 75, p. 997-1010.

Dunham, R.J., 1962, Classification of carbonate rocks according to depositional texture, *in* Ham, W.E. ed., Classification of Carbonate Rocks: Memoir American Association of Petroleum Geologists, v. 1, p. 108-121.

Dunn, M.T., 2004. The Fayetteville Flora I: Upper Mississippian (middle Chesterian/lower Namurian A) plant assemblages of permineralized and compression remains from Arkansas, USA: Review of Palaeobotany and Palynology, v. 132, p. 79-102.

Dunn, M.T., Krings, M., Mapes, G., Rothwell, G.W., Mapes, R.H., and Keqin, S., 2003. *Medullosa steinii* sp. Nov., a seed fern vine from the Upper Mississippian: Review of Palaeobotany and Palynology, v. 124, p. 307-324.

Dutro, J.T., Gordon, M. Jr., and Huddle, J.W., 1979, Paleontological zonation of the Mississippian system *in* Lawrence, C.G., Connor, C., and others, Paleotectonic investigations of the Mississippian System in the United States: Part II. Interpretive summary and special features of the Mississippian System: Geological Survey Professional Paper 1010, 407-429.

El-ghali, M., Mansurbeg, H., Morad, S., Al-Aasm, I., and Ajdanlisky, G., 2006, Distribution of diagenetic alterations in fluvial and paralic deposits within sequence stratigraphic framework: Evidence from the Petrohen Terrigenous Group and the Svidol Formation, Lower Triassic, NW Bulgaria: Sedimentary Geology, v. 190, p. 299-321.

Ettensohn, F.R., 1998, The Mississippian section at Pound Gap: A tectono-stratigraphic overview *in* Chestnut, D.R., Jr., Eble, C.F., Greb, S.F., and Dever, G.R., Jr., Geology of the Pound Gap Roadcut, Letcher County, Kentucky. Kentucky Society of Professional Geologists, 169p.

Ettensohn, F.R., and Chesnut, D.R.,Jr., 1998. Geology of the Pound Gap Roadcut, Letcher County, Kentucky. Kentucky Society of Professional Geologists, 169p.

Ettensohn, F.R., Dever, G.R., and Grow, J.S., 1988, A paleosol interpretation for profiles exhibiting subaerial exposure "crusts" from the Mississippian of the Appalachian Basin *in* Reinhardt, J., Sigleo, W.R., eds., Paleosols and weathering through geologic time: Principles and Applications: Geological Society of America Special Paper, v. 216, p. 49-79.

Falcon-Lang, H.J., 1999, The Early Carboniferous (Courceyan-Arudian) monsoonal climate of the British Isles: evidence from growth of rings in fossil woods: Geology Magazine, v. 136, p. 177-187.

Feakes, CR., and Retallack, G.J., 1988, Recognition and chemical characterization of fossil soils developed on alluvium; A Late Ordovician example *in* Reinhardt, J., and Sigleo, W.R. eds., Paleosols and Weathering Through Geologic Time: Principles and Applications: Geological Society of America Special Paper, v. 216, p. 35-48.

Fielding, C.R., Frank, T.D., Birgenheier, L.P., Rygel, M.C., Jones, A.T., and Roberts. J., 2008, Stratigraphic imprint of the Late Palaeozoic Ice Age in eastern Australia: a record of alternating glacial and nonglacial climate regime: Journal of the Geological Society, London, v. 165, p. 129-140.

Fitzpatrick, E.A., 1993, Soil Microscopy and Micromorphology. John Wiley and Sons, New York. 304 pp.

Gallet, S., Jahn, B., Lanoe, B., Dia, A., and Rossello, E., 1998, Loess geochemistry and its implications for particle origin and composition of the upper continental crust: Earth and Planetary Science Letters, v. 156, v. 157-172.

Greb S.F., and Caudill, M.R., 1988, Well-developed paleosols of the Upper Pennington Formation *in* Ettensohn, F.R., and Chesnut, D.R. eds., Jr., 1998. Geology of the Pound Gap Roadcut, Letcher County, Kentucky: Kentucky Society of Professional Geologists, 169 pp.

Greb, S.F., and Chesnut, D.R., Jr., 1996, Lower and lower Middle Pennsylvanian fluvial to estuarine deposition, Central Appalachian basin-Effects of eustasy, tectonics, and climate: Geological Survey of America Bulletin, v. 108, p. 303-317.

Greb, S.F., and Eble, C.F., 1998, The Mississippian-Pennsylvanian Boundary at Pound Gap *in* Ettensohn, F.R., and Chesnut, D.R. eds., Jr., 1998. Geology of the Pound Gap Roadcut, Letcher County, Kentucky: Kentucky Society of Professional Geologists, 169 pp.

Greb, S.F., 1998a. Lower Pennsylvanian fluvial sandstones at Pound Gap *in* Ettensohn, F.R., and Chesnut, D.R. eds., Jr., 1998. Geology of the Pound Gap Roadcut, Letcher County, Kentucky. Kentucky Society of Professional Geologists, p.5-8.

Greb, S.F., 1998b. Tidal estuarine sedimentation in the Pennington Formation *in* Ettensohn, F.R., and Chesnut, D.R. eds., Jr., 1998. Geology of the Pound Gap Roadcut, Letcher County, Kentucky. Kentucky Society of Professional Geologists, p. 43-48.

Greb S.F., and Caudill, M.R., 1988, Well-developed paleosols of the Upper Pennington Formation *in* Ettensohn, F.R., and Chesnut, D.R. eds., Jr., 1998. Geology of the Pound Gap Roadcut, Letcher County, Kentucky. Kentucky Society of Professional Geologists, p. 38-42.

Greb, S.F., and Eble, C.F., 1998. The Mississippian-Pennsylvanian Boundary at Pound Gap *in* Ettensohn, F.R., and Chesnut, D.R. eds., Jr., 1998. Geology of the Pound Gap Roadcut, Letcher County, Kentucky. Kentucky Society of Professional Geologists, p. 9-13.

Guo, Z.; Liu, T.; Fedoroff, N.; Wei, L.; Ding, Z.; Wu, N.; Lu, H.; Jiang, W.; and An, Z. 1998, Climate extremes in Loess of China coupled with the strength of deep-water formation in the North Atlantic: Global and Planetary Change, v. 18, p. 113-128.

Harnois, L. 1988, The CIW Index: a new chemical index for weathering: Sedimentary Geology, v. 55, p. 319-322.

Harris, A.G., Harris, L.D., and Epstein, J.B., 1978, Oil and gas data from Paleozoic rocks in the Appalachian Basin: Maps for assessing hydrocarbon potential and thermal maturity (conodont color alteration isograds and overburden isopachs): U.S. Geological Survey I-917-E.

Heironymus, B.; Kotschoubey, B.; and Boulegue, J. 2001, Gallium behavior in some contrasting lateritic profiles from Cameroon and Brazil: Journal of Geochemical Exploration, v. 72, p. 147-163.

Hodsen, M.E. 2002, Variation in element release rate from different mineral size fractions from the B horizon of a granitic podzol: Chemical Geology, v. 190, p. 91-112.

Hoefs, J., 2004, Stable Isotope Geochemistry: Springer, 244 pp.

Horne, J.C., Ferm, J.C., Caruccio, F.T., and Baganz, B.P., 1978, Depositional Models in Coal Exploration and Mine Planning in Appalachian Region: American Association of Petroleum Geologists Bulletin: v. 62, p. 2379-2411.

Hower, J.C., Fiene, F.L., Wild, G.D., and Helfrich, C.T., 1983, Coal metamorphism in the upper portion of the Pennsylvanian Sturgis Formation in western Kentucky: Geological Society of America Bulletin, v. 94, p. 1475-1481.

ICS, 2004. A geologic time scale 2004. International Commission on Stratigraphy.

International Commission on Stratigraphy, 2005. Geologic Time Scale.

Jahn, B.; Gallet, S.; and Han, J. 2001, Geochemistry of Xining, Xifeng and Jixian sections, Loess Plateau of China: eolian dust provenance and paleosols evolution during the last 140ka: Chemical Geology, v. 178, p. 71-94.

Johnson, R.A., and Wichern, D.W. 2007, Applied multivariate statistical analysis 7ed. New Jersey, Prentice Hall 773p.

Kahmann, J.A., Seaman, J., and Driese, S.G., 2008, Evaluating Trace Elements as Paleoclimate Indicators: Multivariate Statistical Analysis of Late Mississippian Pennington Formation Paleosols, Kentucky, U.S.A.: Journal of Geology, v. 116, p. 254-268.

Kahmann, J.A., and Driese, S.D., 2008, Paleopedology and geochemistry of Late Mississippian (Chesterian) Pennington Formation paleosols at Pound Gap, Kentucky, USA: Implications for high-frequency climate variations: Palaeogeography, Palaeoclimatology, Palaeoecology, v. 259, p. 357-381.

Kabata-Pendias, A., 2001,Trace elements in soils and plants, 3rd ed. CRC Press, 413pp.

Kemp, R.A., 1999. Micromorphology of loess-paleosol sequences: a record of paleoenvironmental change: Catena, v. 35, p. 179-196.

Kim, J.C., Lee, Y., and Hisada, K., 2007, Depositional and composition controls on sandstone diagenesis, the Tetori Group (Middle Jurassic-Early Cretaceous, central Japan: Sedimentary Geology, v. 195, p. 183-202.

Kraus, M.J., 1987, Integration of channel and floodplain suites, II. Vertical relations of alluvial paleosols: Journal of Sedimentary Research, v. 57, p. 602-612.

Lees, A., and Buller, A.T., 1972, Modern temperate-water and warm-water shelf carbonate sediments contrasted: Marine Geology, v.13, p. 67-73.

Lynn, W.C., and Willams, D., 1992, The making of a Vertisol: Soil Survey Horizons, v. 33, p. 45-50.

Marques, J.J., Schulze, D.G., Curi, N., and Merztmann, S.A., 2004, Trace element geochemistry in Brazilian Cerrado Soils: Geoderma, v. 121, p. 31-43.

Maynard, J.P., Eriksson, K.A., and R.D., Law, 2006, The Upper Mississippian Bluefield Formation in the Central Appalachian basin: A hierarchical sequence-stratigraphic record of a greenhouse to icehouse transition: Sedimentary Geology, v. 192, p. 99-122.

McCarthy, P.J., Martini, I.P., and Leckie, D.A., 1998, Use of micromorphology for palaeoenvironmental interpretation of complex alluvial paleosols: an example from the Mill Creek Formation (Albian), southwestern Alberta, Canada:Palaeogeography, Palaeoclimatology, Palaeoecology, v. 143, p. 87-110.

McCarthy, P.J., 2002, Micromorphology and development of interfluve paleosols: a case study from the Cenomian Dunvegan Formation, NE British Columbia, Canada: Bulletin of Canadian Petroleum Geology, v. 50, p. 158-177.

McCarthy, P.J., Martini, I.P., and Leckie, D.A., 1998, Use of micromorphology for palaeoenvironmental interpretation of complex alluvial paleosols: an examplefrom the Mill Creek Formation (Albian), southwestern Alberta, Canada: Palaeogeography, Palaeoclimatology, Palaeoecology v. 143, p. 87-110.

McLennan, S.M. 1989, Rare earth elements in sedimentary rocks; influence of provenance and sedimentary processes: Reviews in Mineralogy and Geochemistry, v. 21, p. 169-200.

McKee, E.D., Crosby, E.J., and others, 1976, Paleotectonic investigations of the Pennsylvanian System in the United States: U.S. Geological Survey Professional Paper 853, 541pp.

Menning, M., Weyer, D., Drozdzewski, G., Van Amerom, H.W.J., and Wendt, I., 2000, A Carboniferous time scale 2000: Discussion and use of geological parameters as time indicators from Central and Western Europe: Geologisches Jahrbuch, v. A156, p. 3-44.

Meyers, P.A., 1994, Preservation of elemental and isotopic source identification of sedimentary organic matter: Chemical Geology, v. 114, p. 289-302.

Miall, A.D., 1978, Facies types and vertical profile models in braided river deposits: a summary, *in* Miall, A.D., ed., Fluvial sedimentology: Canadian Society of Petroleum Geologists, Memoir 5, p. 597-604.

Mitra, S., 1988, Three-dimensional geometry and kinematic evolution of the Pine Mountain thrust system, southern Appalachians: Geological Society of America Bulletin: v. 100, p. 72-95.

Miller, D.J., and Eriksson, K.A., 1997, Late Mississippian prodeltaic rythmites in the Appalachian Basin: A hierarchical record of tidal and climatic periodicities: Journal of Sedimentary Research, v. 67, p. 653-660.

Miller, D.J., and Eriksson, K.A., 1999, Linked sequence development and global climate change: The Upper Mississippian record in the Appalachian basin: Geology, v. 27, p.35-38.

Miller, D.J., and Eriksson, K.A., 2000, Sequence stratigraphy of Upper Mississippian strata in the Central Appalachians: A record of glacioeustasy and tectonoeustasy in a foreland basin setting: American Association of Petroleum Geologists Bulletin, v.84, p. 210-233.

Mitchum, R.M., and Van Wagoner, J.C., 1991, High-frequency sequences and their stacking patterns: sequence stratigraphic evidence of high-frequency eustatic cycles: Sedimentary Geology, v. 70, p. 131-160.

Mitra, S., 1988, Three-dimensional geometry and kinematic evolution of the Pine Mountain thrust system, southern Appalachians: Geological Society of America Bulletin, v.100, p. 72-95.

Mora, C.I., Sheldon, B.T., Elliott, W.C., and Driese, S.G., 1998, An oxygen isotope study of illite and calcite in three Appalachian Paleozoic Vertic paleosols: Journal of Sedimentary Research, v. 68, p. 456-464.

Mora, C.I., and Driese, S.G., 1999, Palaoenvironment, palaeoclimate and stable carbon isotopes of Palaeozoic red-bed palaeosols, Appalachian Basin, U.S.A. and Canada: Special Publication of the International Association of Sedimentologists, v. 27, p. 61-84.

Moore, D.M., and Reynolds, R.C., 1997, X-Ray diffraction and the identification and analysis of clay minerals 2nd ed. Oxford University Press. 378pp.

Muggler, C.C., and Buurman, P. 2000, Erosion, sedimentation and pedogenesis in a polygenetic Oxisol sequence in Minas Gerais, Brazil: Catena, v. 41, p. 3-17.

Nelson, W.A., and Read, J.F., 1990, Updip to downdip cementation and dolomitization patterns in a Mississippian aquifer, Appalachians: Journal of Sedimentary Petrology, v. 60, p. 379-396.

Nesbitt, H.W., and Markovics, G., 1997, Weathering of granodioritic crust, long-term storage of elements in weathering profiles and petrogenesis of siliciclastic sediments: Geochimica et Cosmochimica Acta, v. 61, p. 1653-1670.

Nettleton, W.D., and Sleeman, J.R., 1985, Micromorphology of Vertisols *in* Douglas, L.A., and Thompson, M.L., eds. Soil Micromorphology and Soil Classification: Soil Science Society of America, Special Publication, v. 15, p. 165-196.

Niemann, J.C., and Read, J.F., 1988, Regional cementation from unconformity-recharged aquifer and burial fluids, Mississippian Newman limestone, Kentucky: Journal of Sedimentary Petrology, v. 58, p. 688-705.

Nio, S.D., and Yang, C.S., 1991, Sea-level fluctuations and the geometric variability of tide-dominated sandbodies: Sedimentary Geology, v. 70, p. 161-172.

Nordt, L.C., Wilding, L.P., Lynn, W.C., and Crawford, C.C., 2004, Vertisol genesis in a humid climate of the coastal plain of Texas, USA: Geoderma, v. 122, p. 83-102.

Olivie-Lauquet, G.; Grau, G.; Dia, A.; Riou, C.; Jaffrezic, A.; and Henin, O. 2001, Release of trace elements in wetlands: role of seasonal variability: Water Research, v. 35, p. 943-952.

Parfitt, R.L., Theng, B.K.G., Theng, J.S., and Whitton, T.G.S., 1997, Effects of clay minerals and land use on organic matter pools: Geoderma, v. 75, p. 1-12.

Parrish, J.T., 1993, Climate on the supercontinent of Pangea: Journal of Geology, v. 101, p. 215-233.

Parker, A. 1970. An index of weathering for silicate rocks: Geological Magazine, v. 107, p. 501-504.

Pemberton, S.G., and MacEachern, J.A., 1995, The sequence stratigraphic significance of trace fossils: Examples from the Cretaceous foreland basin of Alberta, Canada *in* Van Wagoner, J.C., and Bertram, G.T., Sequence stratigraphy of foreland basin deposits: Outcrop and subsurface examples from the Cretaceous of North America: American Association of Petroleum Geologists Memoir, v. 64, 429-476.

Pemberton, S.G., MacEachern, J.A., and Frey, R.W., 1992, Trace fossil facies models: environmental and allostratigraphic significance *in* Walker, R.G., James, N.P., Facies Models: Geological Association of Canada, p. 47-72.

Pe-Piper, G., Dolansky, L., and Piper, D.J.W., 2005, Sedimentary environment and diagenesis of Lower Cretaceous Chaswood Formation, Southeastern Canada: The origin of kaolin-rich mudstones: Sedimentary Geology, v. 178, p. 75-97.

PiPujol, M.D., and Buurman, P., 1994, The distinction between ground-water gley and surface-water gley phenomena in Tertiary paleosols of the Ebro basin, NE Spain: Palaeogeography, Palaeoclimatology, Palaeoecology, v. 110, p. 103-113.

Pritchard, D.W., 1967, What is an estuary: physical standpoint?, *in* Lauff, G.H., ed., Estuaries: American Association for Advancement of Science, v. 83, p. 3-5.

Prochnow, S. J., Nordt, L.C., Atchley, S.A., and Hudec, M.R., 2006, Multi-proxy paleosol evidence for middle and late Triassic climate trends in eastern Utah: Palaeogeography, Palaeoclimatology, Palaeoecology, v. 232, p. 54-72.

Quinlan, G.M., and Beaumont, C., 1984, Appalachian thrusting, lithospheric flexure, and the Paleozoic stratigraphy of the Eastern interior of North America: Canadian Journal of Earth Sciences, v.21, p. 973-996.

Reed, J.S., Eriksson, K.A., and Kowalewski, M., 2005, Climatic, depositional and burial controls on diagenesis of Appalachian Carboniferous sandstones: qualitative and quantitative methods: Sedimentary Geology, v. 176, p. 225-246.

Retallack, G.J. 1986, Reappraisal of a 2200 Ma paleosol from near Waterval Onder, South Africa: Precambrian Research, v. 32, p. 195-232.

Retallack, G.J., 1988, Core concepts in paleopedology: Quaternary International, v. 51/52, p.203-212.

Retallack, G.J., 1992, What to call early plant formations on land, Palaios, v. 7, p. 508-520.

Retallack, G.J., 2001, Soils of the Past: An Introduction to Paleopedology, 2nd ed. Blackwell Science, Malden, USA, 404 pp.

Retallack, G.J., and Sheldon, N.D., 2001, Equation for compaction of paleosols due to burial: Geology, v. 29, p. 247-250.

Retallack, G.J., and Wright, V.P., 1990, Micromorphology of lithified paleosols *in*: Douglas, L.A. ed. Soil Micromorphology: A Basic and Applied Science: Elsevier, Amsterdam 641-652.

Robinson, A., 2002, A chronosequences study of modern Vertisols and application to interpreting the time significance of Paleozoic paleo-Vertisols. Masters Thesis, Univ of Tennessee- Knoxville, 176 pp.

Rossetti, D., 2000, Influence of low amplitude/high frequency relative sea-level changes in a wave-dominated estuary (Miocene), São Luis Basin, northern Brazil: Sedimentary Geology, v. 133, p. 295-324.

SAS Institute Inc., 2004, SAS OnlineDoc ® 9.1.3. North Carolina, SAS Institute Inc.

SAS Institute Inc., 2007, JMP User's Guide. North Carolina, SAS.

Sable, E.G., and Dever, G.R., 1990, Mississippian Rocks in Kentucky: U.S. Geological Survey Professional Paper 1503, 125pp.

Sarg, J.F., 1988, Carbonate sequence stratigraphy: SEPM Special Publication, v. 42, p. 155-181.

Schroeder-Adams, C., 2006, Estuaries of the past and present: A biofacies perspective: Sedimentary Geology, v. 190, p. 289-298.

Scotese, C.R., and McKerrow, W.S., 1990, Revised world maps and introduction, *in* McKerrow, W.S., Scotese, C.R., eds., Paleogeography and Biogeography: Geological Society of London Memoir, v. 21, p. 1-24.

Scribner, A.M.; Kurtz, A.C.; and Chadwick, O.A. 2006, Germanium sequestration by soil: Targeting the roles of secondary clays and Fe-oxyhydroxides: Earth and Planetary Science Letters, v. 243, p. 760-770.

Shang, C., and Tiessen, H., 2003, Soil organic C sequestration and stabilization in karstic soils of Yucatan: Biogeochemistry, v. 62, p. 177-196.

Sheldon, N.D., Retallack, G.J.,and Tanaka, S., 2002, Geochemical climofunctions from North American Soils and application to paleosols across the Eocene-Oligocene boundary in Oregon: Journal of Geology, v. 119, p. 687-696.

Sheldon, N.D. 2006, Abrupt chemical weathering increase across the Permian-Triassic boundary: Palaeogeography, Palaeoclimatology, Paleaoecology, v. 21, p. 315- 321.

Shotyk, W.; Weiss, D.; Kramers, J.D.; Frei, R.; Cheburkin, A.K.; Gloor, M.; and Reese, S. 2001, Geochemistry of the peat bog at Etang de la Gruere, Jura Mountains, Switzerland, and its record of atmospheric Pb and lithogenic trace metals (Sc, Ti, Y, Zr, and REE) since 12,370 ^{14}C yr BP: Geochimica et Cosmochimica Acta v. 65, p. 2337-2360.

Smith, L.B., and Read, J.F., 2000, Rapid onset of Late Paleozoic glaciation on Gondwana: Evidence from Upper Mississippian strata of the Mid-Continent, United States: Geology, v. 28, p. 279-282.

Sloss, L., 1963. Sequences in the cratonic interior of North America: GSA Bulletin, v. 74, p. 93-113.

Soil Survey Staff, 1998, Keys to Soil Taxonomy, Eighth Edition: Washington D.C. U.S. Government Printing Office, 324 pp.

Sterckeman, T.; Douay, F.; Baize, D.; Fourrier, H.; Proix, N.; and Schvartz., C. 2004, Factors affecting trace element concentrations in soils developed on recent marine deposits from northern France: Applied Geochemistry, v. 19, p. 89-103.

Sterckeman, T.; Douay, F.; Baize, D.; Fourrier, H.; Proix, N.; and Schvartz., C. 2006, Trace elements in soils developed in sedimentary materials from Northern France. Geoderma, v. 136, p. 912-929.

Stewart, B.W.; Capo, R.C.; and Chadwick, O.A. 2001, Effects of rainfall on weathering rate, base cation provenance, and Sr isotope composition of Hawaiian soils: Geochimica et Cosmochimica Acta, v. 65, p. 1087-1099.

Stewart, W.N., 1983, Paleobotany and the evolution of plants: Cambridge University Press, New York, 405pp.

Stiles, C.A.; Mora, C.I.; and Driese, S.G. 2001, Pedogenic iron-manganese nodules in Vertisols: a new proxy for paleoprecipitation?: Geology, v. 29, p. 943-946.

Stiles, C.A.; Mora, C.I.; and Driese, S.G. 2003, Pedogenic processes and domain boundaries in a Vertisol climosequence: evidence from titanium and zirconium distribution and morphology: Geoderma, v. 116, p. 279-299.

Stoops, G., 2003, Guidelines for Analysis and Description of Soil and Regolith Thin Sections. Soil Science Society of America, Madison, WI. 184 pp. + CD w/images.

Strahler, A.N., and Strahler, A.H., 1973, Environmental geoscience: Interaction between natural systems and man. Hamilton Publishing, Santa Barbara, 511pp.

Stuzenbaker, C.D., 1999, Aquatic and wetland plants of the Western Gulf Coast. Texas Parks and Wildlife, 465pp.

Tankard, A.J., 1986, Depositional response to foreland deformation in the Carboniferous of eastern Kentucky: American Association of Petroleum Geologists Bulletin, v.70, p. 853-868.

Tinker, S.W., 1998. Shelf-to-basin distributions and sequence stratigraphy of a steep-rimmed carbonate margin: Capitan depositional system, McKittrick Canyon, New Mexico and Texas: Journal of Sedimentary Research, v. 68, p. 1146-1174.

Trakooniyingcharoen, P., Kheoruenromne, I., Suddhiprakam, A., and Gilkes, R.J., 2006, Properties of kaolins in red Oxisols and red Ultisols in Thailand. Applied Clay: Science, v. 32, p. 25-39.

Tyler, G. 2004, Vertical distribution of major, minor, and rare elements in a Haplic Podzol: Geoderma, v. 119, p. 277-290.

Tyler, G., and Olsson, T. 2002, Conditions related to solubility of rare and minor elements in forest soils: Journal of Plant Nutrition and Soil Science, v. 165, p. 594-601.

Van Siclen, D.C., 1958, Depositional topography; examples [Louisiana-Texas] and theory: American Association of Petroleum Geologists Bulletin, v. 42, p. 1897-1913.

Van Wagoner, J.C., Posamentier, R.M., Mitchum, R.M., Vail, P.R., Sarg, J.F., Loutit, T.S., and Hardenbol, J., 1988, An overview of the fundementals of sequence stratigraphy and key definitions, *in* C.W., Wilgus et al., eds., Sea level changes: an integrated approach: SEPM Special Publication, v. 42, p. 39-45.

Van Wagoner, J.C., 1995, Overview of Sequence Stratigraphy of Foreland Basin Deposits: Terminology summary of papers, and glossary of sequence stratigraphy *in* Van Wagoner, J.C., and Bertram, G.T., Sequence stratigraphy of foreland basin deposits: Outcrop and subsurface examples from the Cretaceous of North America: American Association of Petroleum Geologists Memoir, v. 64, ix-xxi.

Wilding, L.P., and Tessier, D., 1988, Genesis of vertisols: Shrink-swell phenomena, *in* Wilding, L.P., and Puentes, R., ed. Vertisols: Their Distribution, Properties, Classification and Management: College Station, Texas, Texas A&M University Printing Center, 55-81.

Wilson, J.L., 1965, Cyclic and Reciprocal Sedimentation in Virgillian Strata of southern New Mexico: Geological Society of America, v. 78, p. 805-817.

Wilson, J. L., 1975, Carbonate Facies in Geologic History: Springer-Verlag, New York, 471p.

deWitt, W., and McGrew, L.W., 1979, The Appalachian Basin Region *in* Paleotectonic investigations of the Mississippian system in the United States, Part I: Introduction and regional analysis of the Mississippian system: Geological Survey Professional Paper 1010, 13-48.

Woodward, H.P., 1961, Preliminary subsurface study of southeastern Appalachian Interior Plateau: American Association of Petroleum Geologists Bulletin, v. 45, p. 1634-1655.

Wright, V. P., and Marriott, S.B., 1993, The sequence stratigraphy of fluvial depositional systems: the role of floodplain sediment storage: Sedimentary Geology, v. 86, p. 203-210.

Wright, V.P. and Tucker, M.E., 1991, Calcretes. Oxford, Blackwell Science 347pp.

Wynn, T.C., and Read, J.F., 2007, Carbon-oxygen isotope signal of Mississippian slope carbonates, Appalachians, USA: A complex response to climate-driven fourth- order glacio-eustasy: Palaeogeography, Palaeoclimatology, Palaeoecology, v. 256, p. 254-272.

Yin, Q., and Guo, Z., 2006, Mid-Pleistocene vermiculated red soils in southern China as an indication of unusually strengthened East Asian monsoon: Chinese Science Bulletin, v. 51, p. 213-200.

Zhang, C., Wang, L., Li, G., Dong, S., Yang, J., and Wang, X., 2002, Grain size effect on multi-element concentrations in sediments from the intertidal flats of Bohai Bay, China: Applied Geochemistry, v. 17, p. 59-68.

Ziegler, A.M., Scotese, C.R., McKerrow, W.S., and others, 1979, Paleozoic paleogeography: Annual Review of Earth and Planetary Science, v. 7, p. 473-502.